



KATHOLISCHE UNIVERSITÄT
EICHSTÄTT-INGOLSTADT



ALFRED-WEGENER-INSTITUT
HELMHOLTZ-ZENTRUM FÜR POLAR-
UND MEERESFORSCHUNG

Master Thesis

to attain the academic degree

Master of Science (M.Sc.) in Physical Geography

Estimating excess ground ice in Arctic tundra landscapes by a statistical analysis of drained thermokarst lake basins - A comparison between research sites in Alaska

Abschätzung von überschüssigem Bodeneis in arktischen Tundralandschaften
anhand einer statistischen Analyse von Alasen -
Ein Vergleich zwischen Untersuchungsgebieten in Alaska

submitted by

Lisa Annika Schramm

to Prof. Dr. Michael Becht
Institute of Geography,
Catholic University of Eichstätt - Ingolstadt

Potsdam, 24. September 2019

Lisa Annika Schramm,

geboren am 13.07.1994 in Esslingen am Neckar

Adresse: Im Holder 15, 73734 Esslingen

Email: lisaschramm@web.de

Matrikelnummer: 707538

Gutachter KU:

Prof. Dr. Michael Becht

Lehrstuhl für Physische Geographie

Mathematisch- Geographische Fakultät der KU Eichstätt-Ingolstadt

Ostenstraße 18, 85072 Eichstätt

Michael.Becht@ku.de

Betreuer AWI:

Dr. Moritz Langer

Forschungsgruppe PermaRisk am Alfred- Wegener- Institut

Telegrafenberg A43, 14473 Potsdam

Moritz.Langer@awi.de

Abstract

Excess ice is determining the sensibility of permafrost landscapes in a warming climate. As excess ice thaws several morphodynamical processes can occur, which can change the Arctic landscape significantly. Up until now, the excess ice content is only known for small areas of the Arctic, but not Arctic wide. Mappings that cover large areas are mostly based on classifications of the land surface and are therefore not very precise. The limited amount of data about excess ice affects the precision of the modelling of the degradation of Permafrost, because it affects the sensitivity of permafrost landscapes including all biogeochemical and geophysical processes.

To estimate the amount of excess ice in a landscape, differences in altitude formed by thermoerosion processes were analyzed. Height differences are formed by melting excess ice in the ground, causing subsidence. It is presumed that the content of excess ice around the thermoerosion structures is about as thick as the subsidence of the structure itself. Some factors, like erosion, slope and others, must be kept in mind when interpreting the results. The research question of the thesis is: Is it possible to make a rough estimation of the excess ice content of permafrost soil in tundra landscapes by an analysis of a digital elevation model (DEM)?

The Barrow Peninsula and the Seward Peninsula, both located in Alaska, U. S., are the two research sites of this work, characterized by current thermokarst lakes and former ones, which are nowadays Drained Thermokarst Lake Basins (DTLBs).

For the analysis of the basin height in comparison to the surrounding area, the Arctic DEM is used as main data resource together with data of the DTLBs. ArcGIS and R were used to calculate the height of the lakes and DTLBs and to statistically analyze the results.

Various height differences and elevation distribution patterns for the two research sites were found out without a significantly related distribution pattern with the age or general elevation of the DTLBs.

The discussion includes the importance of the distribution pattern of the elevation data for the interpretation of the excess ice and which other factors must be considered in the interpretation, like the age of the DTLB, the landscape type and soil and permafrost properties. Problems occurred, e.g. regarding the comparability between the research sites because of the age classes and due overlapping of buffers. Furthermore, ideas of an improvement of the method are proposed.

The result includes the mean difference of the buffer height minus the basins height, but several other factors need to be included, such as the active layer thickness, the permafrost depth and more. Therefore, the named difference can not be equalized to the excess ice volume.

Zusammenfassung

Überschüssiges Bodeneis spiegelt die Sensibilität von Permafrostlandschaften in einem sich erwärmenden Klima wider. Durch das Tauen von Bodeneis werden verschiedene morphodynamische Prozesse in Gang gesetzt, welche die Arktische Landschaft sehr deutlich verändern können. Bisher ist das Ausmaß von überschüssigem Bodeneis, excess ice, nur bekannt für kleinräumige Gebiete, aber nicht die gesamte Arktis. Kartierungen, welche größere Flächen abdecken, basieren zumeist auf Klassifizierungen der Landoberfläche und sind dadurch nicht sehr genau. Die limitierte Datenmenge zu excess ice ist ein Ungenauigkeitsfaktor in der Modellierung der Permafrost Degradierung, da es auch die gesamte Sensitivität von Permafrostlandschaften beeinflusst, inklusive aller biogeochemischen und biogeophysikalischen Prozessen.

Um die Menge an überschüssigem Bodeneis zu analysieren, wurde ein Vergleich von der Höhe von ausgelaufenen Thermokarstsee, Alasen, und der direkten Umgebung berechnet. Diese Differenzen sind durch das Abtauen von Bodeneis und der dadurch resultierenden Bodenabsackung entstanden. Es wird dabei angenommen, dass die Absenkung der Seebecken in etwa die Höhe des Bodeneisgehaltes entspricht. Jedoch müssen Faktoren, wie Erosion, Hangneigung und weitere, bei der Interpretation mit herangezogen werden. Die Fragestellung der Masterthesis lautet: Ist es möglich eine grobe Abschätzung über den Gehalt von Bodeneis eines Permafrostbodens in einer arktischen Tundralandschaft durch eine Analyse eines Digitalen Höhenmodells zu berechnen?

Die Untersuchungsgebiete dieser Arbeit sind die Barrow Halbinseln und der Norden der Seward Halbinsel, welche beide in Alaska, USA, zu verorten sind. Beide Gebiete sind charakteristisch geprägt von rezenten Thermokarstseen sowie ehemaligen, heute ausgelaufenen Thermokarstseen, auch Alase genannt.

Für die Analyse der Seebeckenhöhe und des umliegenden Geländes, wird das Arctic DEM als hauptsächliche Datenquelle in Kombination mit Daten für die Alase verwendet. ArcGis und R werden für die Datenverarbeitung, die Höhenberechnungen und die statistische Analyse der Ergebnisse verwendet. Verschiedene Höhendifferenzen und Verteilungen der Höhendaten für beide Untersuchungsgebiete ohne einen signifikanten Zusammenhang zwischen der Verteilung und Alter oder der generellen Höhe des DTLBs wurden herausgefunden.

Die Diskussion beinhaltet die Wichtigkeit der Verteilungen der Höhendaten für die Interpretation von excess ice and welche anderen Faktoren bei der Interpretation beachtet werden müssen, wie das Alter der Becken, der Landschaftstyp und Boden- sowie Permafrost-eigenschaften. Probleme sind unter anderem bei der Vergleichbarkeit der Untersuchungsgebiete auf Grund der verschiedenen Altersklassen und durch sich überlappende Bufferbereiche entstanden. Weiterhin werden Idee für eine Verbesserung der Methode vorgeschlagen.

Das Ergebnis beinhaltet die durchschnittliche Höhendifferenz der Bufferflächen minus der Beckenflächen, wobei noch andere Faktoren einberechnet werden müssen, wie die Dicke des active layers, die Permafrostmächtigkeit und weitere. Es kann nicht die genannte Höhendifferenz mit dem Volumen des excess ice gleichgesetzt werden.

Content

Abstract	I
Zusammenfassung	II
Content	III
List of Figures	V
List of Tables	VII
List of Appendixes	VIII
Abbreviations	IX
1. Introduction	1
1.1. Permafrost in the Arctic	1
1.2. State of the Art of Mapping Permafrost	2
1.3. Landscape Structures and Processes in Permafrost Environments.....	3
1.4. Project at Alfred-Wegener-Institute	6
1.5. Aim of the Thesis	7
2. Study region	7
2.1. Barrow Peninsula.....	8
2.2. Northern Seward Peninsula	11
3. Methodology	14
3.1. Data.....	14
3.1.1. Arctic DEM.....	14
3.1.2. Landsat Data	15
3.1.3. World Imagery in ArcGIS.....	15
3.1.4. DTLB Data.....	16
3.2. Data Processing in ArcGIS	18
3.3. Statistical Analysis in R.....	19
4. Results	20
4.1. Sensitivity Study - Determination of the Buffer Size.....	20
4.2. Details of Barrow research site.....	25

4.3. Details of Seward Peninsula research site	31
4.3.1. Age group 1.....	31
4.3.2. Age group 2.....	35
4.3.3. Age group 3.....	37
4.3.4. Age group 4.....	39
4.3.5. Age group 5.....	40
4.3.6. Errors and Inaccuracies	43
4.4. Comparison of Barrow and Seward.....	44
5. Discussion	46
5.1. Interpretation of the results.....	46
5.2. Evaluation of the Results and Outlook	50
6. Conclusion.....	51
Acknowledgements	53
Bibliography.....	54
Eidesstaatliche Erklärung	58
Appendix	59

List of Figures

Figure 1: Distribution of permafrost on the northern hemisphere (National Snow and Ice Data Center 2019).....	3
Figure 2: Aerial Picture (ESRI World Imagery) of Thermokarst lakes and DTLBs in the research area of Barrow.....	5
Figure 3: Overview map (ESRI Nat. Geographic) of the research areas in Alaska. Barrow in the north is marked in red, Seward in the west in purple.	8
Figure 4: Map of Barrow on ESRI Nat. Geographic basemap.....	9
Figure 5: Thermokarst lakes and DTLBs Barrow Peninsula (Frohn et al. 2005)	10
Figure 6: Lakes Barrow Peninsula; Barrow DTLBs (Hinkel et al. 2003).....	10
Figure 7: Climate graph of the city of Barrow (Climate Data)	11
Figure 8: Map of the northern Seward Peninsula (ESRI Nat. Geographic).....	12
Figure 9: Aerial image of a thermokarst lake before (a, 1978) and after drainage (b, 2003) on the northern Seward peninsula (Grosse et al. 2013).....	12
Figure 10: Climate Graph of Deering (Climate Data).....	13
Figure 11: Coverage of the Arctic DEM release 7 (Polar Geospatial Centre 2018).....	14
Figure 12: DTLBs of Barrow research area on ESRI World Imagery.....	16
Figure 13: DTLBs of Seward Peninsula research area on ESRI World Imagery	17
Figure 14: Outline of DTLB ID 8 at Barrow based on Hillshade of the Arctic DEM.....	18
Figure 15: Hillshade of DTLB ID 14 at Barrow with the outlines of the DTLB and different radii of buffer	21
Figure 16: World Imagery of DTLB ID 14 at Barrow with the outlines of the DTLB and different buffer radii	21
Figure 17: Histograms DTLB ID 14 buffer 50 m (green), 100 m (orange), 150 m (red)	22
Figure 18: Histograms DTLB ID 8 buffer 50 m (green), 100 m (orange), 150 m (red)	23
Figure 19: DTLB ID 19 at Barrow on ESRI World Imagery.....	23
Figure 20: Histograms DTLB ID 19, buffer 50 m (green), 100 m (orange), 150 m (red)	24
Figure 21: Graph of basin area and basin height.....	26
Figure 22: Graph of differences in buffer - basin heights	27
Figure 23: Histograms of Barrows DTLB ID 8, 14, 19	27
Figure 24: Density plot of DTLB 14 (a) and 17 (b) (normal distribution).....	28
Figure 25: Density plot of DTLB 18 (a) and 19 (b) (bimodal distribution).....	28
Figure 26: Density plot of DTLB 4 (a) and 6 (b) (multimodal distribution)	29

Figure 27: World Imagery of Barrow DTLB 6	29
Figure 28: a) Hillshade of Barrow, DTLB 14 zoomed to north-east of basin and b) World Imagery of Barrow, DTLB 14 zoomed to south of basin.....	30
Figure 29: a) Density & Frequency plot and b) Map of DTLB 1 of age group 1 (OID 1)	33
Figure 30: a) Density & Frequency plot and b) Map of DTLB 12 of age group 1 (OID 258)	33
Figure 31: a) Density & Frequency plot and b) Map of DTLB 14 of age group 1 (OID 296)	34
Figure 32: a) Density & Frequency plot and b) Map of DTLB 15 of age group 1 (OID 334)	35
Figure 33: a) Density & Frequency plot and b) Map of DTLB 2 of age group 2 (OID 13)	36
Figure 34: a) Density & Frequency plot and b) Map of DTLB 78 of age group 2 (OID 223)	36
Figure 35: Extract of the Seward map of age group 3	37
Figure 36: a) Density & Frequency plot and b) Map of DTLB 8 of age group 3 (OID 21)	38
Figure 37: a) Density & Frequency plot and b) Map of DTLB 109 of age group 3 (OID 269)	39
Figure 38: a) Density & Frequency plot and b) Map of DTLB 5 of age group 4 (OID 41)	39
Figure 39: a) Density & Frequency plot and b) Map of DTLB 32 of age group 4 (OID 189)	40
Figure 40: a) Density & Frequency plot and b) Map of DTLB 1 of age group 5 (OID 8)	41
Figure 41: a) Density & Frequency plot and b) Map of DTLB 6 of age group 5 (OID 161) ..	42
Figure 42: a) Density & Frequency plot and b) Map of DTLB 9 of age group 5 (OID 293) ..	42
Figure 43: DTLBs 137 & 139 overlapping	43

List of Tables

Table 1: Arctic DEM data	15
Table 2: DTLB data of Seward Peninsula after Jones et al. 2011	17
Table 3: DTLB and buffer values of Barrow	25
Table 4: Seward age group 1 DTLB and buffer sizes	31
Table 5: Recalculated values of DTLB 2 and 78 of age group 2	36
Table 6: Recalculated values of DTLB 8 and 109 of age group 3	38
Table 7: Recalculated values of DTLB 5 and 32 of age group 4	40
Table 8: Seward age group 5 DTLB and buffer sizes	41
Table 9: Combined data of Barrow and Seward	44
Table 10: Comparison r^2	45
Table 11: Classification of age classes for Barrow and Seward after Jones et al. 2011 and Hinkel et al. 2003	48
Table 12: Extract of table to classify DTLBs from Hinkel et al. 2003	49
Table 13: Mean differences of buffer - basin height.....	49

List of Appendixes

Appendix 1: Table Barrow, various buffer radii	59
Appendix 2: Table Barrow, addition to table 3	60
Appendix 3: Table Seward age group 1, addition to table 4	61
Appendix 4: Table Seward age group 2	62
Appendix 5: Table Seward age group 3	67
Appendix 6: Table Seward age group 4	74
Appendix 7: Table Seward age group 5, addition to table 8	77

Abbreviations

ACP	Arctic Coastal Plain (Alaska)
ALT	Active Layer Thickness
AWI	Alfred-Wegener-Institute
DTLB	Drained thermokarst lake basin
DCCED DCRA	Department of Commerce, Community, and Economic Development - Divison of Community and regional affairs of Alaska
ICP	Inner Coastal Plain (Alaska)
LGM	Last Glacial Maximum
N/A	no value data
NGA	National Geospatial- Intelligence Agency USA
NCSCD	Northern Circumpolar Soil Carbon Database
NSF	National Science Foundation USA
OCP	Outer Coastal Plain (Alaska)
SOC	Soil Organic Carbon

1. Introduction

1.1. Permafrost in the Arctic

“The cryosphere is, however, not simply a passive indicator of climate change; changes in each component of the cryosphere have a significant and lasting impact on physical, biological and social systems.”
IPCC - Climate Change 2013 - The Physical Science Basis (Vaughan et al. 2013)

Polar Amplification describes the phenomenon of an exceeding mean surface temperature warming of the poles over the global average of temperature increase. The cryosphere, which largest parts are the poles, is very sensitive to a change in climate (Vaughan et al. 2013). Frozen ground, as important part of the cryosphere and its changes are not obvious to see, like melting of glaciers, but it is not as ubiquitous as for example the decrease on the Greenland ice sheet. Still, Permafrost is a sensitive part in climate change and is a significant part of the Arctic environment. This is why research on Permafrost, and of the thawing Permafrost, is indispensable for climate change discussion (Grosse et al. 2011; Vaughan et al. 2013). Thawing of permafrost can have a big impact on the whole ecosystem by changing the flora and fauna, as stated in the quotation of the IPCC report. Also, an effect on the exchange of greenhouse gases from permafrost ground and other biogeochemical processes was found, which therefore directly impacts climate change. Additionally, by destabilizing the ground, influences on infrastructure can occur, with consequences for human settlements and population in permafrost regions (Vonk/Gustafsson 2013; Hope/Schaefer 2016).

Permafrost is a temperature- based phenomenon, which is therefore difficult to measure. So far, permafrost is one of the most uncertain, but important, factors influencing climate change. Within the permafrost the ice content of the ground can have a huge variety, depending on various climatological and geological factors, from nearly no ice content to areas existing of nearly pure ice (Regmi et al. 2012). Thermokarst gullies, lakes, Drained Thermokarst Lake Basins (DTLB), retrogressive thaw slumps and other erosional structures are an indicator of thermokarst processes in ice-rich permafrost grounds. These processes and occurring structures show the impact on thawing of ice-rich permafrost ground. Up to now it is not possible to detect ground ice and its spatial distribution by any tool of remote sensing. Methods for investigating ground ice remotely by analyzing surface structures or other indicators are not yet sufficiently working (Bockheim/Hinkel 2012; Regmi et al. 2012). Considering the rapid warming measured in the terrestrial Arctic with an increase of the mean annual air temperature by 0.5° C per decade since 1981, which is two to three times the average global warming. Therefore an improvement on the research of degrading permafrost in Arctic landscapes is crucial (Rowland et al. 2010; Comiso/Hall 2014).

1.2. State of the Art of Mapping Permafrost

The current knowledge on the directly measured content of excess ice in permafrost ground is mostly limited to several field data samples of a few areas. Some of them are done by sampling and geomorphological mapping, while other data is gained by geophysical and airborne methods (Jorgenson et al. 2003; Gilbert et al. 2016). Up to the moment there is neither a detailed pan- Arctic map of excess ice, nor of thermokarst lakes or drained thermokarst lake basins available, just some maps created by very largely extrapolated data from a combination of point measurements and land surface or climate maps. Summarizing this existing data, there is no detailed information on ground ice for large areas of the Arctic, neither gained by direct investigations, nor by investigating landscape features originating by ground ice or thawing of ground ice (Heginbottom 2002; Grosse et al. 2013). Due to these difficulties of data acquisition, the general processes of Arctic tundra landscapes are most likely not fully understood yet. Thermokarst lakes and DTLBs are ubiquitous landforms in the Arctic tundra landscape, but their lifespan and dynamic processes need further research (Grosse et al. 2013; Liu et al. 2014).

The maximum of the formation of thermokarst lakes and drained basins in the Arctic can be dated back into the Pleistocene- Holocene transition and the Holocene thermal maximum. Thermokarst lakes as well as drained basins are geomorphological features of thawing excess ice in permafrost ground (Grosse et al. 2013). Such lakes on the central part of the Seward peninsula in the Imuruk area were first mentioned by David Hopkins in 1949. He describes the lakes and drained lakes discovered in his 1947/48 field work as lakes established by the subsidence caused by the thawing of perennially frozen ground (Hopkins 1949). The thermokarst lake drainage cycle was also mentioned the first time together with the formation, growth and drainage of the lakes (Hopkins 1949; Grosse et al. 2013). Presently it is known, that thermokarst lakes are having a big influence on surface energy balances with feedbacks to the ground thermal regime in permafrost landscapes as well as the land- atmosphere energy exchange (Grosse et al. 2013; Boike et al. 2015).

Currently produced data products of permafrost include maps of global or regional focus as well as selective data based on cores of the ground, which are just of local scale. One example is the Circum Arctic Map of Permafrost and Ground Ice Conditions by Brown et al. (1997) is a map including the northern hemisphere and marks points of known ground ice bodies. An updated version of this map was published in 2002 (Brown et al. 1997; Brown et al. 2002). Further on, there is the map on “Permafrost Characteristics of Alaska” by Jorgenson et al. (2008), giving an overview on the permafrost categories, like continuous or discontinuous and on punctual permafrost depth, but no information on ground ice is included (Jorgenson et al. 2008). While there is no map or database for Drained Thermokarst Lake Basins known, since 2017 there is a database based on remote sensing data for ponds and lakes in arctic permafrost regions by Muster et al. (Muster et al. 2017).

1.3. Landscape Structures and Processes in Permafrost Environments

Permafrost is defined by the temperature of the ground (soil or rock and included ice and organic material) and the thermal state of the lithosphere, which has to be below or at 0°C for a minimum time of two continuous years. Permafrost does not have to contain water, but it can. Permafrost ground does not have to be perennially frozen, but perennial frozen ground is always considered as Permafrost. The thickness of a Permafrost layer can differ between several centimeters to more than 1000 m (Heginbottom 2002; van Everdingen 2005; Dobinski 2011).

In figure 1 different shadings of purple from light to dark show the extent of isolated, sporadic, discontinuous and continuous permafrost on the northern hemisphere. Permafrost covered areas make up to 23 million km², from which the biggest parts are in Siberia, Alaska, northern Canada and the Tibetan plateau (National Snow and Ice Data Center 2019). In addition to permafrost in the Arctic area, there is also a certain amount of alpine permafrost under specific conditions in high alpine regions.



Figure 1: Distribution of permafrost on the northern hemisphere (National Snow and Ice Data Center 2019)

Arctic permafrost is often found in tundra landscapes, a mostly treeless terrain, with a continuous cover of vegetation (van Everdingen 2005). In high latitudes tundra landscapes, thermokarst is a widely spread process, which can shape big areas very characteristically. The process hereby is the thawing of ice- rich permafrost or the melting of ground ice, which often causes thaw settlement. Thermokarst landscapes or terrains are characteristically shaped by thermokarst lakes, thermokarst mounds, gullies, thaw slumps and drained thermokarst lake

basins (DTLBs). Another name for DTLBs is the term **Alas**. Not included in thermokarst processes is the annual thawing of the active layer. The thawing of ice can be caused naturally by a warming climate, but also a human caused disturbance of the thermal regime of the ground (van Everdingen 2005).

Although **ground ice** refers to all kinds of ice in frozen ground, **excess ice** is specified as ‘the volume of ice in the ground, which exceeds the total pore volume that the ground would have under natural frozen conditions’ (van Everdingen 2005; Grosse et al. 2013). Excess ice is exceeding the soil porosity, creating an oversaturated soil, and can build ice wedges, ice lenses and ice veins. Excess ice is not including ice found in pores and its content is usually given on a volumetric basis. Soil containing excess ice can settle, when thawing, under its own weight until it reaches a stable state. Ice wedges cause the ground to expand vertically, whilst ice lenses are spread more horizontally (van Everdingen 2005; Bockheim/Hinkel 2012; Lee et al. 2014). Permafrost grounds can have a very different amount of ice, depending on the soil type, the amount of sediments, bedrock and organic material. One type of ice-rich permafrost is the Siberian Yedoma, containing up to 70 % or more ice of the volume in the uppermost 30 meters. Not just these big amounts, but also smaller amounts of ice will cause a subsidence when thawing (Grosse et al. 2010).

Thermokarst lakes usually fill basins formed by thaw settlement of the ground caused by melting of ice-rich permafrost and ground ice. The lakes can vary in size from 0.5 to < 100 km² in their area and between less than a meter to up to about 20 m in depth. Typically, lakes form in areas with an ice content of 30 % by volume or more. It is possible that those mostly shallow lakes expand toward a certain direction and form so called **oriented lakes**. These are characterized by a common orientation. In Barrow, northern Alaska, most lakes are elliptical with an N - W orientation, whereas in northern Siberia there are oriented triangular shaped lakes. On Baffin Island, Canada there are nearly perfectly round shaped lakes. About 25 to 40 % of the Arctic lowland landscapes, Alaska, Siberia and Canada, are covered by thermokarst lakes. Especially in the Arctic Coastal Plain of northern Alaska (ACP) where most lakes are shallow, the energy balance and the stability of the permafrost gets strongly influenced by the thickness of the lake ice (van Everdingen 2005; Arp et al. 2012; Grosse et al. 2013).

Underneath a thermokarst lake there is usually a layer of unfrozen ground, a so called **Talik**. It forms due to local anomalies in thermal, hydrological, hydrogeological, or hydrochemical conditions. The lake and Talik can expand due to unstable permafrost conditions on the lake shores in its width, but also due to temperature anomalies in its depth, like a change in the active layer (van Everdingen 2005; Larsen/Fondahl 2016).

The bigger thermokarst lakes become, the more likely a drainage can occur and **Drained Thermokarst Lake Basins (DTLBs)** develop. Such drainage events occur at different frequencies and can take place over a long period of time or in a short and sudden event. Most cases are triggered by an ice-wedge erosion, but a headward stream erosion, tapping, bank overflow, or coastal erosion can also be possible causes, as well as human impacts, like traffic, mining or construction work. Lakes do not always drain completely, but partially, which leads to residual ponds within the basins. The draining can take place subterrestrial, e.g. through an opening in the Talik, or superficial (Hinkel et al. 2003; van Everdingen 2005; Hinkel et al. 2007). After a lake is drained, the volume of the ground ice usually increases rapidly due to

new aggradation of permafrost in the unfrozen basin sediments (Bockheim/Hinkel 2012). An example of a tundra landscape with oriented thermokarst lakes and DTLBs of the research area of Barrow is shown in figure 2. The two red outlined DTLBs are part of the dataset of Barrow.

Barrow



Figure 2: Aerial Picture (ESRI World Imagery) of Thermokarst lakes and DTLBs in the research area of Barrow.

A concept of the **Thermokarst Lake Drainage Cycle** was established in the 1950s to describe the cycle of appearing and draining of the lakes as best as possible. One cycle must consist of two or more of the following sequences:

- A thermokarst lake develops in ice-rich permafrost.
- The lake grows, a drainage of the lake happens.
- New permafrost forms in the drained basin, including the formation of new ground ice.
- Due to increasing ice volume of the ground, the basin surface inflates to approximately almost the old surface height.
- The new ground ice, like ice wedges and ice lenses, starts degrading.

From this point the cycle repeats itself again. The age of the lake and the drainage event time can vary significantly. Due to the lack of proof of a rapid regrowth of ground ice formation, the inflation of the ground to the first lake height is an uncertain assumption and therefore often questioned. Furthermore, this cycle is based on the thermokarst lake areas of Northern Alaska and it is not yet proven if this concept is applicable to other regions (Hinkel et al. 2003; Bockheim/Hinkel 2012; Grosse et al. 2013).

1.4. Project at Alfred-Wegener-Institute

The Alfred-Wegener-Institute for Polar and Marine Science (AWI) is a Research Institute belonging to the German Helmholtz Association. The Permafrost Research Unit is based in Potsdam, whereas the AWI headquarters are in Bremerhaven, Germany.

The Permafrost section has two main focuses: One topic is “the observation and quantification of current periglacial processes and environmental changes and their causes in order to assess the modern state of permafrost and its future transformation”, whereas the second topic is about “the reconstruction of periglacial landscape dynamics of the last 200,000 years, delivering important information on the temporal variability of environmental and climatic change, ecosystem dynamics, and the carbon cycle“. Location wise the focuses are mainly on Alaska and Siberia, but also Canada and Svalbard (AWI 2019).

Within the Permafrost research unit, there is the PermaRisk junior research group under the leadership of Dr. Moritz Langer with the focus on “Simulating erosion processes in a permafrost landscape under a warming climate - a risk assessment for ecosystems and infrastructure“. The work for this thesis was done within this group (AWI PermaRisk 2019).

Three main research questions have been set up by the PermaRisk group to get a better understanding of permafrost erosion and mass wasting processes:

- How will a warming climate affect the intensity of erosion and mass movement process within permafrost landscapes?
- How will erosion affect landscape characteristics, human infrastructure, and essential ecosystem functions such as the energy, water, and nutrient balance within the Arctic?
- Do erosion processes and the associated changes in landscape characteristics introduce positive and/or negative feedbacks to permafrost degradation?

Therefore, the land surface model CryoGrid3, initially developed by the AWI in cooperation with the University of Oslo, will be extended and improved. The model will include certain features for snow cover and surface subsidence as well as a model to simulate the evolution of thermokarst lakes in addition to the full surface energy balance scheme. With the output of the model, the risk assessment should be more precise and the prevention of damage of infrastructure in the Arctic can be established faster and more comprehensively. In general, a more detailed and more precise simulation of permafrost environments in a warming climate under different scenarios will be processed. The three focus areas of the PermaRisk group are Deadhorse/Prudhoe Bay, Alaska; Churchill, Canada; and the Lena Delta, Siberia (AWI 2019; AWI PermaRisk 2019).

1.5. Aim of the Thesis

A future improvement on the understanding of thermokarst lakes in Arctic permafrost and the content of excess ice in tundra landscapes is necessary to gain more information on the landscape features and their spatial distribution. Therefore, the aim of the thesis is to investigate and calculate excess ground ice based on remote sensing data. The knowledge is essential for all processes in the permafrost landscape, for the thermokarst lake drainage circle, and for man-made infrastructure in these areas. A benefit of remote sensing based methods is that they are cost efficient by using existing data and field investigations are not particularly needed once the methods are proofed with field data of different investigation sites.

A new method is tested in this study by only using remote sensing data to obtain information on the excess ice content in Arctic tundra landscapes. The research question is:

Is it possible to make a rough estimate of the excess ice content of permafrost ground in Arctic tundra landscapes by a statistical analysis of drained thermokarst lake basins of a digital elevation model (DEM)?

For this task a comparison of drained thermokarst lake basins at two research sites close to the town of Barrow and on the northern Seward peninsula, both in Alaska, U. S., was done. As main data source, the open source Arctic DEM is used.

2. Study region

Both research areas of this study are located in Alaska in the United States of America north of 66° N. The Seward Peninsula (fig. 3, purple) is at the west coast at the Bering Sea, whereas the city of Barrow and the surrounding research area (fig. 3, red) are on the Outer Coastal Plain (OCP) on the north coast. The map is giving a spatial overview on position of the research sites within Alaska and the neighboring countries, Canada in the east and Russia in the west, with the Bering strait and sea in between. A very distinctive difference between the two research sites is that in Barrow are much more water filled lakes nowadays than on the northern Seward Peninsula.

Thermokarst lakes and Drained Thermokarst Lake Basins cover large areas of Alaska, but mostly on the Arctic Coastal Plain (ACP), the Arctic Foothills and the Seward Peninsula (Hinkel et al. 2012). The number of lakes and lake basins is decreasing from the coastal areas towards the interior. More and also larger lakes are found in the outer coastal plain (OCP) than in the Inner Coastal Plain (ICP). About 20 % of the ACP is covered by lakes and 26 % with drained thermokarst lake basins based on an analysis of satellite data (Hinkel et al. 2012). The lakes have formed a very dynamic landscape due to the lake drainage cycle. The accumulation of soil organic carbon in form of peat within the lakes makes these areas important for the high-latitude carbon cycle (Hinkel et al. 2012; Regmi et al. 2012).

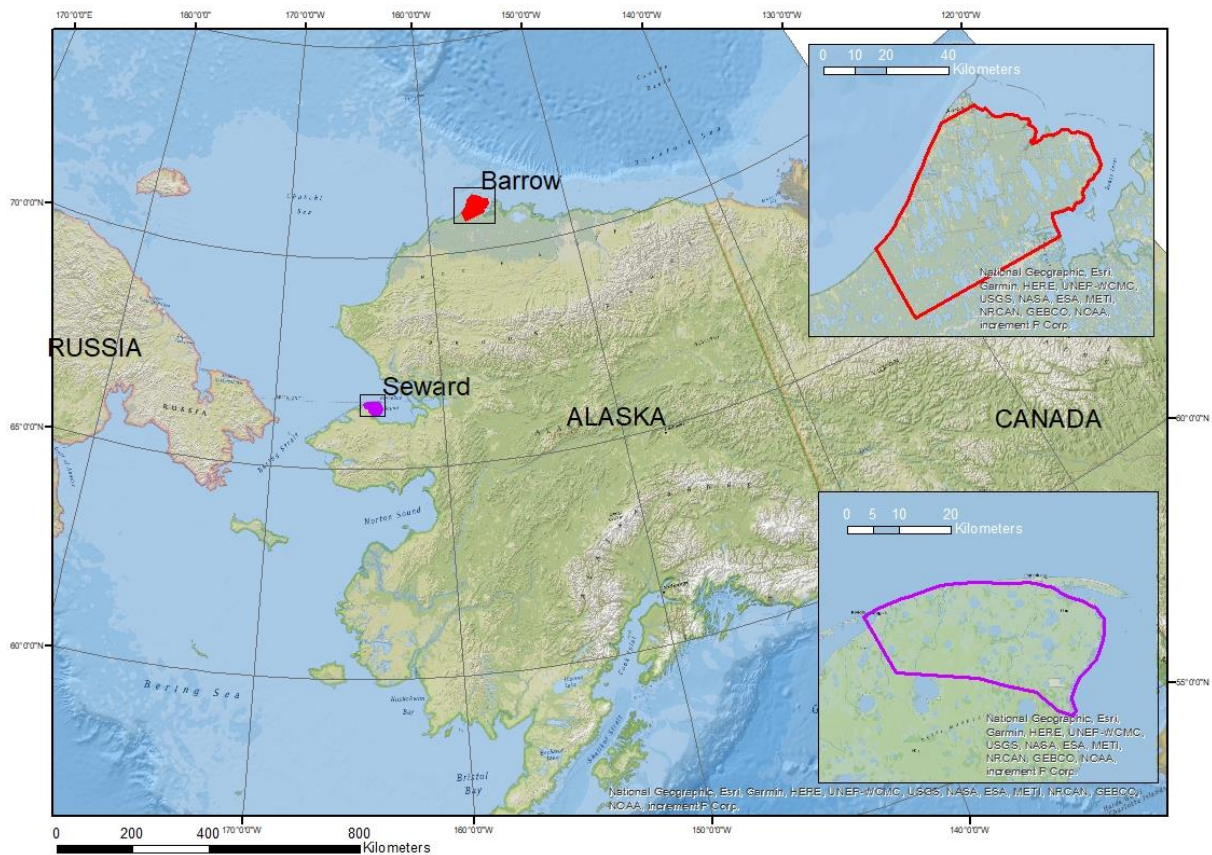


Figure 3: Overview map (ESRI Nat. Geographic) of the research areas in Alaska. Barrow in the north is marked in red, Seward in the west in purple.

2.1. Barrow Peninsula

The city of Barrow (fig. 4, red dot) is located at the west side of the peninsula on the north coast of Alaska on the Outer Coastal Plain north of the Inaru river, which flows into the Admiralty bay. The research site is located south of the city of Barrow at $71^{\circ} 18' N$ and $156^{\circ} 46' W$, with a total area of about 2700 km². The altitude of the area ranges from -10 to 23 m a.s.l. according to the Arctic DEM. Characteristic of the area are the elongated lakes, mostly oriented in a nearly N-S direction, as well as a high density of lakes and drained thermokarst lake basins, which formed in ice-rich silty deposits. Polygonal tundra covers approximately 65 % of the area (Hinkel et al. 2003). The elliptical shape of the lakes was documented for the first time in 1962 by Carson et al. (Carson/Hussey 1962). A hypothesis on how the oriented lakes have formed is through a certain prevailing wind direction, but it is still not completely proven and controversially discussed (Grosse et al. 2013).

A total of 1600 km² of the Barrow region is covered by 592 lakes (> 1 ha), which makes up 22 % of the surface. In addition, 558 Drained Thermokarst Lake Basins cover about 50 % of the surface (Hinkel et al. 2003). Their altitude against sea level varies between -3.01 m and 16.66 m and their size between 0.63 and 11.95 km².

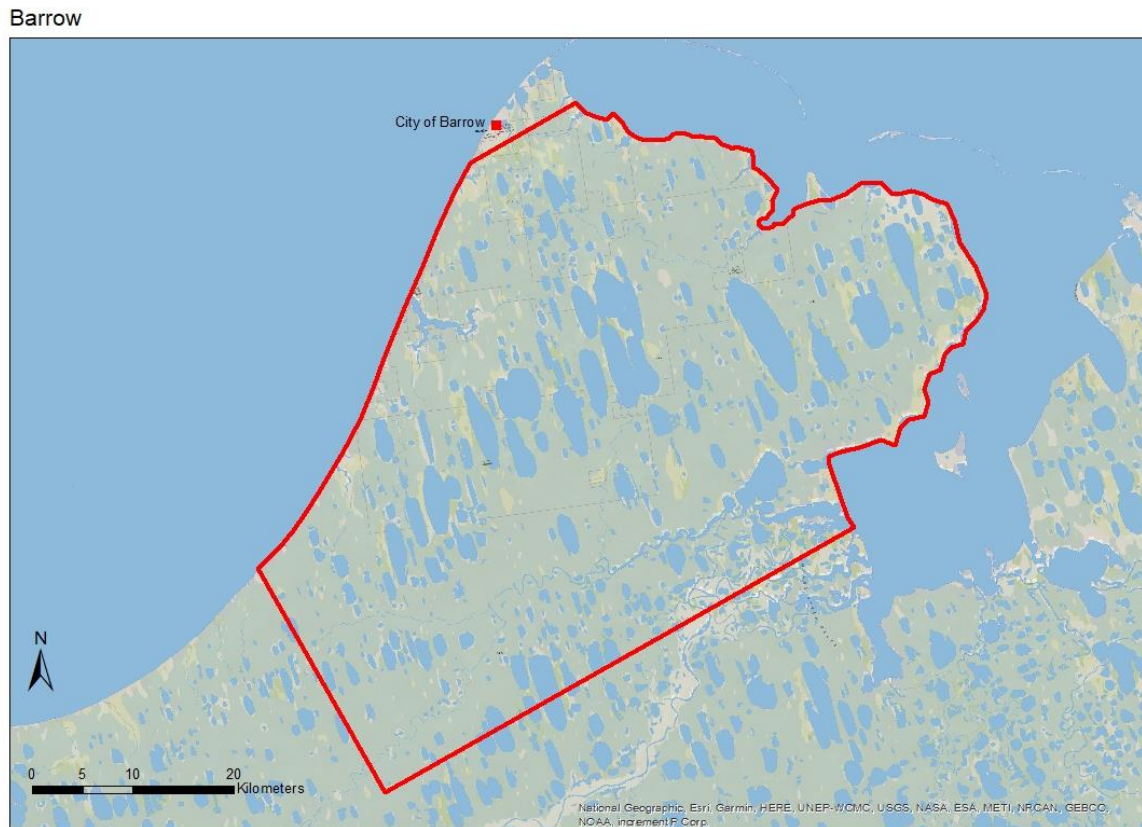


Figure 4: Map of Barrow on ESRI Nat. Geographic basemap

The ground around Barrow can be described as unconsolidated sediments in the Late Pleistocene Gubik formation, which are very frost- susceptible. Sediments in form of marine silts can be frequently found in the area. The soils of Barrow can be categorized into Turbels, Orthels and Histels (Bockheim et al. 1999; Bockheim/Hinkel 2012). Continuous permafrost is as deep as 400 m with an active layer thickness of about 30 to 90 cm. By analyzing soil cores, it was found out that pore ice and ice lenses/ veins, cover up to 50 to 75 % of the volume of the uppermost 2 m of the ground around Barrow (Bockheim/Hinkel 2005). Additionally, ice wedges contain another 10 to 20 % of ice volume. A total of 80 % of excess ice content in the uppermost 10 m is mentioned by Bockheim/Hinkel (2012). Due to the high ice content of the ground, the area has a high number of large and deep (> 2 m) lakes, which drain in various frequencies. Most lakes can be characterized with a talik beneath the lake bed before the draining occurs. From 1949 to 2012, a minimum of 7 out of 9 partial – or total – drainage events of lakes are suspected to be caused by human activity on the barrow peninsula. An estimated number of 50 lakes drained between 1975 to 2000 (Bockheim/Hinkel 2012; Hinkel et al. 2003; Hinkel et al. 2007). Drained thermokarst lake basins are dated back to 0 to 5.5 kya BP according to Grosse et al. (2013) and 3500 BP according to Hinkel et al. (2003).

An overview on the amount of Lakes in comparison to drained lake basins is given in figure 5 (Frohn et al. 2005). Various age stages of drained basins are shown in figure 6 from young (a), medium (b), old (c) to ancient (d).

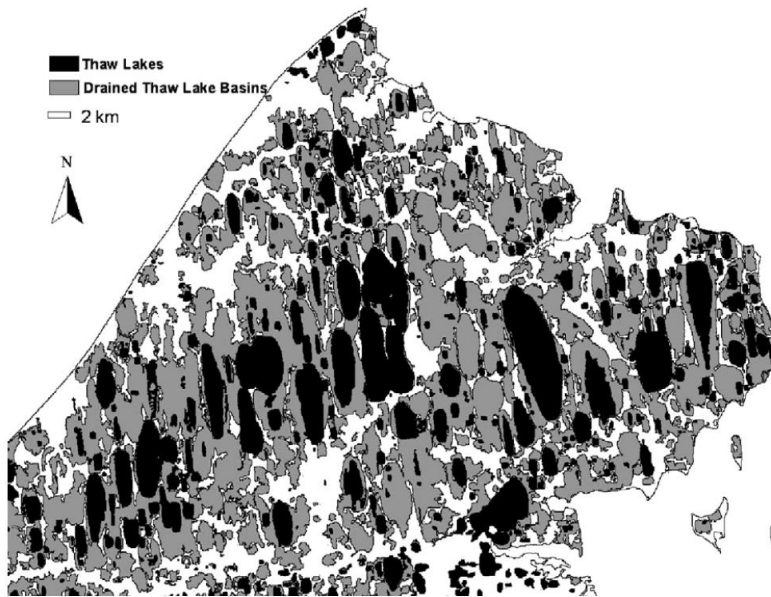


Figure 5: Thermokarst lakes and DTLBs Barrow Peninsula (Frohn et al. 2005)

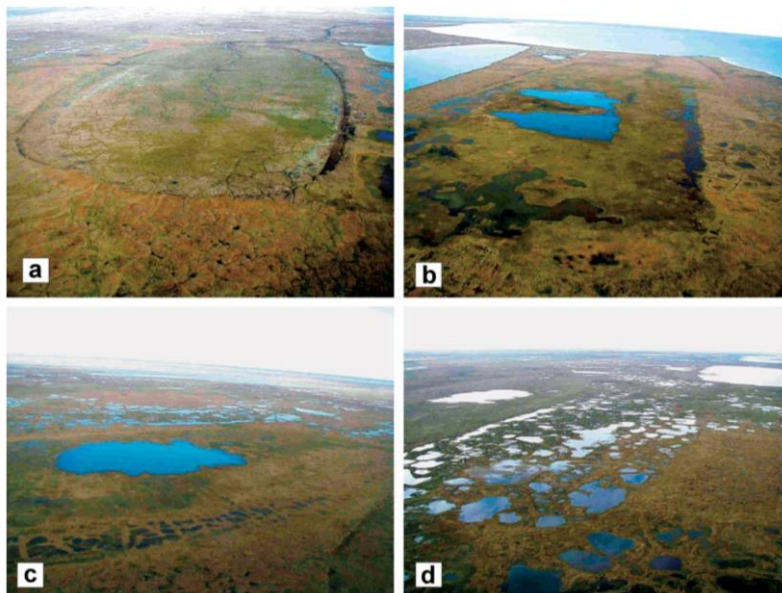


Figure 6: Lakes Barrow Peninsula; Barrow DTLBs (Hinkel et al. 2003)

The climate of the Barrow Peninsula can be characterized as a cold maritime climate. After Köppen-Geiger it is categorized as an ET Tundra climate. With a mean annual air temperature of $-12.0\text{ }^{\circ}\text{C}$, the mean temperature of July is the warmest with $4.7\text{ }^{\circ}\text{C}$, whereas February is the coldest with a mean of $-26.6\text{ }^{\circ}\text{C}$. The mean annual precipitation amounts to 106 mm. Most precipitation, 63 %, occurs as rain between July and September. The annual snowpack average is between 20 to 40 cm, whereas snow drifting creates very variable heights (Hinkel et al. 2003; Bockheim/Hinkel 2012).

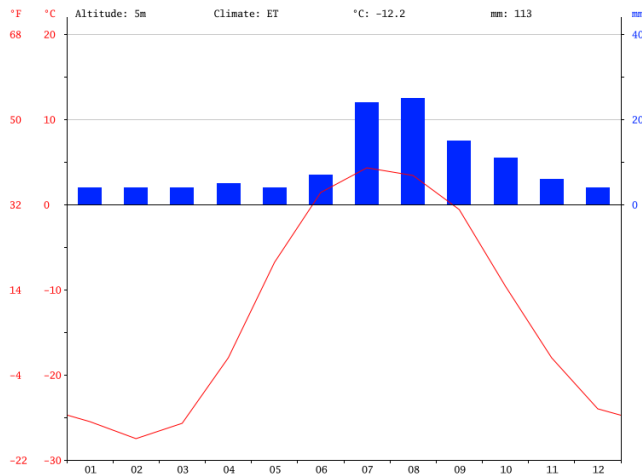


Figure 7: Climate graph of the city of Barrow (Climate Data 2019a)

Vegetation is established in drained or partially drained basins. Vegetation communities succeed one another as edaphic conditions change, and surface organic material accumulates above lacustrine sediments. Ground heave, polygon development, and slope processes combine to slowly obliterate the basin, and it eventually appears as wet sedge meadow tundra characterized by *Carex aquatilis* Wahlenb., tall cottongrass (*Eriophorum angustifolium* var. *triste* Honckeny), white cottongrass (*E. Scheuchzeri* Hoppe), and Fisher's tundra grass (*Dupontia fisheri* R. Br.). Because thaw-lake basins often develop in older basins, nested patterns form a palimpsest that dominates the landscape (Hinkel et al. 2003).

2.2. Northern Seward Peninsula

The research site of the northern Seward Peninsula is located in northwestern Alaska, USA, with the northernmost tip of the peninsula at Cape Espenberg at 66° 33' N 163° 37' W, merging into the Chukchi Sea in the North. During the Last Glacial Maximum (LGM) the whole Peninsula was unglaciated, nowadays it is a zone of continuous permafrost. The peninsula is one of the major lake districts in Alaska, with more than 70 % of the landscape influenced by thermokarst lakes or the remaining drained lake basins. It can be clearly seen that thermokarst processes are actively reworking and forming the landscape. Whereas the whole peninsula of more than 6000 km² is covered by around 7 % of extant lakes, the research area of this study covers only about 780 km² of the northernmost part. The altitude of the site differs from about -41 m to 431 m a.s.l. (Jones et al. 2011; Jones et al. 2012). The lakes and DTLBs on Seward peninsula are mostly almost round and not oriented. Within the basins some pingos have formed with heights of up to 15 m as well as small streams and thermoerosion gullies. So far, there is no known frequency of the lake drainage cycle for the Seward peninsula. Since 1950, about 60 lakes have drained, of which details were investigated in situ (Regmi et al. 2012).

Seward Peninsula



Figure 8: Map of the northern Seward Peninsula (ESRI Nat. Geographic)

On the Seward peninsula, mostly silt and loam textures are found together with loess deposits, which are typical for an aeolian transportation. Also, peat and lacustrine silt deposits are typical for the thermokarst lake basin deposits of the region. And due to the yedoma-like late-Pleistocene permafrost deposits the sediments are mainly very ice-rich, including ice lenses and ice wedges as segregated ground ice. Prevailing soil types include gelsols, historthels, aquiturbels, aquorthels, fibristels, and hemistels, based on the Bering Land Bridge National Preserve soil map (Jones et al. 2011; Jones et al. 2012).

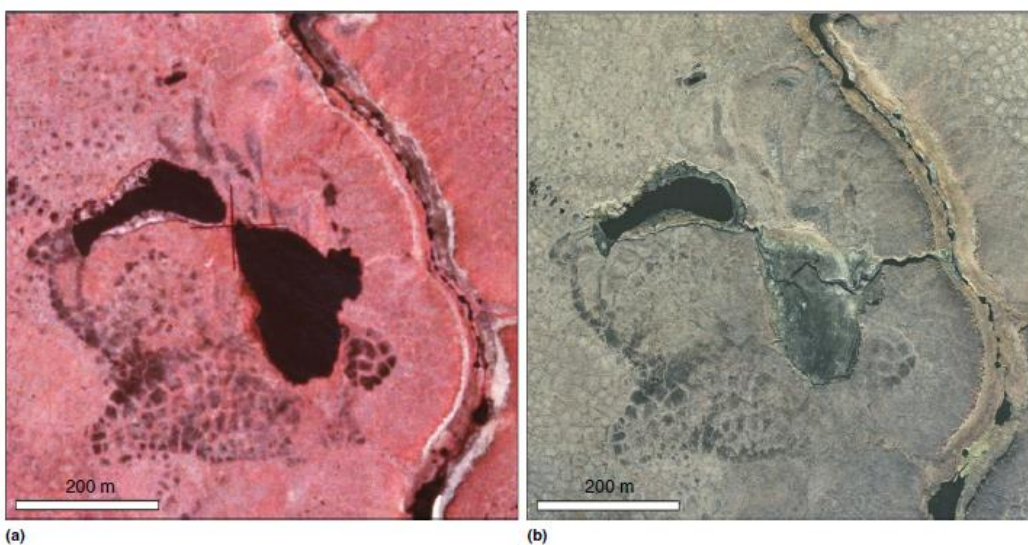


Figure 9: Aerial image of a thermokarst lake before (a, 1978) and after drainage (b, 2003) on the northern Seward peninsula (Grosse et al. 2013)

The aerial pictures from 1978 (fig. 9 a) and 2003 (fig. 9 b) show the lake drainage of a rather small thermokarst lake in the north of the Seward peninsula, compared by Grosse et al. (2013). From the first to the second image, the right lake is completely drained and the top left one also partially drained. The drainage event happened by the deepening of the shown channel in the east of the lakes towards the river. Due to the big size of the channel, it is presumed that it was a catastrophic and sudden drainage event (Grosse et al. 2013).

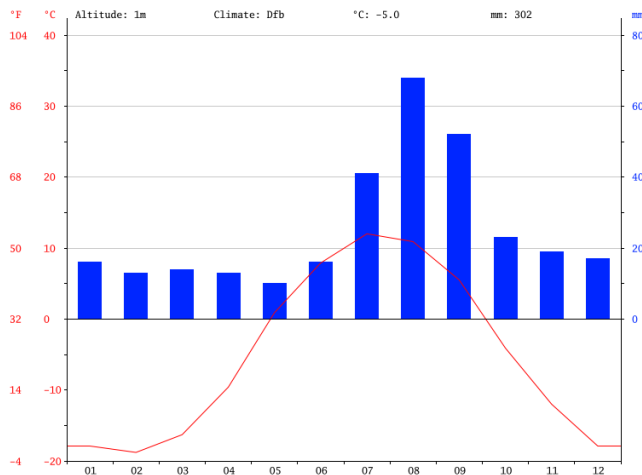


Figure 10: Climate Graph of Deering (Climate Data 2019b)

Figure 10 shows the climate graph of Deering, a town about 80 km southeast of the northernmost point of the Seward Peninsula. The climate of the Seward Peninsula can be denominated as Dfc (subarctic) climate after Köppen- Geiger, rather than the categorizing as Dfb (hemiboreal) climate for Deering on the mainland. For the period of 1971 to 2000, the mean annual air temperature of the region is $-6.1\text{ }^{\circ}\text{C}$ with a mean annual precipitation 255 mm of precipitation, from which $\sim 130\text{ mm}$ were registered as rain between July and September. All climate data is recorded in Kotzebue, about 60 km northeast of the site, but with a similar coastal position (Jones et al. 2011; Regmi et al. 2012). The mean annual ground temperature is at $-3\text{ }^{\circ}\text{C}$ according to Jones et al. (2011).

The site of the northern Seward Peninsula is classified as Bering Tundra with tundra- type vegetation (Jones et al. 2011). Productive grasses, like *Calamagrostis canadensis* and *Dupontia fisherii*, are dominant in very young drained basins as well as the sedge *Carex aquatilis*. Based on the age of a basins the vegetation changes to less productive plant communities, which can include *Carex bigelowii*, *Eriophorum angustifolium* and *Sphagnum* sp. tundra with *Betula nana*, *Salix* sp. and prostrate ericaceous shrubs. Whereas on the oldest DTLBs with the dry surfaces, which are developed from the heave of reforming of ground ice and the existence of ice wedge polygon ridges, might only grow abundant lichen (Jones et al. 2011; Regmi et al. 2012).

3. Methodology

The main data set of this study is the Arctic DEM, next to digitalized DTLBs, Landsat and ESRI World Imagery data. The work processes include parts in ArcGIS and R.

3.1. Data

3.1.1. Arctic DEM

The Arctic Digital Elevation Model (DEM) is the most important data of this work. It is provided as open source data by the National Geospatial- Intelligence Agency (NGA) and National Science Foundation (NSF) of the USA.

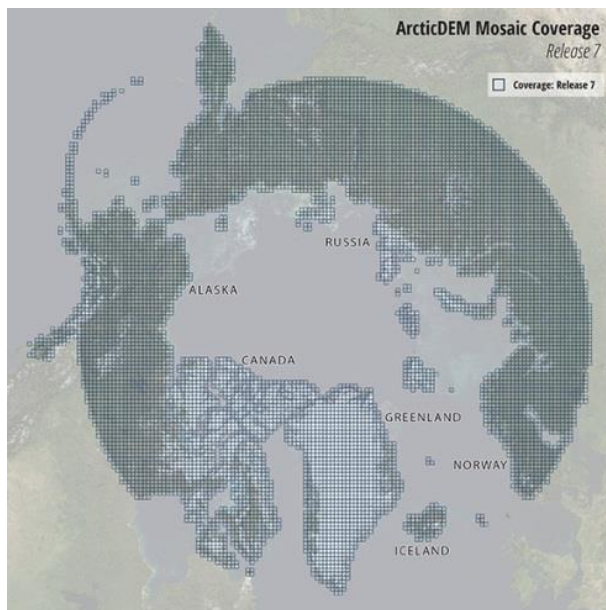


Figure 11: Coverage of the Arctic DEM release 7 (Polar Geospatial Centre 2018)

There are stereoscopic images available of the digitalGlobe satellites Worldview 1, 2 and 3 as well as from the GeoEye-1 satellite available for all land areas north of 60° northern latitude, including Greenland and the Kamchatka peninsula. The data is processed by the “Surface Extraction from TIN- based Search- space Minimization” (SETSM) software at Ohio State University into a 2- meter elevation model in the Polar stereographic projection referenced to the WGS84 ellipsoid. In September 2018 there was the seventh data release of the Arctic DEM. The latest update includes an overall resolution improvement from 5 to 2 m post-processing. Whereas there are files in strip form with measurements of 16 to 18 km width and 110 to 120 km length available, in

this study mosaic tiles of 50 x 50 km squares were used. There are a total of 2,488 tiles available with 9,228 sub- tiles covering an area of 23,070,000 km². The bigger mosaic images are merged together from multiple mostly smaller strip files of different years and seasons, while the strip files are from one exact date (Polar Geospatial Centre 2018). The vertical resolution of the Arctic DEM is very high with a 10 cm accuracy (Candela et al. 2017). For downloading the Arctic DEM “The ArcticDEM Index and Download web viewer” was used by selecting the correct tile. The datasets used for this work are listed in table 1 (ESRI 2019a).

Table 1: Arctic DEM data

Research site	Arctic DEM data sets
Barrow	48_21_2_1_2m_v3.0_reg_dem.tif 48_21_2_2_2m_v3.0_reg_dem.tif
Seward	53_18_1_1_2m_v3.0_reg_dem.tif 53_18_1_2_2m_v3.0_reg_dem.tif 53_18_2_1_2m_v3.0_reg_dem.tif 53_18_2_2_2m_v3.0_reg_dem.tif

3.1.2. Landsat Data

Landsat Images were used to digitalize the DTLBs of Barrow in combination with the ESRI World imagery. Landsat images (Landsat- 8 Data) for Barrow and Seward Peninsula were downloaded at the EO Browser and included Bands 2, 3, 4 in order to get an RGB image. The bandwidth of the three bands are the following: Band 2 with a bandwidth of 0.450 - 0.515 μm , Band 3 with a bandwidth of 0.525 - 0.600 μm and Band 4 with a bandwidth of 0.630 - 0.680 μm . The resolution of all bands is of 30 m/ px. The data includes several different dates at each site, but always in July or August to have the least snow cover (Sinergize 2019).

3.1.3. World Imagery in ArcGIS

The World Imagery by ESRI was last updated in September 2018. It has a worldwide resolution of 1 m aerial or satellite images available for ArcGIS online map or ArcGIS Desktop. By a combination of TerraColor 15 m and SPOT 2.5 m imagery for most of the world and DigitalGlobe data for the United States and Western Europe is available. For the US, including the Alaskan World Imagery Data, a resolution of 1 m or better is the minimal standard. Whereas in some parts of the world the accuracy is as detailed as 0.03 m (ESRI 2019b).

For Alaska, the coverage is made with aerial images (SOA DCRA Profile Imagery), which are contributed by the Alaska DCCED DCRA (Department of Commerce, Community, and Economic Development - Division of Community and Regional Affairs). For Alaskan communities all data is from 2013 and 2014. The resolution for the Barrow area is between 0.15 to 0.6 m. For the area of the Seward Peninsula, the resolution is not exactly known due to the fact, that it is not listed as a certain area of Alaskan communities in the list of contributors of the World Imagery. But the minimum standard of 1 m resolution is given for whole Alaska (Stewart 2018; ESRI 2019b).

The World Imagery by ESRI has always been used as a base map in ArcGIS Desktop.

3.1.4. DTLB Data

For the research site of **Barrow**, a dataset of 20 manually digitalized DTLBs was created with the help of Landsat RGB aerial pictures and ESRI World Imagery data. The outlines of the DTLBs were saved as a shapefile, numbered sequentially per basin and including the size of each. In the map below (fig. 12), the 20 basins (red), each with its number, can be identified. The basins vary between 0.63 and 11.95 km² in size in a total area of 2700 km². The buffer zones of 100 m for each basin are shown in thin blue shadings. The elevation of basins and buffer are always given in meters above sea level.

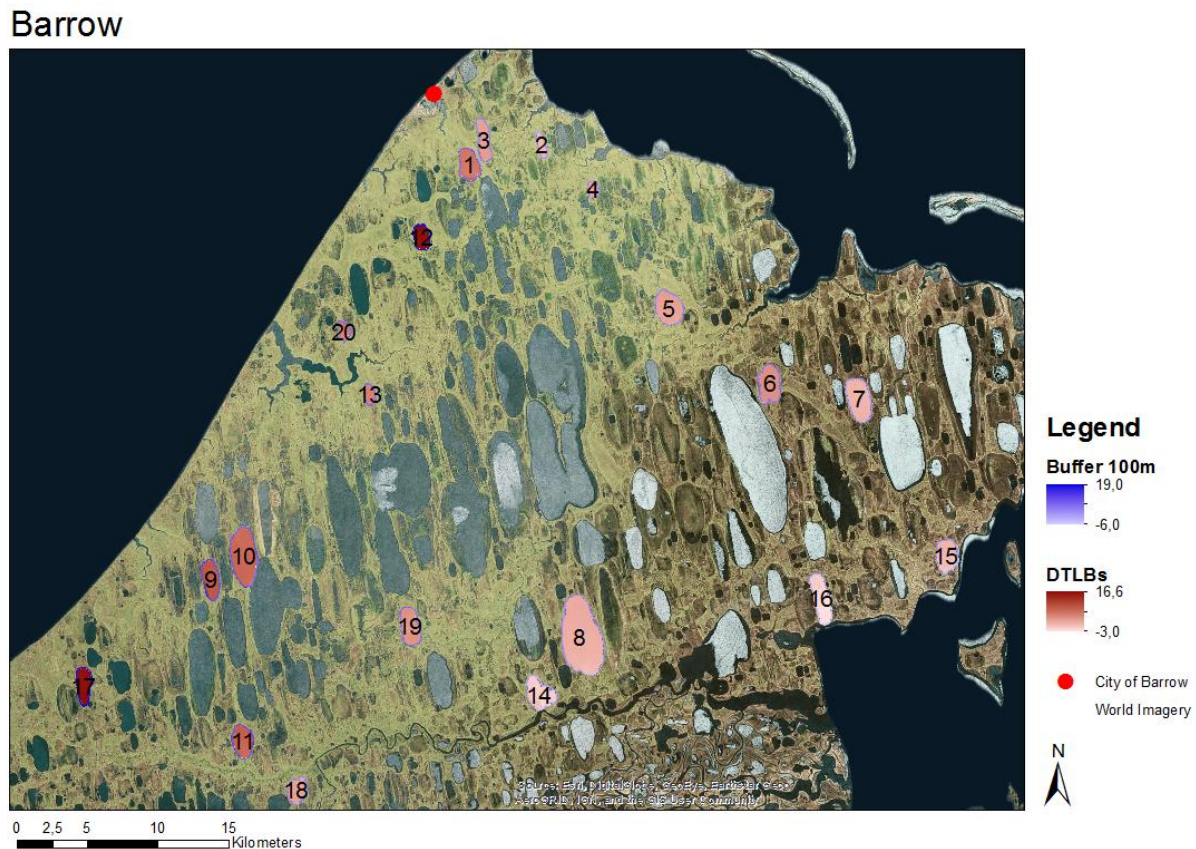


Figure 12: DTLBs of Barrow research area on ESRI World Imagery

For the research site of the **Seward Peninsula**, an existing dataset of a former project by Jones et al. (2011) was used, which contains a total of 466 Drained Thermokarst Lake Basins in six age classes. The age and count per class are shown in table 1. It differs from only 9 basins in age group 5 to 188 in group 3. The age classes are set logarithmically from 0 - 50 years, 50 - 500 years, 500 - 2000 years, 2000 - 5000 years up to > 5000 years and an unknown age class (Jones et al. 2011). The outlines of all basins of the dataset on a World Imagery map can be seen in figure 13. The mapped basins are very concentrated on the north of the Peninsula in a total area of 780 km². Here the DTLBs vary in size between 0.03 and 4.83 km².

Table 2: DTLB data of Seward Peninsula after Jones et al. 2011

Age class	Age	Count
Age class 1	0 - 50 years, modern	20
Age class 2	50 - 500 years, young	140
Age class 3	500 - 2000 years, medium	188
Age class 4	2000 - 5000 years, old	82
Age class 5	> 5000 years, ancient	9
Age class 0	unknown	27

Seward

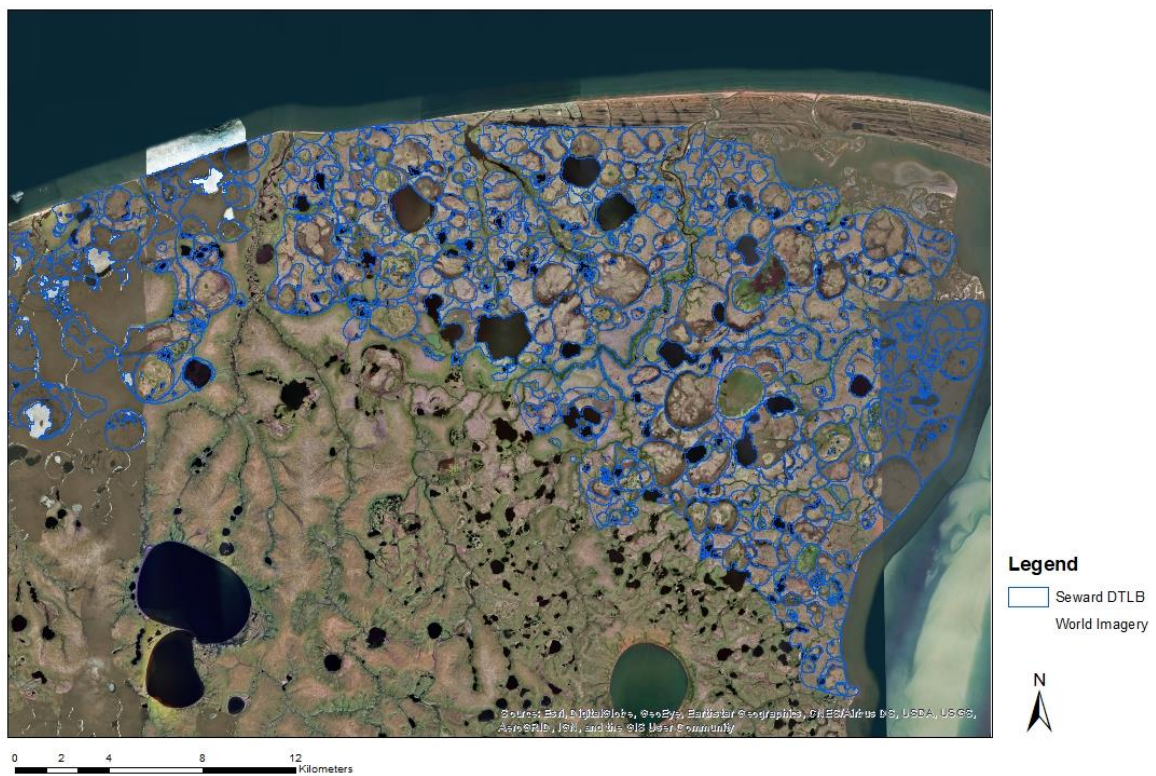


Figure 13: DTLBs of Seward Peninsula research area on ESRI World Imagery

3.2. Data Processing in ArcGIS

The Geographic Information System ArcGIS by ESRI and the open source software SAGA GIS were used to process the Arctic DEM and the DTLB shape files.

For each research area, two to four Arctic DEM Mosaics (each 50 x 50 km) were downloaded and merged together. The merged file was always clipped to the exact extend of the research area, mainly to get a smaller file for the later analysis in R. The 32- Bit floating- point pixel type and depth were kept preserving the accuracy of the elevation value.

Landsat RGB aerial pictures were used in GIS in addition to the ESRI World Imagery to digitalize the DTLBs for the Barrow side. For Seward, an existing shape file of DTLBs from another project was used (see 3.1.4.). Figure 14 shows how a characteristic basin and its surrounding buffer looks. Basin and buffer of DTLB 8 of the Barrow site are shown with other DTLBs close by, but not overlapping each other.

On the basis of the DTLB shape files, buffer areas around the drained lakes with a width of 100 m were created. In order to set a fitting radius size, buffer with radius widths of 50 m, 100 m and 150 m of the basin outline were sampled during the work. The results and interpretation of the different buffer sizes are discussed in chapter 4.1. Sensitivity Study.

At the end of the workflow in GIS three files were exported for the further work in R: a DEM raster of the desired research area, a DTLB shape file and the according buffer shape file.

Subsequently, the elevation data of the DTLBs and buffer was imported to ArcGIS again in order to create detailed maps for every research area. In addition, overview maps of the research sites on the base of World Imagery were generated.

Barrow

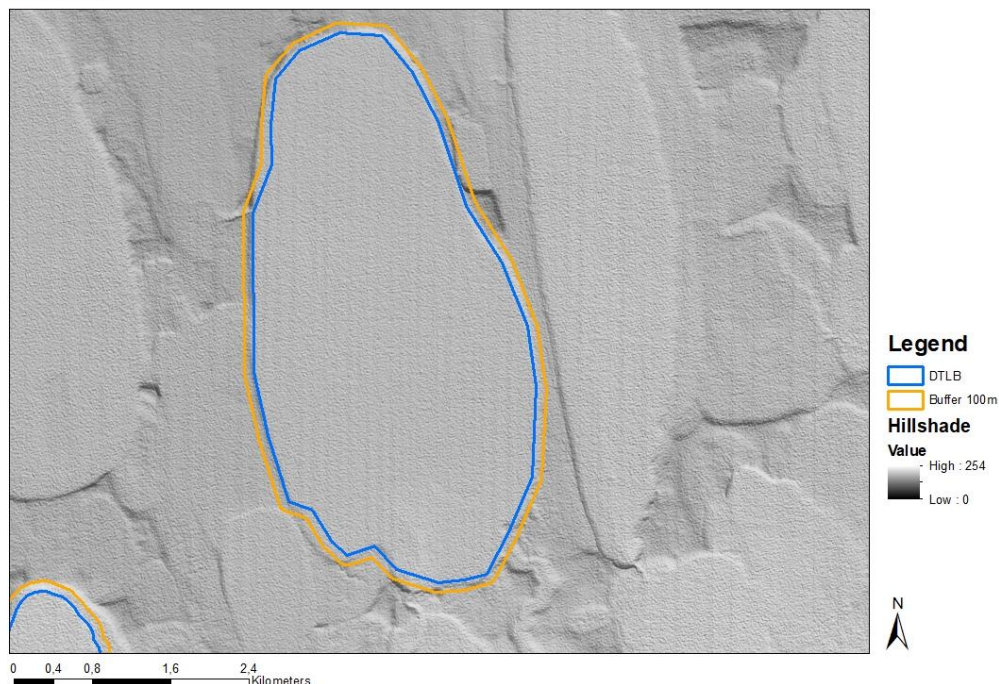


Figure 14: Outline of DTLB ID 8 at Barrow based on Hillshade of the Arctic DEM

3.3. Statistical Analysis in R

Three GIS exported files - DEM raster tif file, DTLB shape file, and the buffer shape file - comprise the basic data for further analysis in R.

For the two shape files, raster tif files with the according elevation data out of the Arctic DEM were produced. The main aim is to collect elevation data from each DTLB in comparison to the according buffer zone around it. The elevation values for each DTLB and buffer were extracted. With this data a table with all statistical information was created. The table contains the DTLB ID, DTLB size [m²], buffer size [m²], minimum, maximum, median, mean, and the differences of buffer - DTLB mean/ median/ max/ min (all in meter). These tables were created for Barrow and Seward, here separately per age class.

The Coefficient of Determination is calculated for various variables in R to see their relation to each other. The coefficient is calculated automatically with the `r.squared` function. The closer the result is to 0, the lower the relation, the higher to +1 or -1 the result is, the more the variables are related.

The elevation values of a DTLB and the according buffer were visualized by creating density and frequency plots. The density plots are more detailed, since no value bins are created as for the frequency plots. Within this step the elevation data of every DTLB and buffer got categorized in normal/ unimodal distributed, bimodal or multimodal distributed. This categorization will be discussed in chapter 5.1. Interpretation of Results.

Additionally, the DTLB and buffer raster layer with the elevation data were exported to create maps in ArcGIS.

4. Results

4.1. Sensitivity Study - Determination of the Buffer Size

For the analysis of the difference in altitude between the DTLB and the surrounding area, buffer zones were created, as mentioned in chapter 3. To determine the best fitting size of the buffer, tests with radii of 50, 100 and 150 m distances of XYZ to the outline of the DTLBs were done. In order to find the right size, the surrounding areas had to be analyzed on how close other structures next to the DTLB occur. Additionally, the area of the buffer should be smaller than the area of the DTLBs, but not too small in comparison to the biggest DTLBs. Nevertheless, not all buffers fit perfectly around the basins, but some overlap with other DTLBs, gullies, present day lakes or other landscape structures. The sensitivity study was only done for the Barrow research site. A table with DTLB and buffer areas for the various buffer radii, as well as their mean, median, maximum and minimum values can be found in the appendix 1.

The maps and histograms show that a buffer with a radius of 50 m is too small because it often lies still on the slope of the DTLB and does not reach the higher surroundings outside the slope. This problem can be seen in figure 15 and 16 with the light green 50 m buffer outline, which is the closest to the blue outline of the basin. The buffer mostly covering the slope can be detected best in the east of the basin. Generally, figure 15 and 16 are showing the same DTLB at the Barrow research site with the outlines of the DTLB outline in blue and buffer radius with 50 m in light green, 100 m in orange, 150 m in red on the base of a Hillshade of the 2 m Arctic DEM and World Imagery.

For the smallest DTLBs a 50 m buffer would be an acceptable size, but even for those ones, the problem of an unclear boarder of the slopes might occur. Whereas for bigger basins the 50 m buffer is also very small, regarding the area ratio between basin and buffer. So, depending on the total size of the DTLB, a 50 m radius of a buffer is covering a too small area in terms for an appropriate size of a zone to analyze later, and sometimes not even covering the correct area, regarding the slope of a basin.

On the other hand, the 150 m buffer radius around basins seems to be too big measured. Independently of the size of the DTLB itself, almost all buffers with a radius of 150 m are covering smaller or larger parts of other structures, which could falsify further analysis. These structures are mostly drainage channels, gullies, other drained basins or recent lakes. For the example of DTLB 14 in figures 15 and 16 in the south-east, in the south and in the north other basins are covered with the red outlined 150 m buffer.

Also, in figure 19, the coverage of another basin including a deeper drainage channel on the west side of the basin by the 150 m buffer can be seen. In the east of the basin the 150 m buffer zone intersects an area of polygonal tundra, which has various heights because of water filled structures and other geomorphological features. Therefore, the height of the surrounding of the DTLB includes these structures, which are affecting and falsifying the further interpretation of the result.

Barrow

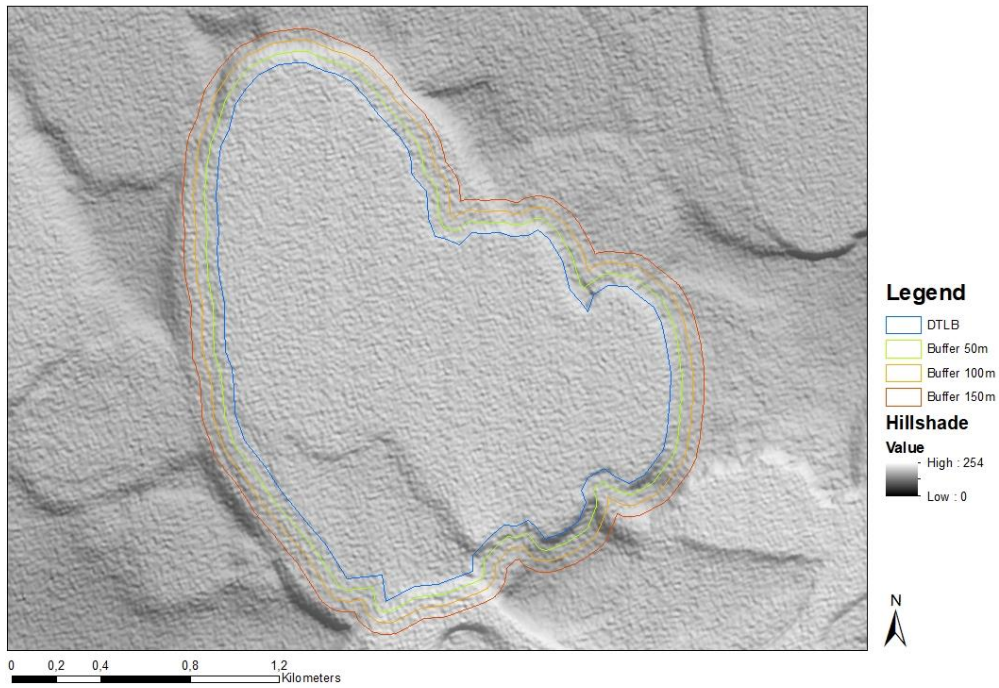


Figure 15: Hillshade of DTLB ID 14 at Barrow with the outlines of the DTLB and different radii of buffer

Barrow

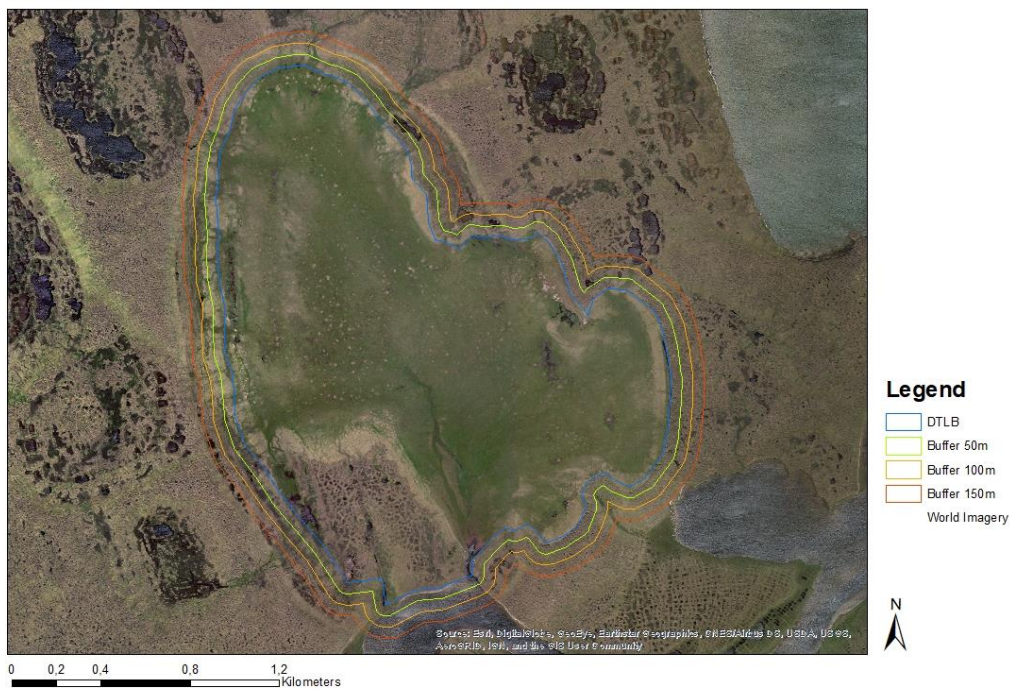


Figure 16: World Imagery of DTLB ID 14 at Barrow with the outlines of the DTLB and different buffer radii

Further on, the histograms of the heights of the basins and buffers show a similar outcome as the interpretation of the maps. Each histogram shows the frequency on the y- axis against the height in meter a.s.l. on the x- axis. Each set of histograms shows the different radii of 50, 100 and 150 m from left to right of one basin. The colors of the buffer radii are the same in the map as in the histograms with green for 50 m, orange for 100 m and red for 150 m.

The first set of histograms shows the DTLB 14 as the maps in figure 15 and 16 do. The histograms of DTLB 14 in figure 17 are showing heights between 0 to 2.5 m for the basin and buffer heights with a frequency between 0 and < 80,000. The average height of the DTLB is at 0.75 m a.s.l., which is the third lowest value of the Barrow research site. The height points of the 50 m buffer in green are so few that they have a low frequency and do not show a distinct peak of the height. The only notable detail is the slightly shifted height to the right side of the x-axis of the whole buffer in comparison to the DTLB in blue. The histogram of the 150 m buffer (red) is showing one big peak at ~1.1 m and one smaller peak at ~1.9 m. There is a broader range of buffer heights (in red), possibly caused by a big coverage of another structure. This can influence the variation in height tremendously and should be mentioned in comparison to the two smaller buffer radii. In this example, the greater variation in height of the 150 m buffer can be explained by other basins in the north and very south, which the buffer covers partially and by another neighboring basin with polygonal tundra in the south- east.

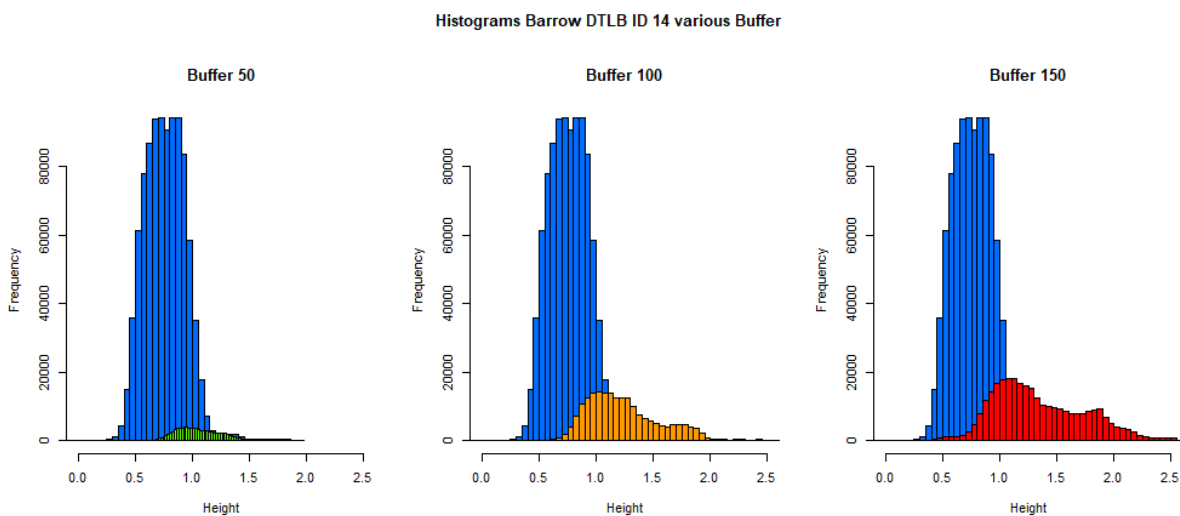


Figure 17: Histograms DTLB ID 14 buffer 50 m (green), 100 m (orange), 150 m (red)

Even though the frequency is much higher in figure 17, the density of the height variance is much higher at the DTLB ID 8 (fig. 18), which is the biggest DTLB of Barrow. The average height of DTLB ID 8 is 3.5 m, whereas the averages for the three buffers vary between 3.99 m for the 50 m buffer, 4.39 m for the 100 m buffer and 4.58 m for the 150 m buffer. Furthermore, the distribution of the height values of the 50 m buffer is shifted to the right compared to the values of the basin. The peaks, like the maxima mentioned, are equally shifted and the distribution of the buffer height is mostly between 3.5 m and 4.5 m, including a few spikes with a maximum at 5.0 m. In comparison to the 50 m buffer, the two bigger ones have a much larger distribution of up to more than 6.0 m.

For the 100 m buffer, the peak can still be seen at slightly less than 4.0 m, but for the 150 m buffer the height values are varying considerably between ~ 3.8 and ~ 4.8 m, without having a distinct peak. Hence, the most fitting buffer size has a 100 m radius. For DTLB 8, the values of radii 100 m have a big variance, but still have a peak and a shift to higher values than the DTLB itself.

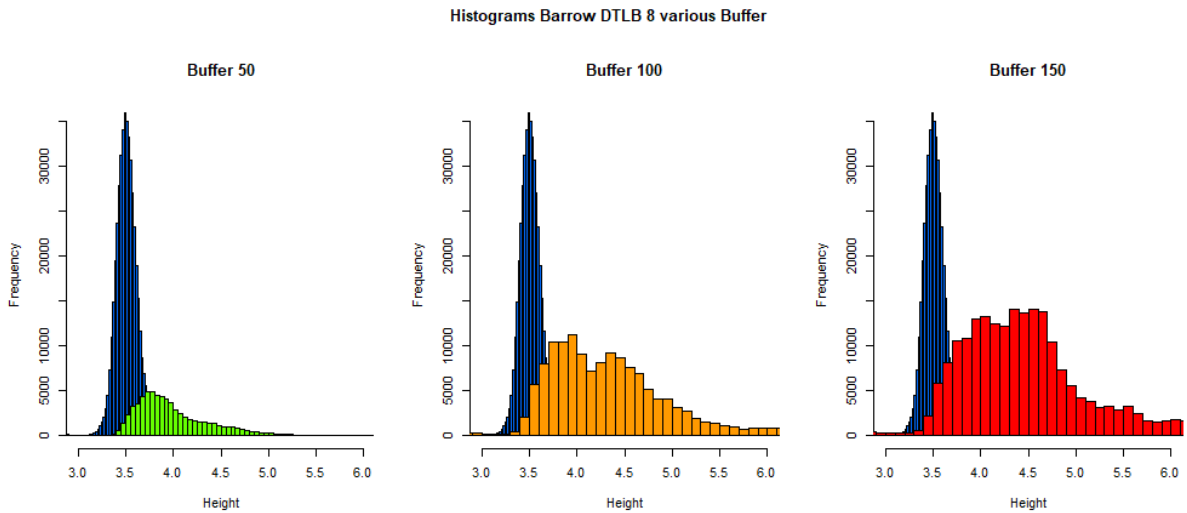


Figure 18: Histograms DTLB ID 8 buffer 50 m (green), 100 m (orange), 150 m (red)

Barrow

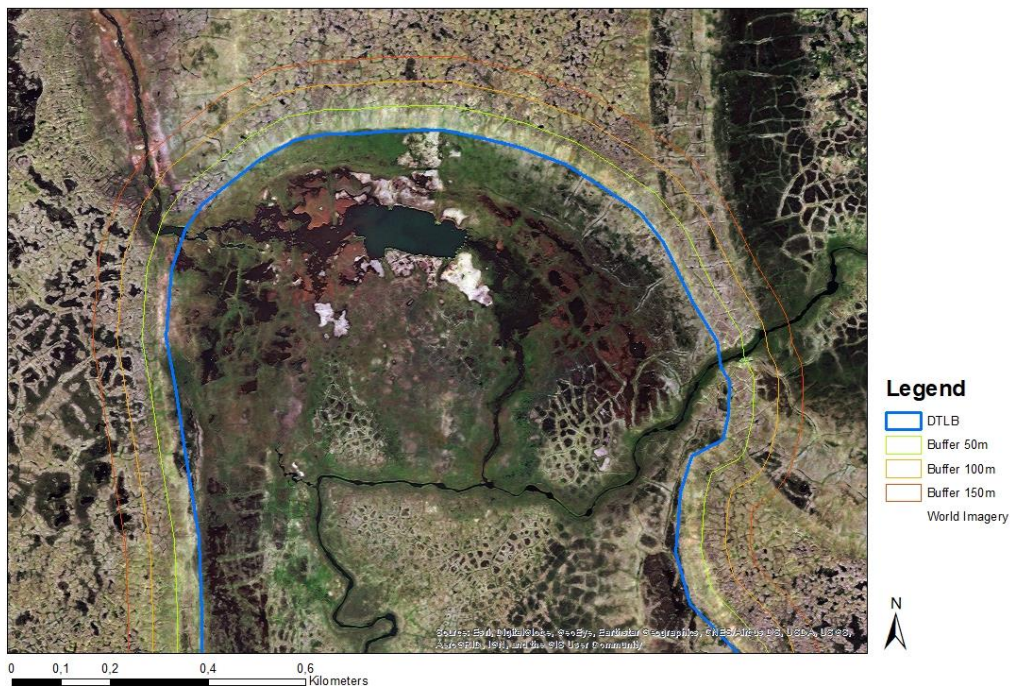


Figure 19: DTLB ID 19 at Barrow on ESRI World Imagery

Another example, DTLB ID 19, is shown in figure 19 with the World Imagery. The buffer of radius 50 m and 100 m both fit very well, without intersecting other structures, except for the two drainage channels in the east and north-west. The 150 m buffer covers a big part of the neighboring basin in the east, which is not good for the analysis of the height data.

The histograms of DTLB ID 19 (fig. 20) show a height distribution of 15 to 17 m for the DTLB, with the peak 15.7 m. The basin has a unimodal distribution, whereas the buffer histograms are all bi- or multimodal distributed. At the 150 m buffer the values vary a lot in the lower and higher heights, which means that other landscape structures are included and therefore the buffer size is not fitting well. The 50 m buffer shows a clear peak and values mostly above the DTLB mean height, but the histogram of the 100 m buffer is showing this even more clearly. The radius of 100 m also includes more values above the average basin height and with a higher distribution of up to 19 m.

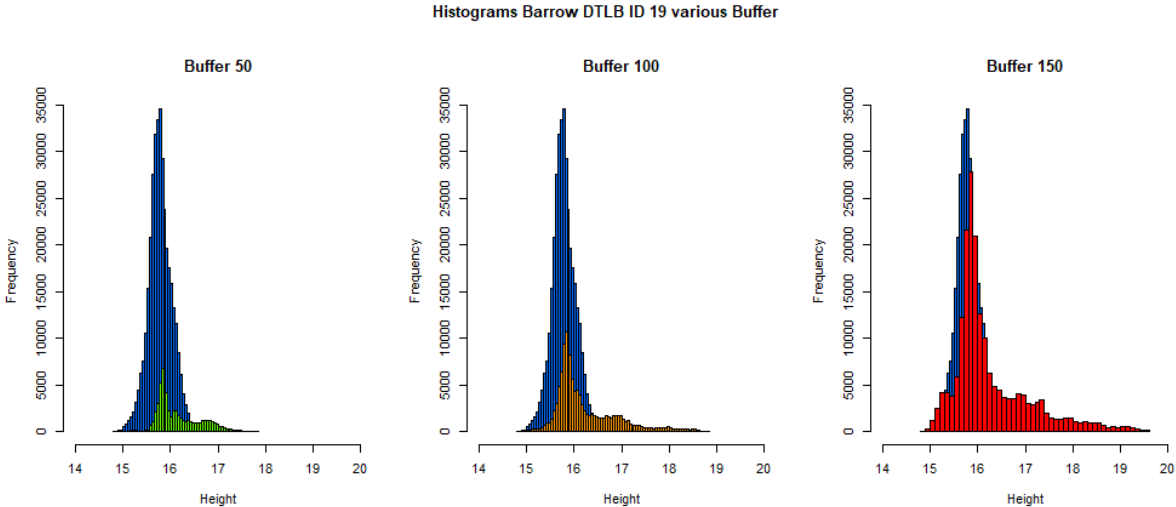


Figure 20: Histograms DTLB ID 19, buffer 50 m (green), 100 m (orange), 150 m (red)

Concluding the sensitivity study, the result is that a 100 m buffer radius is an appropriate size for the purpose of the height analysis. It is a good size because it gives an appropriate coverage of the outside of the basin regarding the difference in elevation between the basin and its surrounding. On the other hand, it does not cover too much of other structures, like neighboring basins or recent lakes.

4.2. Details of Barrow research site

For the Barrow and Seward research sites analysis of the DTLB and buffer heights were carried out. The buffer size is always of 100 m in radius around the DTLB outline. First, some general remarks on the data will be described, followed by a detailed description of the statistics and further interpretation of the data.

The 20 basins of Barrow vary in size between 0.63 km² and 11.95 km², with an average size of 2.83 km², whereas the buffer sizes diverge between 0.33 km² and 1.43 km², with an average of 0.69 km². The heights of the basins range between -2.23 and 16.72 m a. s. l., whereas the buffer heights show slightly higher values from -2.20 to 19.24 m. More values of each DTLB and the according 100 m buffer, like the minima, median and maxima of the altitude values as well as the differences of mean height of DTLB minus buffer, can be seen in table 3. The last row gives the average of the 20 values of each column. The full table with all buffer - basin differences and the median values can be found in appendix 2.

Table 3: DTLB and buffer values of Barrow

ID	DTLB Size [m ²]	Buffer Size [m ²]	Buffer Mean [m]	DTLB Mean [m]	Diff Buffer-DTLB Mean [m]	Buffer Max [m]	DTLB Max [m]	Buffer Min [m]	DTLB Min [m]
1	2,419,723	655,423	7.52	6.85	0.66	9.49	9.37	5.59	5.58
2	737,345	440,012	1.74	1.17	0.57	3.20	2.21	0.37	0.53
3	1,904,419	731,851	7.11	6.29	0.81	9.49	6.97	5.69	5.74
4	633,220	331,547	1.10	0.69	0.41	4.05	2.95	-2.20	-1.04
5	3,417,157	715,237	1.31	1.04	0.27	4.18	2.02	-1.64	-0.61
6	3,046,643	778,813	1.09	0.61	0.48	5.60	2.39	-2.10	-2.27
7	3,868,608	808,340	16.36	15.98	0.37	19.25	16.87	14.60	14.73
8	11,952,064	1,435,557	4.39	3.50	0.88	7.18	4.12	2.49	2.70
9	2,431,961	693,324	6.23	4.79	1.44	9.86	6.02	3.29	3.40
10	5,624,563	1,013,288	7.04	6.76	0.27	9.18	7.80	5.20	5.69
11	2,430,490	626,184	4.03	3.43	0.59	6.81	4.88	2.88	2.91
12	1,436,097	499,587	3.22	2.49	0.72	5.32	3.67	1.06	1.17
13	791,941	385,778	4.74	4.07	0.67	8.84	5.25	3.47	3.61
14	3,013,737	792,560	1.23	0.75	0.48	2.56	1.69	0.25	-2.05
15	2,594,511	681,082	3.50	2.43	1.06	7.77	5.87	0.59	0.72
16	3,105,136	866,977	10.56	9.71	0.84	14.67	12.63	8.94	8.92
17	1,985,544	655,917	8.65	8.25	0.39	13.87	9.32	6.10	6.09
18	1,800,122	566,525	9.38	8.48	0.89	12.56	12.42	7.80	7.73
19	2,753,803	714,249	16.22	15.78	0.44	18.82	16.72	14.87	14.83
20	765,907	387,777	3.15	2.61	0.54	4.48	3.45	2.22	2.17
Ø	2,835,650	689,001	5.93	5.28	0.64	8.86	6.83	3.97	4.02

Some statistical tests were executed, and graphs generated in order to see, if any variables are related between each other. One hypothesis is, that the values of the basin area and the buffer height should be greatly related to one another. The graph in figure 21 confirms increasing in basin area and a therefore increase of the buffer area. Also, the coefficient of determination results in a high dependency of the variables with $r^2 = 0.88$. Other coefficients of determination are showing a result for the relationship of basin area vs. basin height with $r^2 = 0.008$ and for

the buffer area vs. buffer height with $r^2 = 0.02$. This results in no dependency between the average height and area of both basins and buffer.

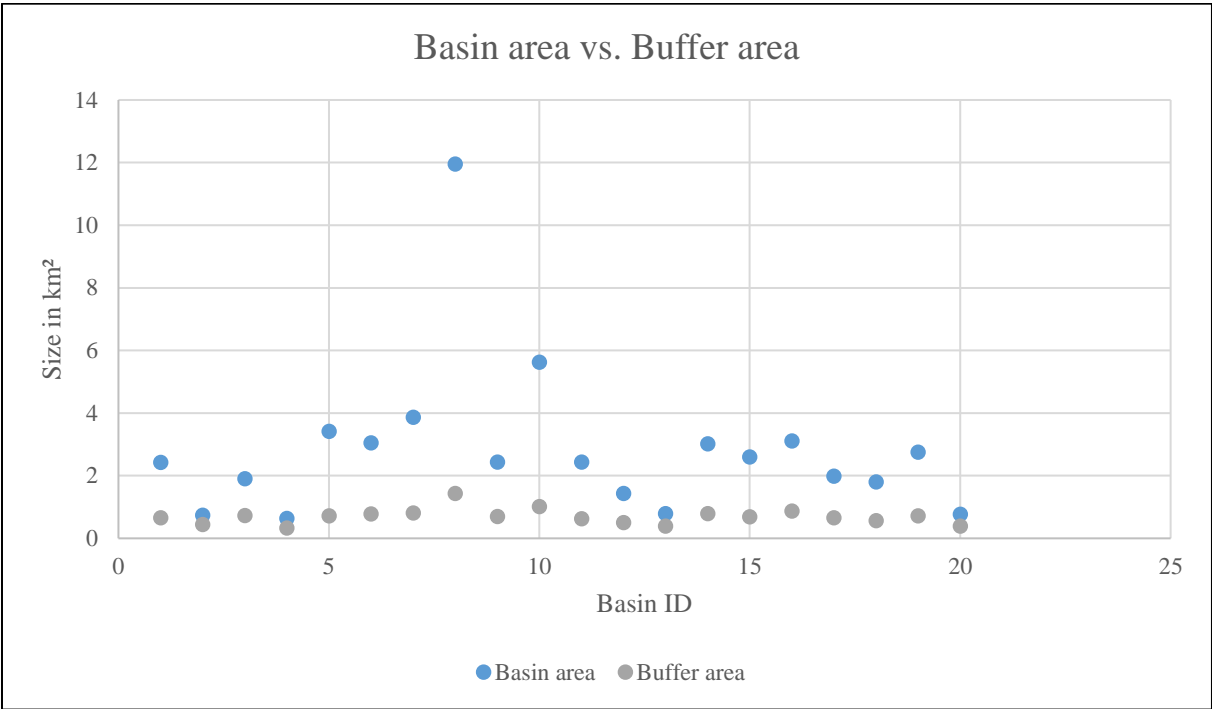


Figure 21: Graph of basin area and basin height

In order to estimate the ground ice content, the height differences between the basins and their surroundings, the buffer zones, were calculated, including the differences of the maximum, mean, median and the minimum values for all 20 DTLBs between basin and buffer zones. The values of the differences are diagrammed in figure 22. The values of the minimum height of buffer minus basin vary slightly. All values are between -1.0 and 0.48 m, except for one outlier, basin 14, with a difference of 2.3 m. This can be explained with several deep points of the basin down to - 2.05 m, which might be inside a man- made channel crossing the whole basin. The differences of the basins and buffer median have a greater value range from 0.19 to 1.24 m. Even greater is the range of the mean height differences with 1.17 m, from 0.27 to 1.44 m. However, the mean values are just slightly higher than the median values, on average + 0.13 m. The greatest differences are amongst the maximum values of the basin and buffer altitudes: 0.14 to 4.54 m. About half the values are between 0 and 2 m, while the other half ranges between 2 to 4 m of difference in the maximum altitude, resulting in an average of 2.07 m of buffer-basin height.

The mean and median differences are more significant for this study than the minimum and maximum values are. Most of these mean and median values are in a range of 0 to 1 m, with only two differences exceeding the one- meter difference with a maximum at 1.44 m. This is a very tight range for the interpretation of excess ground ice in this difference of height, when also having to consider other impacts, like erosional remnants and the slope of the basins, which could be included in the basin or the buffer data in various quantities.

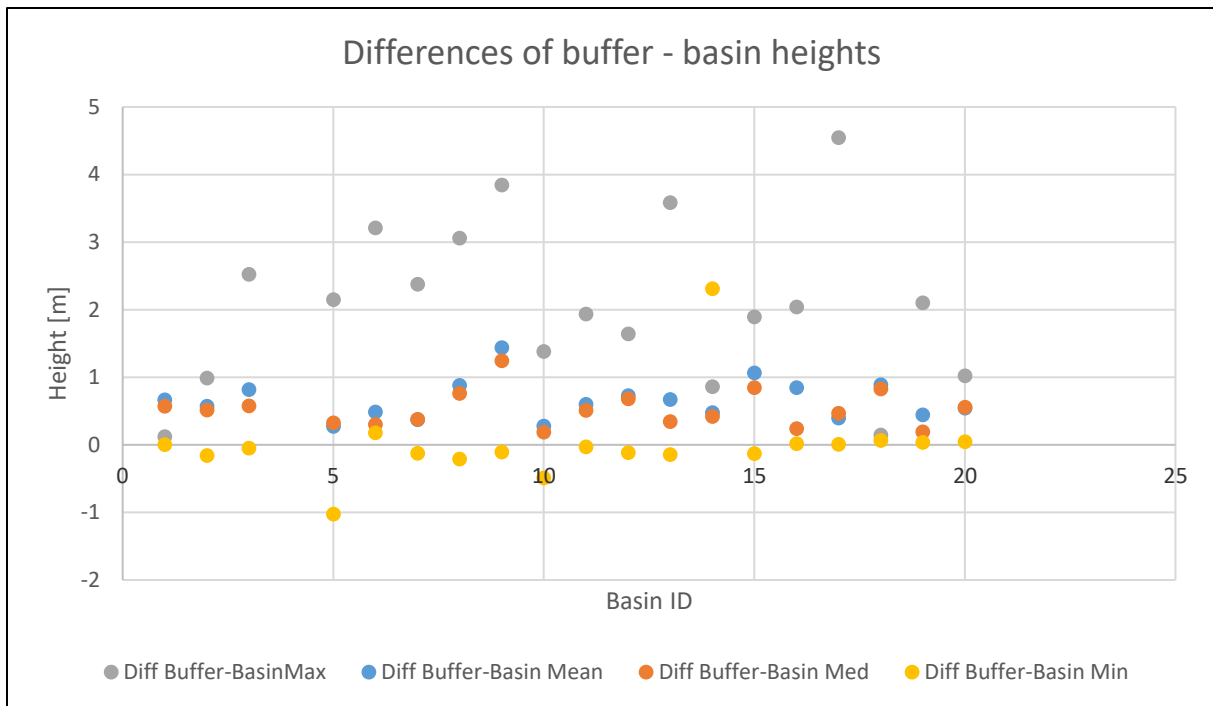


Figure 22: Graph of differences in buffer - basin heights

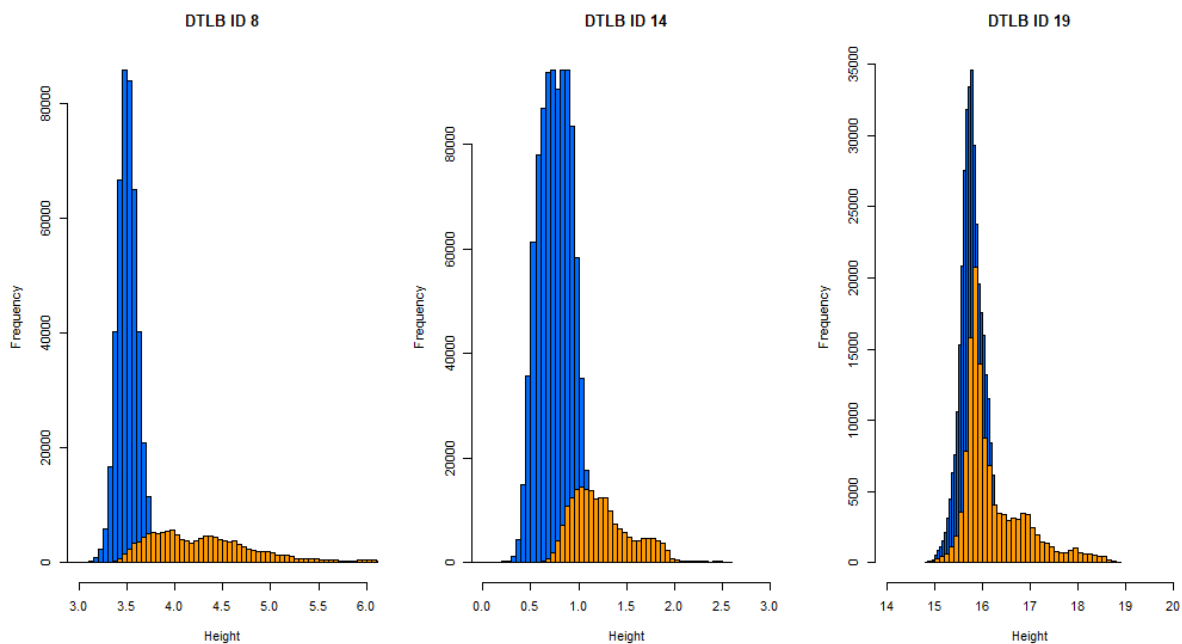


Figure 23: Histograms of Barrows DTLB ID 8, 14, 19

Histograms of the distribution were created to get more detailed information on the elevation data distribution of the DTLBs and buffers. The color scheme is continuously the same with DTLBs in blue and buffers in orange for the whole results chapter, including the lines on the maps and the lines and bars in the diagrams.

It is noticeable that the distributions of the heights of the three DTLBs 8, 14, 19 and the according buffers (100 m) are very different to each other (fig. 23). Whereas DTLB 8 has a very distinguished peak at about 3.5 m, the buffers of it is wide spread. It also does not show

one obvious peak, but two smaller peaks. DTLB 14 and its buffer both have a range of about 1.5 meter, the DTLB itself with a single crest and the buffer with a big and a smaller one. The widest spread values are of DTLB 19 from 15 to 17 m and its buffer from 15 to 19 m, both with a clear peak.

The distribution shapes of the density plots are categorized into three groups for further interpretation: unimodal, bimodal and multimodal. For the density plot the automatic function of kernel smoothing of R is used. It is therefore a clearer graph than the frequency plots, since there are no bins created. For each category two plots of density patterns will be discussed.

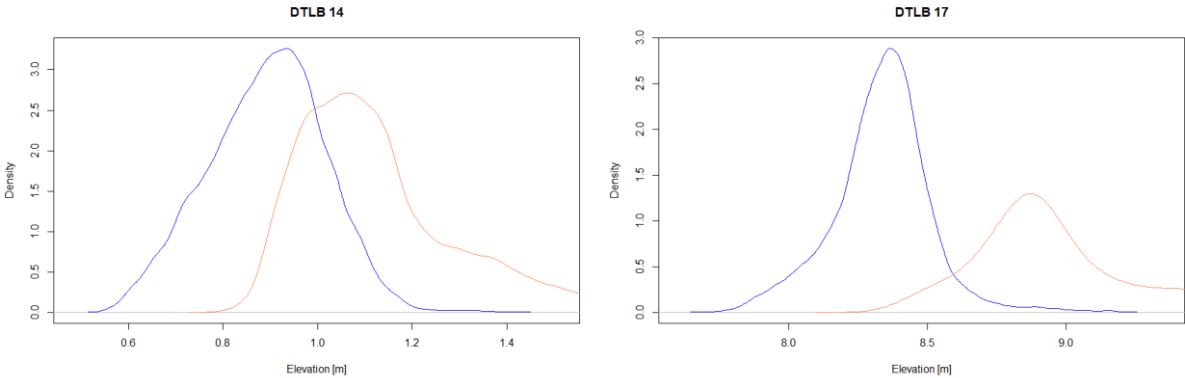


Figure 24: Density plot of DTLB 14 (a) and 17 (b) (normal distribution)

The plots of DTLB 14 and 17 (fig. 24) are showing examples for the unimodal distribution. There is one clear peak at ~ 0.9 m of DTLB 14 and at 1.1 m at its buffer zone. The whole curve of the buffer is displaced of the DTLB curve of about 0.2 m. The values differ slightly, but enough to be visible. In addition, the peak of the buffer is located at a lower density, ~ 2.6 m, in comparison with the DTLB one at about 3.2 m. Therefore, most of the values of the buffer zone are at a higher elevation level as the DTLB. Even closer to a normal distribution is the bell- shaped curve of DTLB 17, with its peak at an elevation of ~ 8.4 m. The according curve of the buffer is a wide spread normal distribution with a dislocation against the basin of about half a meter. Here the overlap of values is small, since the intersection is at a low point against the end of the DTLB curve and at the first third of the buffer curve.

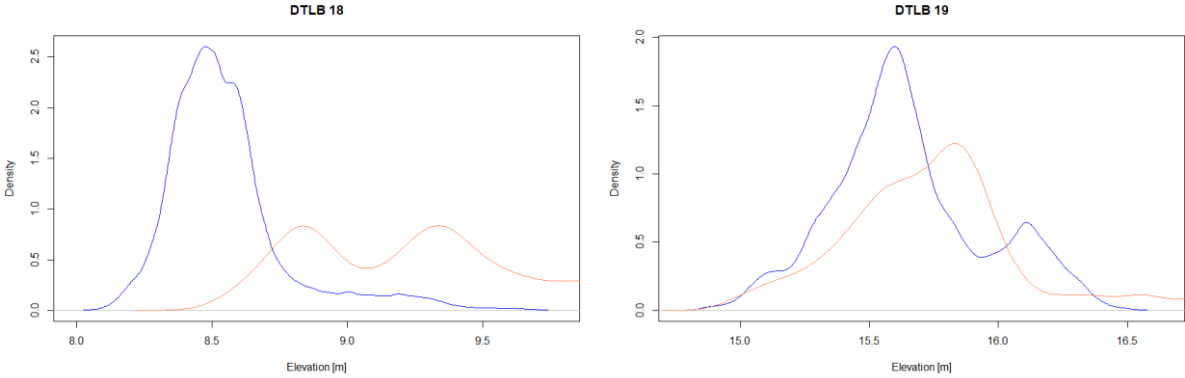


Figure 25: Density plot of DTLB 18 (a) and 19 (b) (bimodal distribution)

The density graph of DTLB 18 (fig. 25 a) is showing a slightly bimodal distribution with a big peak at 8.5 m and a small one at 8.6 m, but with two defined peaks at the buffer values. The buffer is clearly at a higher altitude (8.5 to 9.5 m) than most of the basin, even though it has a wide range of values. Another example of a bimodal distribution is the graph of DTLB 19 (fig. 25 b) with one big peak at 15.6 m and a smaller crest at 16.2 m. The buffer density plot shows only one identifiable peak at 15.9 m. Even with this distribution of the altitude the buffer is on average scarcely above the DTLB altitude mean.

Two examples of multimodal distributions of the height values are DTLB 4 and 6 (fig. 26). The density curve of DTLB 4 has one small peak followed by two big peaks and buffer values with a small crest at 1.2 m followed by a big one at 1.6 m. Here, the density is both times spread over the various peaks, but still creating clearly higher mean values of the buffer than the basin. An example with buffer density peaks much lower and slightly higher than the basin peak occurs at DTLB 6. Also, the DTLB values show a merged peak of two small ones. The lower peak of the buffer can be explained by a basin within the buffer zones, which is of lower altitude than the DTLB analyzed. This lower basin can be seen in figure 27 in the northeast. The buffer zone within the blue outline of the basin and the orange outline of the buffer are blended completely within the other basin. Due to the fact, that polygonal tundra structures formed and the lower height, it can be assumed that the basin is older than DTLB 6.

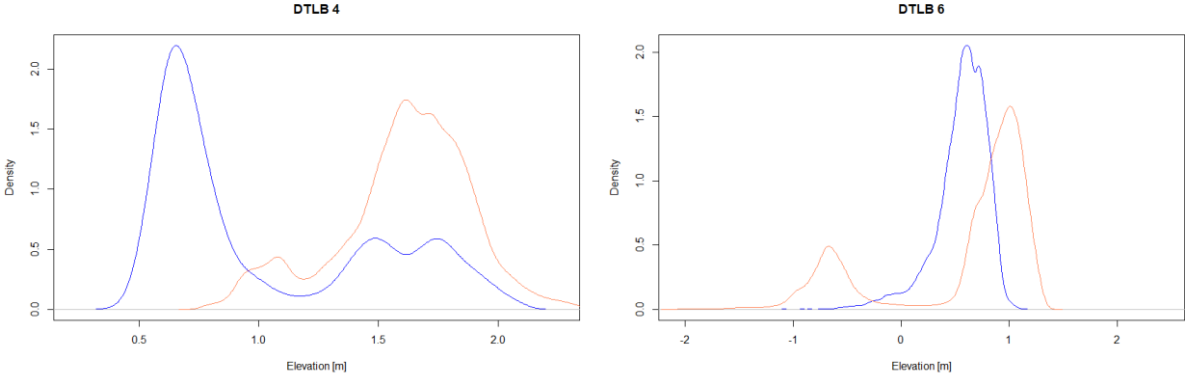


Figure 26: Density plot of DTLB 4 (a) and 6 (b) (multimodal distribution)



Figure 27: World Imagery of Barrow DTLB 6

Except the already described differences in height, various other factors need to be considered before interpreting the data for the amount of excess ground ice. As mentioned in chapter 4.1.4., for Barrow, the DTLB shape files were digitalized with the help of the World Imagery data and Landsat images. Out of this an inaccuracy with the outlines of the digitalized DTLBs occurred due to an approximate correctness of the different age stadium of DTLBs. The Drained Thermokarst Lake Basin (ID 14) in figures 15 and 16 seem to be a mixture of two age stadiums, not one. This can be seen best on the zoomed map in figure 28 a, on the north-east of the basin. Analyzing the vegetation and structure itself, a difference in age can be identified in the south of the basin within a large area (fig. 28 b). The older part is showing a polygonal tundra with a small amount of vegetation, whereas the younger part shows a continuous vegetation cover with no polygonal tundra or a beginning stage of building these structures. It is not possible to correctly compare this basin to a specific age group on Seward, because it contains at least two age stages itself. Furthermore, in figure 28, the buffer is partially running through a water filled stream, which could have arisen errors. However, this is not possible to avoid in bigger datasets. This problem of including different age stadiums of DTLBs could appear in various cases within the Barrow dataset. By knowing the approximate age stadium of the DTLBs the outlines could be digitalized more exactly and therefore the height differences could be interpreted more in detail. Also, the overlapping of the buffer of DTLB 6 into an older basin, like in figure 27, is a source of inaccuracy. But it is important to mention that it is very difficult to eliminate such overlapping, since the basins are often close to each other and therefore also the according buffer zones.

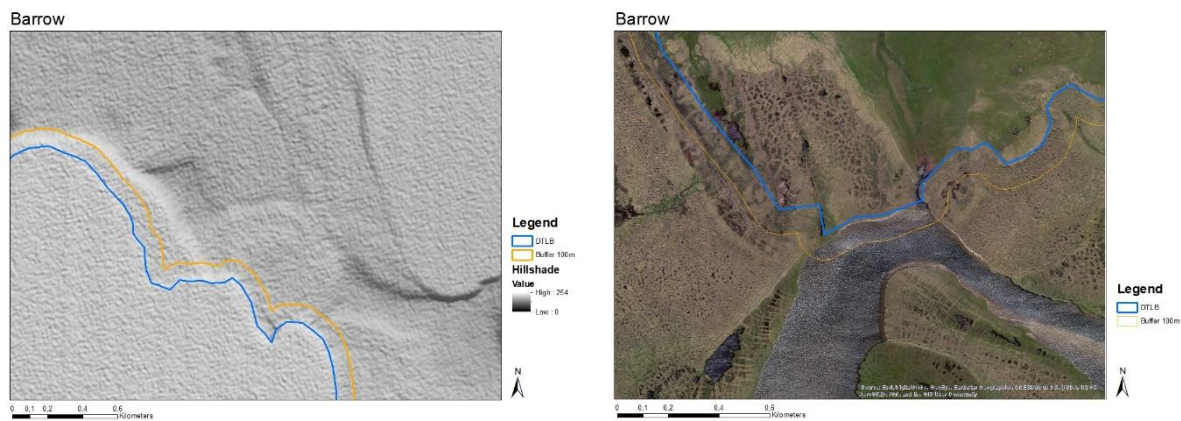


Figure 28: a) Hillshade of Barrow, DTLB 14 zoomed to north-east of basin and b) World Imagery of Barrow, DTLB 14 zoomed to south of basin

4.3. Details of Seward Peninsula research site

The analysis of the DTLB and buffer elevation data for the Seward research area will be explained in this chapter. Due to the five age groups (1 to 5) of the 466 DTLBs at the Seward peninsula, the analysis of this site will follow in several chapters for each class separately. The unknown age group 0 with 27 DTLBs is not studied. As for the Barrow site, an analysis of errors and uncertainties will follow the age group results.

The buffer size is always of 100 m in radius around the DTLB outline, like in Barrow. All graphs and maps continuously show DTLB in blue color, buffer in orange. Further, the graphs are all combined density and frequency plots, showing the density scale on the y- axis and the elevation in meter above sea level on the x- axis. The bars of the graphs always show the frequency, the lines the density. Not all density plots are showing a y- axis from 0 to 1 due to very small distribution of the elevation values. But the integer of the area of the line is proved to be always 1.

4.3.1. Age group 1

There are 20 Drained Thermokarst Lake Basins in **age group 1** on the Seward peninsula, which all drained within the last 50 years.

Table 4: Seward age group 1 DTLB and buffer sizes

ID	Object ID	DTLB Size [m ²]	Buffer Size	Buffer Mean	DTLB Mean	Diff Buffer-DTLB Mean	Buffer Med	DTLB Med	Diff Buffer-DTLB Med
1	1	3588060.9	1108831.6	16.07	14.67	1.39	15.95	14.65	1.30
2	2	95896.4	197336.4	10.04	9.11	0.93	10.15	9.11	1.04
3	3	3594678.3	813143.0	16.85	14.99	1.86	16.38	14.96	1.42
4	4	1054541.9	489509.7	14.42	12.50	1.92	14.09	12.52	1.58
5	133	1722994.9	641490.4	17.29	16.16	1.13	17.20	16.08	1.12
6	137	184393.5	438206.7	24.32	19.72	4.60	21.43	17.93	3.50
7	139	106026.2	207071.4	20.63	18.14	2.48	18.11	17.30	0.81
8	178	566100.8	335422.5	18.09	17.31	0.78	17.89	17.22	0.67
9	186	487649.9	346831.8	18.60	17.19	1.40	17.66	17.12	0.55
10	211	180619.9	210161.7	11.62	11.16	0.46	11.71	11.16	0.56
11	250	300535.7	407779.7	16.70	14.12	2.58	15.73	13.80	1.94
12	258	707493.0	421885.6	24.59	23.08	1.52	23.89	23.17	0.72
13	294	127307.7	186473.8	19.17	18.26	0.91	19.00	18.39	0.61
14	296	370909.9	366250.2	12.73	12.08	0.66	12.76	12.15	0.61
15	334	451883.8	643820.7	15.81	15.70	0.11	15.63	15.66	-0.04
16	349	135551.6	199492.0	14.98	14.12	0.85	15.26	14.10	1.16
17	352	380823.1	322797.9	9.95	8.68	1.27	10.02	8.48	1.55
18	367	235116.4	331970.6	9.70	7.38	2.32	9.98	7.41	2.56
19	420	435936.9	306578.2	12.09	10.46	1.63	11.73	10.46	1.28
20	422	497674.8	317371.6	15.01	13.72	1.28	14.87	13.68	1.19
	Ø	761209.8	414621.3	15.93	14.43	1.50	15.47	14.27	1.21

The sizes of those DTLBs vary between 0.09 and 3.59 km², with an average size of 0.76 km², and an average buffer size of 0.41 km² in a range from 0.19 to 1.10 km². The minimum values of the buffer and basins are as low as 3 to 7 m, but mostly between 10 and 15 m, with an average of 11.4 m for buffer and 11.6 m for basins. The maximums are reached at mostly between 14 and 25 m, but with runaways of up to ~ 40.3 m at both buffer and basin values. Noticeable is the difference of mean values of buffer - basin with 1.5 m for the age group, whereas the median difference is at just 1.21 m. At the mean difference values of the buffer - basin heights the values range between 0.11 to 4.60 meter in altitude change. At all times the mean value is positive, the basins are on average consistently lower than the buffer zones. The last row gives the average of the values of each column. The full table including the buffer - basin differences and the minimum and maximum values can be found in appendix 3.

The coefficient of determination is calculated for the dependency between the buffer and basin area of Seward age group 1. The result is $r^2 = 0.8$. This shows a big dependency between the two variables. The other two tested variables for the Barrow site, the basin size vs. basin mean, and the buffer size against buffer mean, were omitted to present for all Seward sites. A random distribution is the result for these two tests for all age groups.

The frequency and density plots of all 20 DTLBs were created and sorted into the four different distribution categories: normal, bimodal and multimodal distribution and one class for no distinct distribution pattern. Just one basin and buffer elevation values are normally distributed, the one of DTLB 17. Additionally, the basin elevation data of further 11 sole basins is also normally distributed (DTLB 1, 3, 4, 5, 6, 8, 9, 10, 11, 12, 17). Not all the distribution patterns have a perfect bell shape, but always just one distinguished peak. There are no basin and buffer values both bimodal distributed, but four basins, DTLB 2, 7, 16 and 20. Additionally, six buffer values (buffer 1, 8, 9, 10, 11, 12) are bimodal distributed. There are only two basin and buffer distributions, DTLB 13, 14, which belong to the multimodal distribution category. Additionally, nine sole buffer density pattern fit in this category: the ones with ID 2, 3, 4, 5, 6, 7, 16, 17 and 20. No distribution patterns were noticeable for the basin and buffer elevation distributions with the IDs 15 and 18. Here, the patterns were not possible to categorize due to several peaks or other pattern immoderations.

It is apparent, that just a few basin and buffer values are both normally distributed. Further on, often the basin is showing less peaks than the buffer values of the according DTLB. Some buffer distribution patterns show peaks not just above the majority of the basin's elevation, but also a, mostly smaller peak, below the majority of the basin's elevation. This consequences, that more basin areas are even and on similar heights, than buffer areas are. Buffer areas often cover or intersect with some basin slopes, other basins, lake remains or water outlets and hence have a more various distribution and therefore often result in frequency plots with two peaks or more. To discuss these statements more in detail, some examples of frequency & density plots with the according World Imagery map and interpretations will follow.

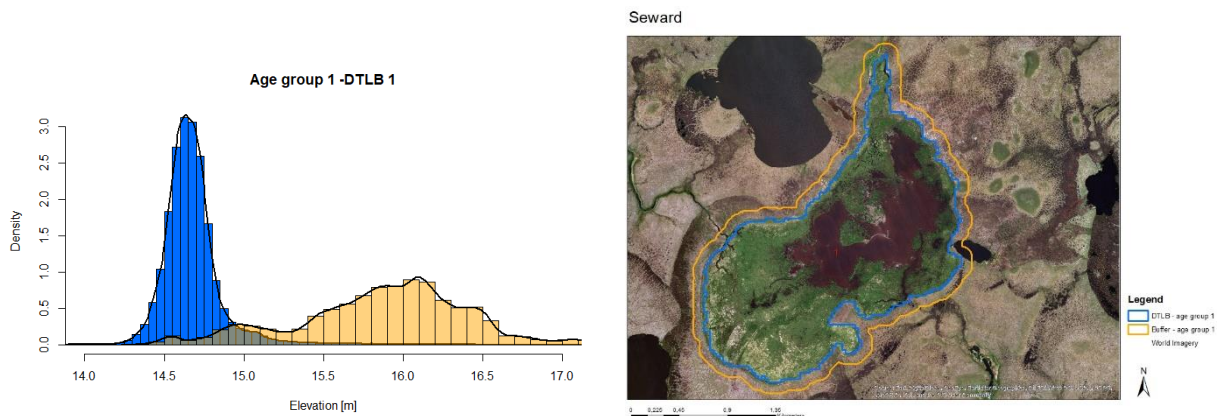


Figure 29: a) Density & Frequency plot and b) Map of DTLB 1 of age group 1 (OID 1)

The first example, DTLB 1, is of a normal distribution pattern, for both, basin and buffer elevation data (fig. 29 a). It is spread from about 14 to 17.5 m. a.s.l., with average heights of 14.67 m for the basin and of 16.07 m for the buffer and with some runaways of the buffer of up to 30 m. Basin 1 is the second biggest of this age group with 3.58 km², but covering a big area of water surface in the middle of the basin (fig. 29 b). Still, the basin height values are evenly distributed in the small range of slightly more than one meter. The basins elevation values are nearly covering the full range from 14.3 to over 17 m, with some outliers above 17 m. The buffer is not intersecting with other basins of buffer of the same age group, but with a small lake in the east and the water outlet in the southeast of the basin. It is apparent, that the basin area is colored in green much more than the surrounding, which leads to the assumption for much more vegetation within the basin than the outside. In the southwest there are first attempts of polygonal tundra with a clear boundary to the deeper polygonal tundra structures, which belong to a basin (OID 395) of age group 3. The clear boundary of a vegetation change and height change stretches around most of the basin outline. In the northeast a basin of age group 4 is sharing this boundary.

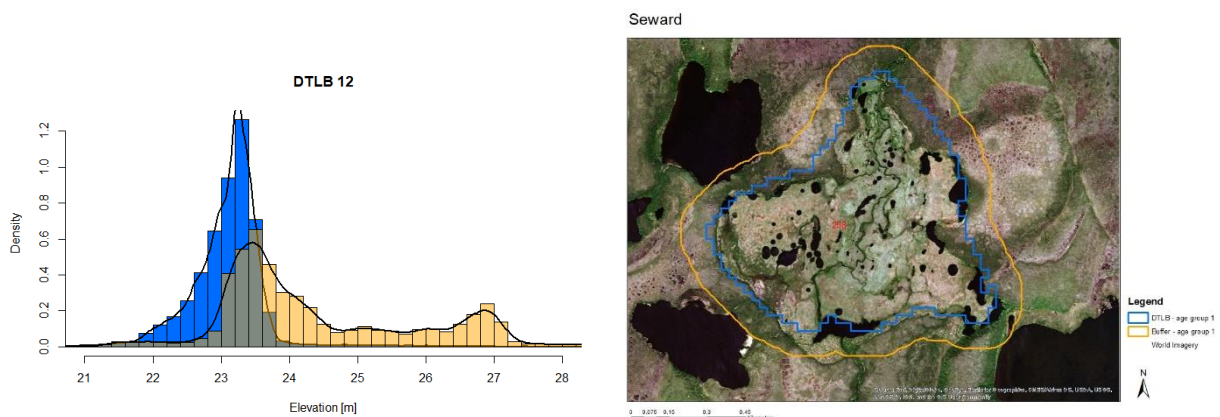


Figure 30: a) Density & Frequency plot and b) Map of DTLB 12 of age group 1 (OID 258)

The values of the basin area of DTLB 12 (OID 258) of this age group are spread in a normal distribution with one clear peak at about 23 m (fig. 30 a). In comparison to this, the buffer values of the according buffer show two peaks just slightly above this at ~ 23.5 and much higher at 26.9 m, but there are also quite some values in between those two peaks. And some outliers even higher than the second peak. The buffer area of 0.42 km² is more than half as big as the

area of the basin area (0.7 km²). The buffer mean elevation of 24.59 m is of 1.52 m higher than the basin elevation of 23.08 m. This basin has the highest elevation for both buffer and basin mean values. The border between the basin and the buffer zone is very distinct. Some lake remains are part of this clear boarder. Additionally, an abrupt change in vegetation and a change in the intensity of the polygonal tundra pattern from the buffer area to no polygonal tundra within the basin (fig. 30 b) are creating this boarder. There are still some small lake remains in the basin, which are a sign of a not full drainage to this point of time. Most of these water remnants are connected by a little stream, crossing the whole basin roughly from north to south. This stream also deepens in the direction of north to south, showing the water flow direction thereby. There is a water outlet from the biggest remaining lake of the basin in the south towards the area south of the buffer zone. It could be possible, that the remaining water will also drain, forming a more even and completely drained basin in the future.

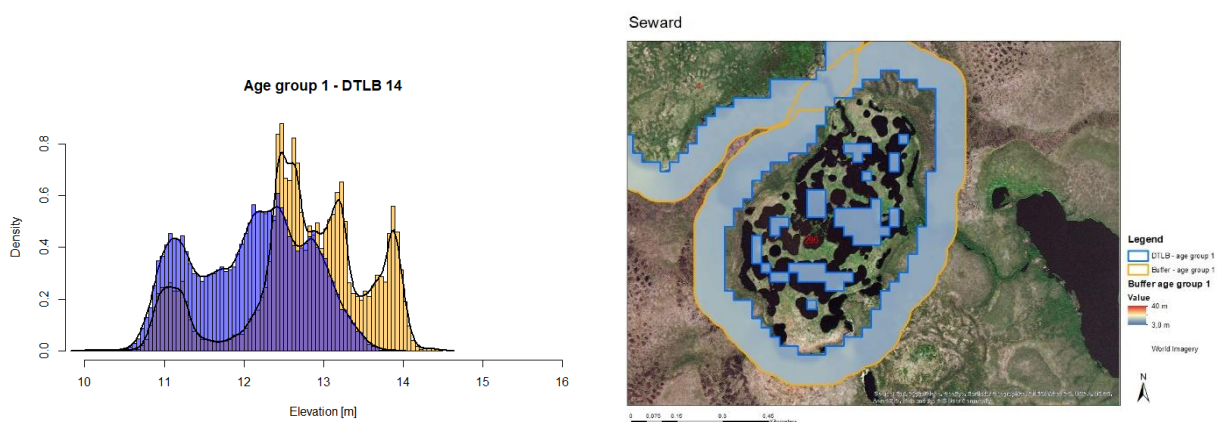


Figure 31: a) Density & Frequency plot and b) Map of DTLB 14 of age group 1 (OID 296)

The basin elevation of DTLB 14 of the age group 1 (OID 296) has a multimodal distribution, (fig. 31 a). The basin has a mean height of 12.08 m, the buffer of 12.73 m. The lowest peak of the buffer elevation, at ~11 m (yellow line in the background), is reflecting the small patches inside the basin, around the water areas, which belong to the buffer area. These low elevation values are lowering the mean buffer height significantly. If overlooking these particular low values between about 10.8 to 11.8 m, the average buffer value would be showing a much greater difference in value to the basin values. There is roughly half the area covered by water filled lake remnants (fig. 31 b). Also, for this basin it could be possible that the basin is still in the process of a drainage event and will be a basin without small ponds in the future. The small outlet in the northwest is flowing from the other DTLB, basin 4, towards this basin, whereas the outlet in the southeast is leading towards the lake in the east. There is still a waterway from the northwest to the southeast outlet and both streams are partially filled with water. Since DLTB 4, which is also in age group 1, is completely drained and showing first indications of polygonal tundra structure, therefore it was most likely drained before this basin, DTLB 14, even though it is in the same age group. The buffer of DTLB 4 and 14 are partially overlapping and the buffer outline of DTLB 14 even intersects very slightly with the basin outline of ID 4.

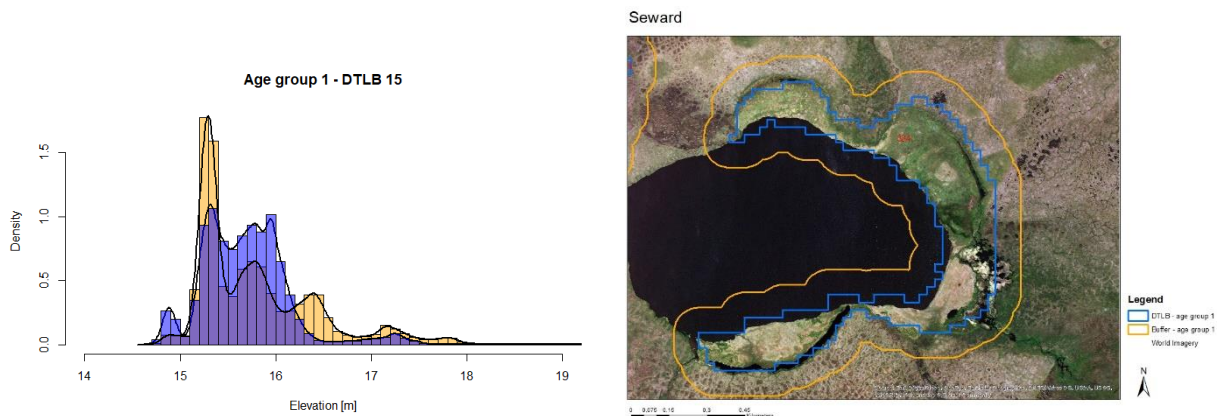


Figure 32: a) Density & Frequency plot and b) Map of DTLB 15 of age group 1 (OID 334)

The elevation distribution of DTLB 15, in blue, is of a multimodal pattern, for both, basin and buffer (fig. 32 a). Older basins, mostly of age group 3, around this one, counting for a big number of low values of the buffer elevation. The lake shore values, which are as low as the lower parts of the basin, are additionally counting low buffer values. In this case, all water surface elevation values were counted into the buffer. The buffer peak at 15.2 m is created of exactly these water surface values. Only the adjoining basin in the northeast, which the buffer covers, has some higher values of 17 to 18 meters (fig. 32 b).

4.3.2. Age group 2

In **age group 2** there are 140 DTLBs of drainage events of an age range of 50 to 500 years. The basins vary in size from 0.02 to 2.71 km², averaging at 0.40 km², and buffers ranging from 0.01 to 0.8 km², averaging at 0.33 km². The elevation range is huge, from -9.64 to 49.8 m within the basins and from -17.7 to 51 m within the buffer. The mean elevation of the basin with 15.13 m and the buffer with 16.35 m are close to each other, with a difference of only 1.22 meter. The full table of elevation values of all DTLBs and buffer of age group 2 can be found in appendix 4.

The coefficient of determination for the basin size compared to the buffer size results in $r^2 = 0.000937$. This value is close to zero, that no dependency can be concluded from this result.

Within the data set of the elevations, there was a significant number of “no value” (N/A) errors due to some overlapping of shape files, holes in the original DTLB shape file due to some water filled areas within certain DTLB and other problems. This will be discussed further in the error/inaccuracy chapter (4.3.6.). For the presentation of the results of age group 2, 3 and 4, the data of the examples was calculated again in order to handle the N/A error problem better. Therefore, there are tables per age group within the results, which are anomalous to the result table per age group in the appendix.

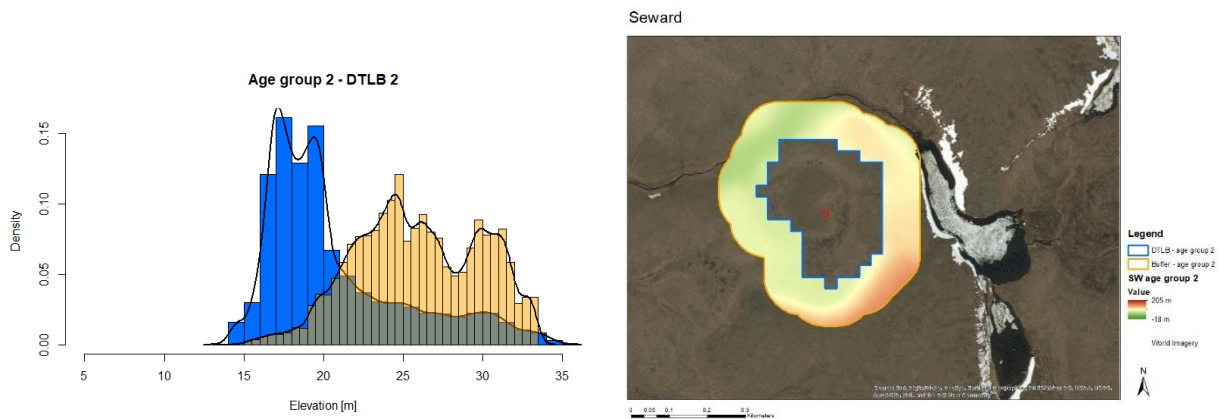


Figure 33: a) Density & Frequency plot and b) Map of DTLB 2 of age group 2 (OID 13)

With an elevation range of 13.6 to 35.4 m, the buffer mean height at 25.9 is 5.2 m higher than the average of the basin elevation at 20.67 m (table 5). Both, basin and buffer have two peaks in their elevation distribution (fig. 33 a). Since this DTLB is small, the buffer area is bigger than the basin area. Furthermore, the elevation range is very high, which gives a wide spread elevation pattern of the density with a very low-density value of just up to 0.15 m. The elevation of the basin and buffer increases from the northwest to the southeast (fig. 33 b).

Table 5: Recalculated values of DTLB 2 and 78 of age group 2

ID	Object ID	DTLB Size [m ²]	Buffer Size [m ²]	Buffer Mean	DTLB Mean	Diff Buffer - DTLB Mean	Buffer Med	DTLB Med	Diff Buffer - DTLB Med
2	13	89443.8	173447.3	25.94	20.67	5.27	25.74	19.29	6.46
78	223	73740.8	375008.5	17.68	17.10	0.58	17.92	16.74	1.18

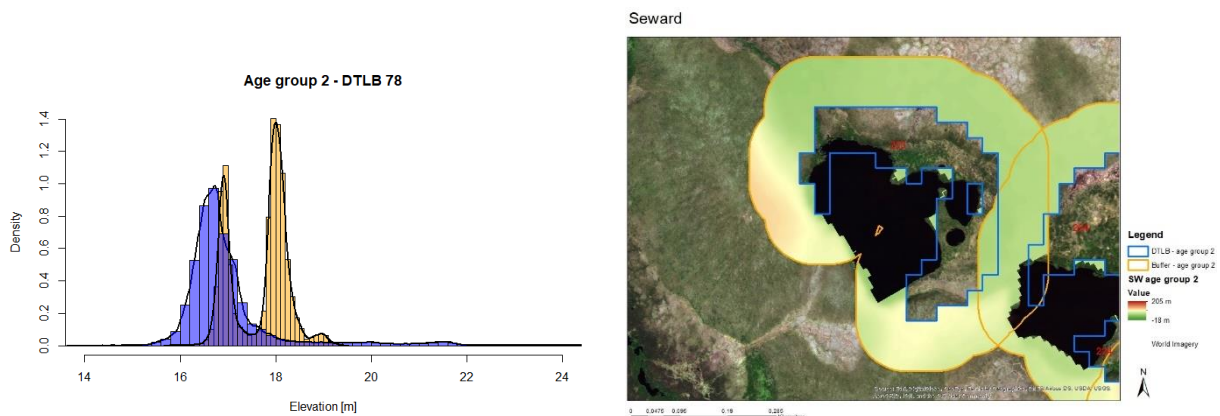


Figure 34: a) Density & Frequency plot and b) Map of DTLB 78 of age group 2 (OID 223)

In comparison to DTLB 2, DTLB 78 of age group 2, has a narrow elevation range, but still two peaks at the buffer values (fig. 34 a). The lower buffer peak mirrors the elevation of the northeast part of the basin, which is completely a land area (fig. 34 b). Whereas the higher peak at ~18.1 m the area in the southwest reflects. The distribution of the basin elevation values is nearly bell shaped. Because of the narrow range, the density is very high of up to 1.4. The difference between the mean buffer height and the mean basin height is just 0.58 meter.

Interesting is the maximum value of the buffer is at only 19.3 m, while the basin maximum is at 32.1 m. But, the minimum value of the basin at 13.7 m is lower than the buffers minimum at 15.8 m.

Also, for this age group there is to notice, that not many distributions of both basin and buffer elevation values are showing a normal distribution, but rather a bimodal or even multimodal pattern. At the same time, the buffer elevation distribution patterns are often showing more peaks than the according basin does.

4.3.3. Age group 3

In **age group 3** are 188 DTLBs of the age range 500 to 2000 since their drainage. For this group the mean buffer area is 0.47 km², about half as big as the basin area with 0.85 km² on average. The buffer heights average is 15.14 m, while the basin heights come to an average of 14.89 m, resulting in a difference of just 0.27 m. In contrast to this, the median is for both the same with 14.9 m. The altitude ranges from an average buffer minimum of 8.75 m and a mean basin minimum of 10.86 m to mean maximum values of 19.35 m for the basins and to 23.67 m for the buffer. The complete table of the values of age group 3 is attached in appendix 5. Like in age group 2 and 4, there are many DTLBs overlapping, intersecting with each other or with the buffer zones around them (fig. 35). This is leading to some errors, as already mentioned for age group 2. Therefore, there are again recalculated tables without N/A errors for the examples. With a coefficient of determination of $r^2 = 0.00119$, as a result for the dependency between the basin area and the buffer area, there is no correlation to be determined.

Seward

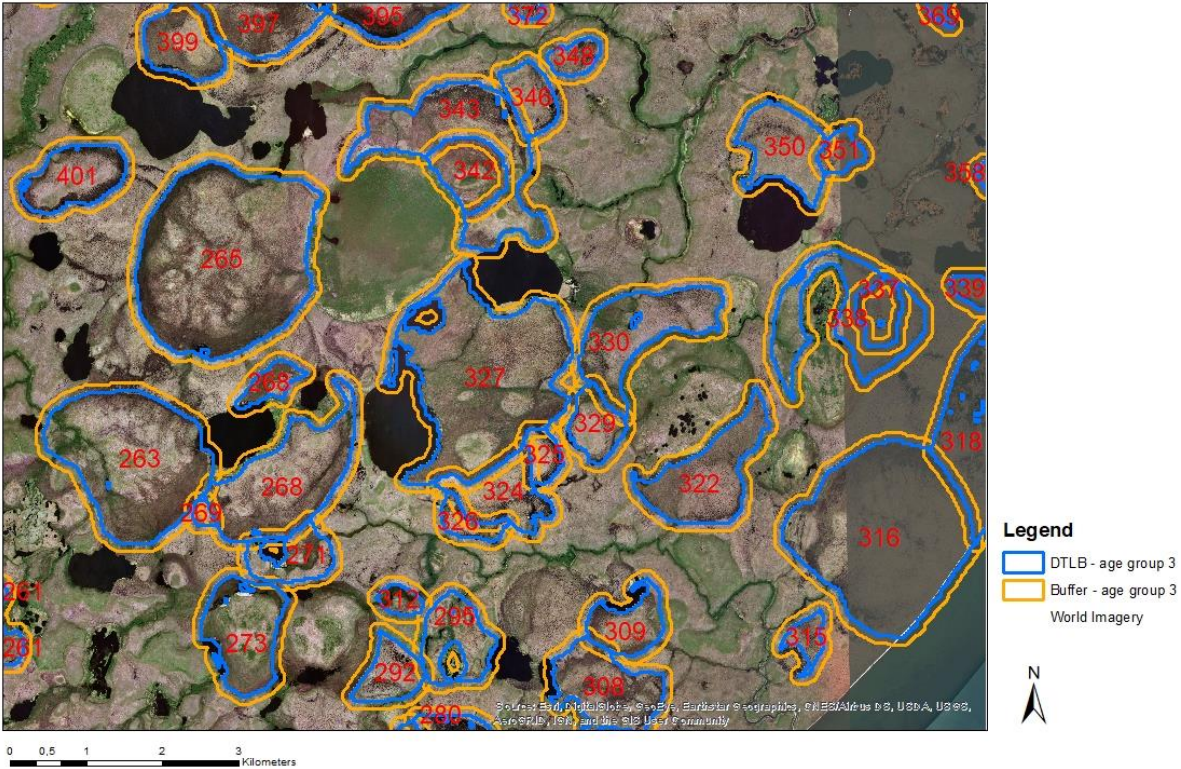


Figure 35: Extract of the Seward map of age group 3

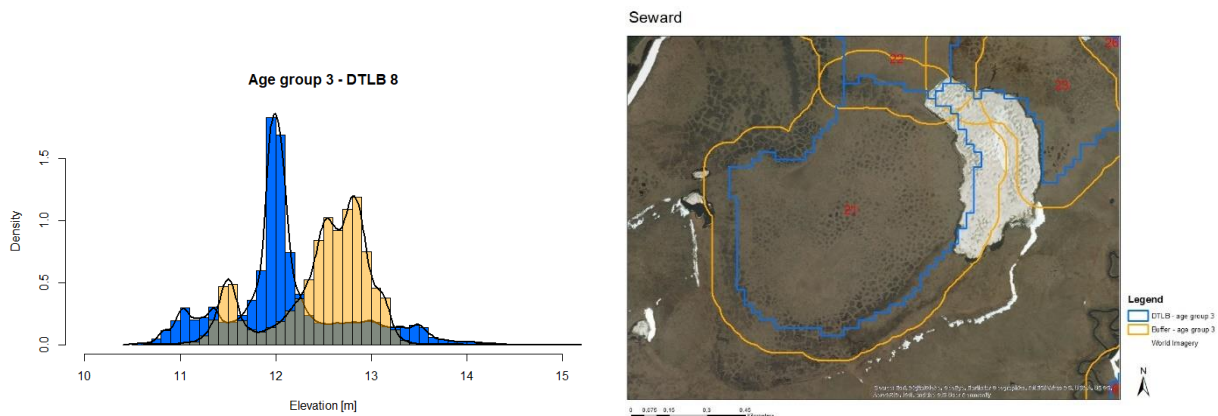


Figure 36: a) Density & Frequency plot and b) Map of DTLB 8 of age group 3 (OID 21)

One example of age group 3 is DTLB 8. It has a size of 0.68 km² and a mean altitude of 12.09 m, with a surrounding buffer of 0.53 km² and an average height of 12.47 m (table 6). The difference in elevation between the basin and its outside is therefore just 0.39 meter. The minimum values of buffer and basin are nearly similar with 10.72 and 10.52 m respectively. The maximum values differ slightly with 14.37 m at the basin heights and 15.12 m at the buffer elevation. Even though the buffer values are creating a small peak below the main peak of the basin, it still creates a higher average of the buffer by the much bigger peak at around 13 m (fig. 36 a). While the basin has a broad range of its elevation, the main peak is clearly at 12 m, averaging all values lower and higher at this height. There is a not completely developed polygonal tundra within the basin and a more distinct one in the buffer zone in the northwest of the basin, which belongs to no specific age class (fig. 36 b). In the south there is as well more distinct polygonal tundra formed.

Table 6: Recalculated values of DTLB 8 and 109 of age group 3

ID	Object ID	DTLB Size	Buffer Size	Buffer Mean	DTLB Mean	Diff Buffer- DTLB Mean	Buffer Med	DTLB Med	Diff Buffer- DTLB Med
8	21	689568.9	531611.8	12.47	12.09	0.39	12.59	12.01	0.58
109	269	76559.6	259725.3	15.14	15.17	-0.03	14.92	15.23	-0.32

For the other example, DTLB 109 of age group 3, the special case of a bigger buffer area (0.25 km²) than basin area (0.07 km²) occurs. The average heights of both elevations are about the same at 15.1 m, the median is showing a difference of a 0.32 m lower buffer zone. The minimum value also differs in just 0.3 m, whereas the maximum values highly vary with 16.22 m within the basin and 21.89 m in the buffer around. This basin is located at an intersection of two other basins of the same age group (fig. 37 b). The two other basins (OID 263, 268) are most likely older than this one due to more polygonal tundra and a lower elevation. The elevation of the buffer of basin 8 is mostly covering the basin of the other two DTLBs and therefore mirroring their elevation values with the two lower peaks in figure 37 a. The third and smallest peak of the buffer values is corresponding to the southern part of the buffer. Because of this, most of the basin values are higher than the buffer of which it is surrounded.

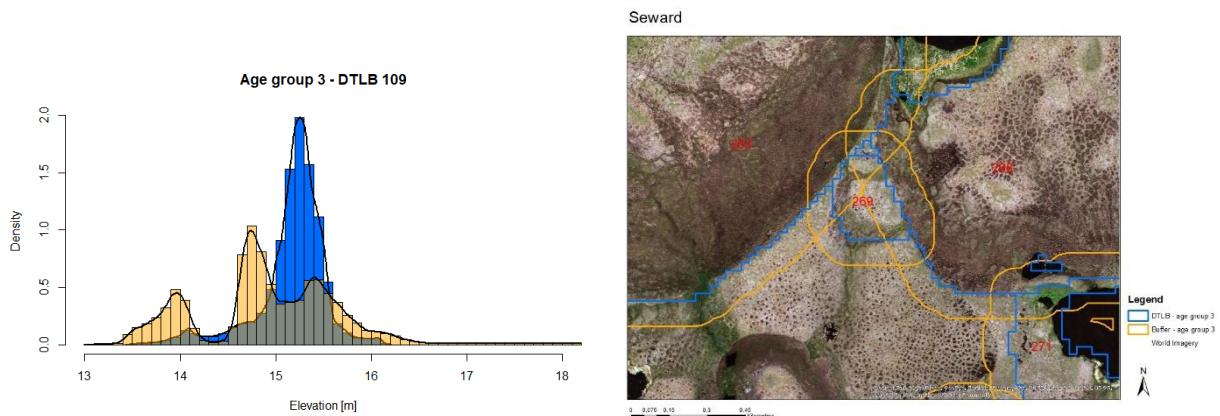


Figure 37: a) Density & Frequency plot and b) Map of DTLB 109 of age group 3 (OID 269)

4.3.4. Age group 4

In **age group 4** are 82 DTLBs of the age range 2000- 5000 years since their drainage. The average buffer area has a size of 0.51 km² with a mean height of 15.60 m and the basin area a size of 0.67 km² with a mean height of 15.52 m. The height difference is therefore as low as 0.08 m. The range of the values varies between minimums of 9.06 m on average for the buffer and of 11.26 m for the basins with maximum values of 20.61 m within the basins and of 24.34 m in their surrounding buffer zones. The full table of this age group is attached in appendix 6.

The coefficient of determination between the basin area and the buffer area for age group 4, resulted in $r^2 = 0.00369$. This result concludes in no correlation between the two values.

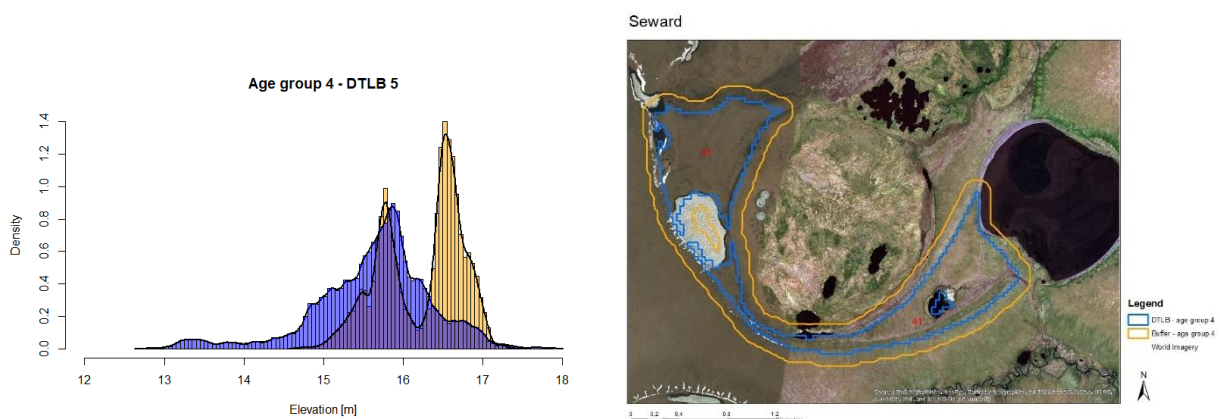


Figure 38: a) Density & Frequency plot and b) Map of DTLB 5 of age group 4 (OID 41)

Example one of this age group is DTLB 5 with a value range from 12.7 to almost 18 m within the basin. The enclosing buffer has a slightly smaller elevation range (table 7). Even though the basin values show a broad range, there is a clear peak to make out at about 15.9 m, compared to the buffer values with two distinct peaks at ~ 15.7 and ~ 16.7 m (fig. 38 a). The two peaks are resulting from the clear difference in altitude between the northern, lower, and southern, higher, side of the basin. The basin, which DTLB 5 is mostly surrounding in the north is of age group 3 (fig. 38 b). All buffer values within this basin are showing values between around 15 to 16 m and therefore corresponding to the lower buffer peak. Resulting of those two distribution patterns are mean height values of 15.64 m within the basin and 16.23 m around it

in the buffer area, resulting in a height difference of just 0.60 m between the two areas. Due to the elongated and thin form and the two parts of the DTLB, the area of the basin is big with 1.43 km² and, the buffer area is also relatively big with 0.32 km². The little ice-covered pond, which lies within the DTLB, is not included in the buffer values, like all ice-covered surfaces of the research area.

Table 7: Recalculated values of DTLB 5 and 32 of age group 4

ID	Object ID	DTLB Size	Buffer Size	Buffer Mean	DTLB Mean	Diff Buffer-DTLB Mean	Buffer Med	DTLB Med	Diff Buffer-DTLB Med
5	41	1436742.8	329021.1	16.23	15.64	0.60	16.43	15.73	0.71
32	189	685841.5	387494.9	12.81	11.57	1.24	11.90	11.60	0.31

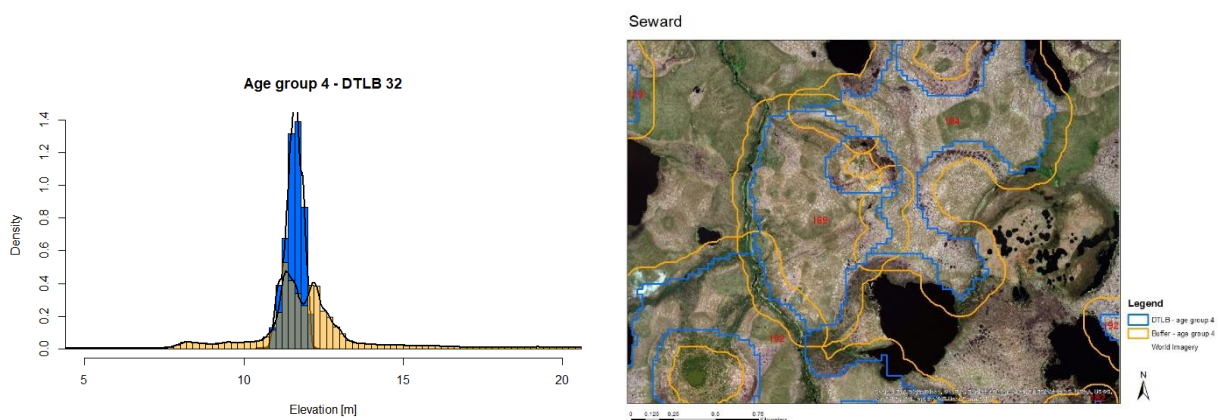


Figure 39: a) Density & Frequency plot and b) Map of DTLB 32 of age group 4 (OID 189)

The second example of age class 4, DTLB 32 (OID 189), has a difference between its basin and buffer twice the height difference of DTLB 5 with 1.24 m. The mean heights are much lower at 12.81 m for the buffer and 11.57 m for the basin. The range of the elevation has a greater variety as number 5, from -1.2 to 32.3 m including both, basin and buffer values and including many outliers out of the main range, which is between around 10 to 15 meters (fig. 39 a). Whereas the basin density shows one clear peak at about 12 m, the buffer density is split up into two peaks at slightly below and slightly above this value. Characteristic for this DTLB is the heavy intersecting and overlapping of mainly buffer areas. In the southeast, the buffer is showing low values, because it cuts a lower basin which is close to a nowadays lake (fig. 39 b). Further, the lowest values of the buffer can be allocated on the west side of the basin, where a water filled stream flows within the buffer zone.

4.3.5. Age group 5

Covering drainage events of ages older than 5000 years, **age group 5** is containing nine basins (table 8). The basins range from 0.17 to 2.26 km² and the according buffers from 0.19 to 1.80 km². The elevation varies between ~ 8 to ~52 m with some outliers reaching up to ~ 120 m. Striking are the four negative differences of buffer - DTLB mean values for DTLB 5, 6, 8 and 9 (OID 159, 161, 283, 293). When comparing the mean and median values and

differences, there is the same pattern to notice: The median values have slightly greater differences. The complete table can be found in appendix 7.

Table 8: Seward age group 5 DTLB and buffer sizes

ID	Object ID	DTLB Size	Buffer Size	Buffer Mean	DTLB Mean	Diff Buffer- DTLB Mean	Buffer Med	DTLB Med	Diff Buffer- DTLB Med
1	8	1124200.6	221625.2	29.23	25.39	3.84	29.43	24.84	4.59
2	61	151155.9	530641.2	33.41	15.91	17.51	36.27	15.42	20.85
3	68	335480.5	199765.5	42.27	20.81	21.46	43.42	21.04	22.38
4	157	248032.7	256617.9	32.59	27.22	5.37	36.02	27.54	8.49
5	159	102325.5	642634.9	20.72	42.63	-21.91	20.57	43.87	-23.29
6	161	175208.9	270732.6	21.17	24.58	-3.41	24.27	24.14	0.13
7	167	2620139.1	1805823.3	23.65	22.55	1.10	23.25	23.07	0.18
8	283	759267.5	222152.8	20.58	21.21	-0.64	19.85	21.17	-1.32
9	293	708517.7	496316.8	18.94	20.71	-1.77	19.08	21.02	-1.94
	Ø	691592.1	516256.7	26.95	24.56	2.40	28.02	24.68	3.34

As for the previous age groups, the coefficient of determination for the dependency of the basin size and buffer size was calculated. The result with $r^2 = 0.637$ is showing a minor dependency.

The elevation distribution patterns are classified into normal distribution, which includes DTLB 2. The bimodal category contains the basins number 1, 4, 6, 9 and buffer ID 2. A multimodal pattern are showing the basin and buffer values of ID 7 and 8. Additionally, buffers number 1, 4, 6 and 9 show a multimodal distribution. For the elevation distributions of DTLBs 3 and 5, no patterns could be found and could therefore not be categorized.

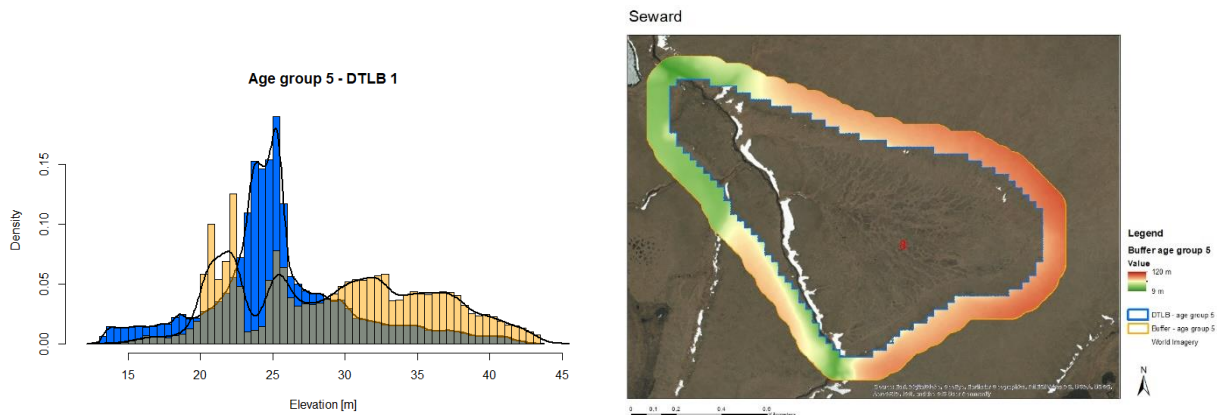


Figure 40: a) Density & Frequency plot and b) Map of DTLB 1 of age group 5 (OID 8)

The elevation range of DTLB 1 of age group 5 (OID 8) (fig. 40 a) is very high from 12.8 m to 43 m for the basin and 14.4 to 43.5 m for the buffer. It is the second biggest basin of age group 5 with an area of 1.12 km² and a surrounding buffer area of 0.22 km². The buffer mean at 29.23 m has a difference of 3.84 m in comparison to the basin mean at 25.39 m. Those elevation values are belonging to the higher ones of this age group. There is a very fine polygonal tundra pattern to notice in the basin and its direct surrounding (fig. 40 b). Furthermore, there is not much vegetation at this basin in contrast to many others, and there are just minor water-filled areas visible within the polygonal tundra structure. A small stream is crossing the basin from northwest to south. The basin looks like the catchment area of the stream from the east towards

the stream. This also corresponds with the higher elevation in the east and the lower elevation in the west.

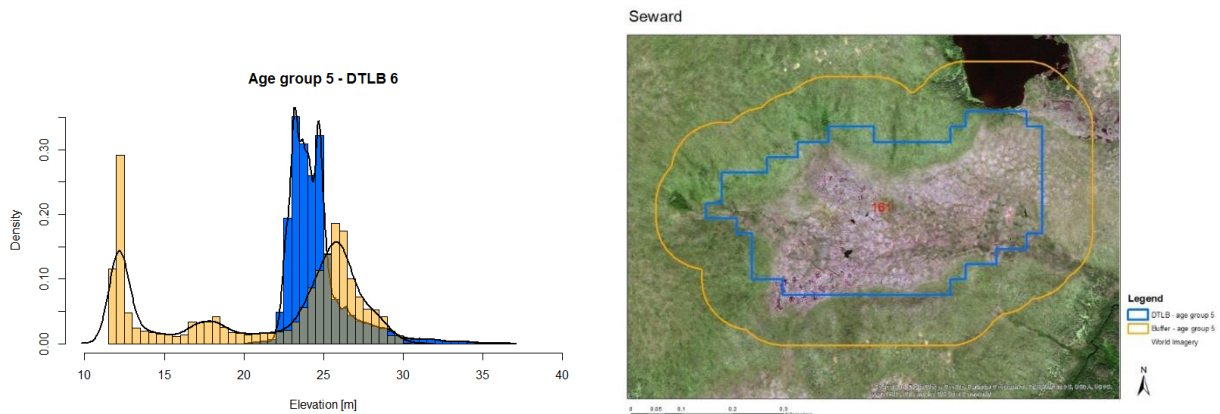


Figure 41: a) Density & Frequency plot and b) Map of DTLB 6 of age group 5 (OID 161)

The elevation values of the basin number 6 (fig. 41 a) are showing a mostly bell shape, overlooking the divided two peaks, whereas the buffer values are having three wide spread peaks below and above the mean basin elevation. In contrast to the elevation distribution and the irregular pattern of the buffer values, the average height of the basin is 24.58 m, and of the buffer is 21.17 m. These values are close, resulting in a difference of -3.41 m. The negative difference is not common, but the low peak of the buffer value at 12 m is reducing the average of all buffer values too much in contrast to the bigger peak at around 26 m, resulting in a lower mean elevation of the buffer than the basin itself. The low buffer peak reflects the area close to the lake shore and the adjacent basin in the northeast, which belongs to age group 2 (fig. 41 b). The high buffer peak is more widely spread, including a bigger value range, which is covering the area in the northwest to south. In general, the basin is showing a very distinct polygonal tundra structure in most parts. Little water- filled ponds already show the beginning of a new DTLB cycle. These ponds will most likely expand and connect to bigger ones in the future, creating a new thermokarst lake, which one day will drain again.

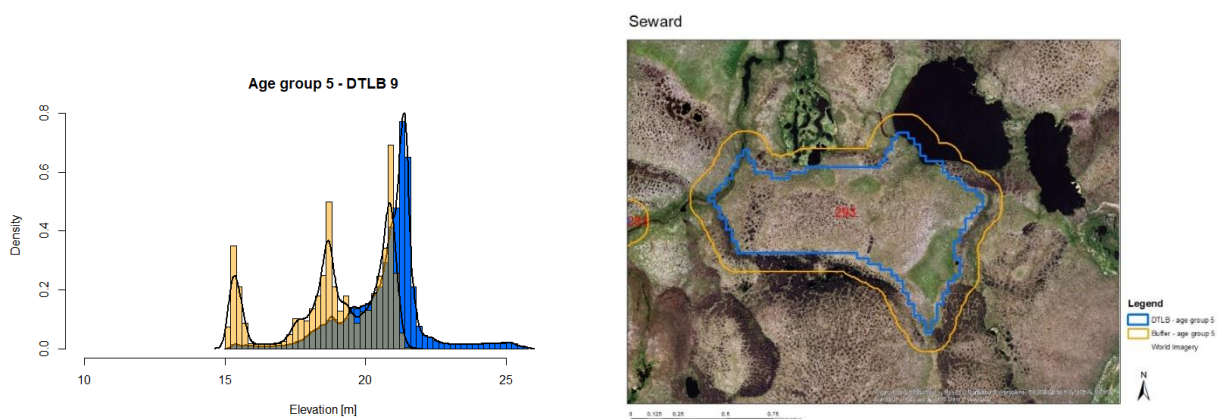


Figure 42: a) Density & Frequency plot and b) Map of DTLB 9 of age group 5 (OID 293)

The density & frequency plot of DTLB number 9 of the age group 5 (fig. 42 a) is showing a distribution of the buffer values mostly overlapping and mostly beneath the lower basin values.

The elevation ranges of the buffer and the basin are very similar, with 15.1 to 21.5 m for the buffer and 15.2 to 25.7 m for the basin. Still, the contrast of the average elevation of both is different with 18.9 m of the buffer and 20.7 m for the basin, resulting in a buffer minus basin result of -1.77 meters. Usually, the mean buffer height should be above the basin's average height. Here, the basin is mostly enclosed by basins of age group 3 and 4. It is possible, that both basins are increasing their ice content again and therefore also increase in their height (fig. 42 b). This means, that they are not exactly basins anymore, but accumulating new ground ice, which is already a next step in the thermokarst lake drainage cycle (see chapter 1.3).

4.3.6. Errors and Inaccuracies

The data set of the Seward DTLBs was primarily for another project of the AWI. Here the basins of the shape files have holes due to nowadays lakes, residual ponds, water outlets or other geomorphological structures. This results in some inaccuracies. An example for this is the buffer of DTLB 15 of age group 1 (OID 334) (fig. 32 b), where half of the buffer area lies within a lake and has therefore not the correct height difference to the DTLB itself and the overlapping DTLBs and buffer of OID 137 and 139 (fig. 43). The figure 35 is showing an extract of the age group 3, where due to the highest count of DTLBs, the highest rate of intersections occurred. This is a big source for errors in GIS attributable to the generation of buffer, which sometimes also include the inside area of the holes in the DTLB shapes. Due to this added complexity, the

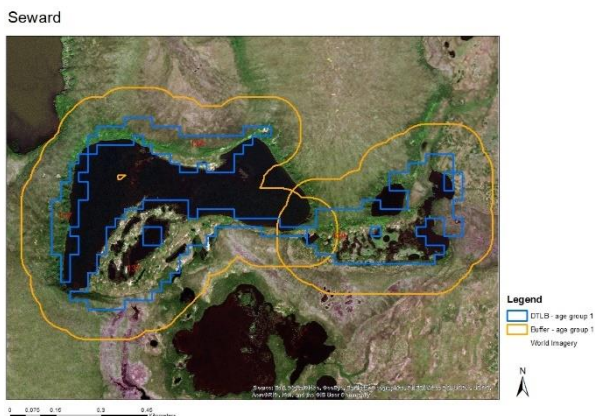


Figure 43: DTLBs 137 & 139 overlapping

height values for the buffer zones were often wrong in their extent, by including the basins itself, written to the data set in R. Therefore, the shape files then added with the elevation data to raster files, had to be clipped to the correct buffer outlines once more in ArcGIS. Also, there are quite a lot of overlapping basins and buffers in the dataset. Other than for the Barrow research site, at the Seward site some basins have buffer zones with at least the same size as the basins, or some buffer are even bigger than the basins.

When analyzing the data in R, another problem occurred, where DTLBs and their buffers showed up with the error “No Value” (N/A). This is most likely because of the unusual patterns that these have. When calculating the results for the tables and the density & frequency plots, the N/A values were omitted in order to get results for all DTLBs. Without omitting the N/A values, age group 2 would have 49 DTLBs with errors out of 140 DTLBs of the age group, which would not count into the results. On the other hand, both, the results with and without the omitted N/A values were controlled in ArcGIS, where the results of the without omitted N/A values do reflect the elevation patterns better than the results with omitted N/As do. Because of this, the density & frequency plots of age groups 3, 4 and 5 were created without omitted N/As, whereas all appendixes show the tables with omitted N/A values.

4.4. Comparison of Barrow and Seward

After the detailed analysis of the results of the two research sites, these will now be evaluated comparatively. In table 9, the average values of the DTLB and buffer sizes, heights and height differences named on the left, are listed for both research sites, Barrow and Seward. For Seward the results are separately listed per age class.

The average sizes of Drained Thermokarst Lake Basins vary significantly between Barrow and Seward. While the average area of basins varies between 0.34 to 0.92 km² for all Seward age groups, in Barrow the average size is 2.83 km². Furthermore, the minimum value, 0.68 km², and maximum, 11.95 km², for Barrow are much greater than the values of the five Seward groups, having 0.03 to 0.09 km² as minimum and 2.36 to 3.59 km² as maximum. In contrast, the average buffer areas do not vary much between the two sites, with a slightly higher value of 0.68 km² in Barrow, compared to Seward with 0.34 to 0.54 km².

The total height of both the research sites is very different is: The site of Barrow is at about 4 to 8 meters above sea level, whereas the Seward peninsula is at 8 to 25 meters a.s.l.. The Seward peninsula is not just at an overall higher altitude but has also a bigger variance in the height of its area.

Table 9: Combined data of Barrow and Seward

	Unit	Barrow	Seward	Seward	Seward	Seward	Seward
[1] Age group		-	1	2	3	4	5
[2] Years since drainage event		unknown	0-50	50-500	500-2000	2000-5000	>5000
[3] Number of DTLBs		20	20	140	188	82	9
[4] Average DTLBs size	[km ²]	2.83	0.76	0.40	0.85	0.67	0.69
[5] Minimum DTLBs size	[km ²]	0.68	0.09	0.02	0.06	0.05	0.10
[6] Maximum DTLBs size	[km ²]	11.95	3.59	2.71	4.82	2.52	2.60
[7] Buffer size mean	[km ²]	0.68	0.41	0.32	0.47	0.51	0.51
[8] Buffer height mean	[m]	5.93	15.93	16.35	15.13	15.60	26.95
[9] DTLBs height mean	[m]	5.28	14.43	15.13	14.89	15.52	24.56
[10] Diff. Buffer-DTLBs height mean	[m]	0.64	1.50	1.22	0.27	0.08	2.40
[11] Buffer height median	[m]	5.79	15.47	15.95	14.93	15.25	28.20
[12] DTLB height median	[m]	5.28	14.27	15.00	14.97	15.56	24.68
[13] Diff. Buffer-DTLB height median	[m]	0.52	1.21	0.95	-0.02	-0.31	3.34
[14] Buffer height max	[m]	8.86	23.52	26.31	23.67	24.34	48.38
[15] DTLB height max	[m]	6.83	20.46	21.03	19.35	20.61	43.61
[16] Diff. Buffer - DTLB max	[m]	2.07	3.06	5.28	4.39	3.73	4.77
[17] Buffer height min	[m]	3.97	11.42	8.68	8.75	9.07	15.69
[18] DTLB height min	[m]	4.03	11.61	10.59	10.86	11.26	16.33
[19] Diff. Buffer - DTLB min	[m]	- 0.06	-0.19	-1.90	-2.11	-2.19	-0.64

Most interesting for this study are the values of the average difference between the basin and its surrounding. The difference of the mean buffer - DTLB altitude (table 9, row 10) varies for both, Barrow and the Seward age groups. The biggest average difference is age group 5 (>5000 years) with 2.40 meters, followed by age group 1 (0 - 50 years) with 1.50 m and age group 2 (50 - 500 years) with 1.22 m. The next value of the decreasing row are the differences of Barrow with 0.64 m. Even less are the values of the two older age groups 3 (500 - 2000) and 4 (2000 - 5000) of Seward with 0.27 and 0.08 m respectively. There is no increase or decrease pattern in basin height against the age of the basins recognized.

When exclusively analyzing the median values of the Seward age classes, there can be seen an increase in the values of the DTLB height median (row 12) from young to old. While the change of values between age classes 1 to 4 are minor, the change to class 5 is significant with more than 10 m. For the buffer median it is similar with no to little variation of around 15 to 16 m of the heights of age classes 1 to 4, and a large increase to class 5, up to 28.2 meters. The same pattern can be seen for the average maximum heights of buffer and basins at Seward peninsula. Age classes 1 to 4 differ slightly around 19 to 21 m for the basins and 23 to 26 m for the buffer. Whereas the max buffer height of age class 5 is at 48 m and the basin is at 43 m. Looking at the differences of the median values, -0.02 to 3.34 m, there is no pattern between the age groups, but a random distribution of increase in height difference. In comparison to this, the average differences of the maximum values are slightly bigger from 3.06 in age group 1, increasing in value from age classes 4, 3, 5 and 2, up to 5.28 m.

Also, for the minimum values of basin and buffer altitude (row 17 and 18), age group 5 is showing the highest mean values, followed by age class 1, then 2, 3 and 4. Conspicuous is, that the minimum buffer values for all age groups at Seward and Barrow are lower than the basin values, even if just slightly. For all values other than the minimum, the basin is usually, as expected, lower than the surrounded buffer area.

Table 10: Comparison r^2

Category	R^2 result
Barrow	$r^2 = 0.88$
SW age 1	$r^2 = 0.801$
SW age 2	$r^2 = 0.0009$
SW age 3	$r^2 = 0.0012$
SW age 4	$r^2 = 0.0037$
SW age 5	$r^2 = 0.637$

Another comparison made for both research sites is the calculation of the coefficient of determination for the variables of the basin area and the buffer area. The comparison of the results is showing high values with over 0.8 for Barrow and for Seward age group 1, meaning a high dependency between the basin and buffer area. For Seward's age group 5 the result of r^2 is at just 0.6, which means that there is a low dependency. For the other three age groups 2, 3 and 4 values of close to 0 are the results, meaning no dependencies between the basin and buffer area.

At both research sites the distribution of the elevation values were very diverse. For Barrow and in Seward for all age groups, there were DTLBs of all classes of unimodal, bimodal, multimodal and without a distinct pattern. No system of distribution between the age classes can be distinguished.

5. Discussion

5.1. Interpretation of the results

The result chapter gave details on the distribution pattern of the elevation data of all DTLBs of both research sites, based on certain examples. Furthermore, with the analysis of the maps in addition to the density & frequency plots, a spatial topographic interpretation was done. Based on the comparison of the elevation data and the topography of the drained basins, some characteristics were noticed.

First, the general difference of elevation between the research sites does not make the data between the sites exactly comparable. For the Barrow site an average of 5 to 6 meter for the research area is calculated, compared to a mean elevation of 14 to 16 m for the Seward area. This results in 10 meters of elevation difference between the two sites, even though both sites are located at a peninsula and therefore directly surrounded by the sea.

The difference of more than 2 km² of the average DTLB size of 2.83 km² at Barrow and between 0.4 to 0.8 km² at Seward, is challenging for an adequate comparison. The difference of the buffer area is slightly higher at the Barrow site than at Seward, with 0.17 to 0.36 m respectively. These differences of both, basins and buffer areas are most likely not just because of natural causes, but also depending on the different sources of DTLB shape files. In contrast to the Seward site, where all basins are included in the data set, this is not the case for Barrow, where a random sampling of basins was done.

Resulting from this big difference between the basin areas of the two sites and the small difference between the buffer areas, different proportions between the basin and buffer area relation are the result. This contrasting relation between the basin and buffer area reflects in the result of the coefficient of determination between those two variables. Whereas there is a great dependency of the basin and buffer area at the Barrow site, at the Seward site just one out of five age groups (AG 1) is showing a dependency between those sizes. The other age classes, 2, 3, 4, and 5, are showing a random relation between the area of the basin and the area of the surrounding area. These results reflect the regular order of DTLBs without holes or rough edges at Barrow and Seward's age group 1 with their buffer areas fitting nicely around them. In contrast to this, DTLBs of the other age groups (2, 3, 4, 5) often show holes, lakes, cutouts or other openings, because of which the buffer zones are not perfectly surrounding the basins, but also fill out other gaps. Therefore, the areas of the buffers are in relation to the basin itself often bigger than for the groups with a "correct" basin/ buffer size relation, including Barrow and Seward age class 1.

Other than the area of the basins, the overlapping of basins is a negative point for the comparison due to data inaccuracies caused by the overlapping. For the Barrow site the DTLBs were digitalized without adjoining basins, so the buffer would not overlap. In contrast to this, there is a remarkable number of adjoining basins at the Seward research site. The more basins there are per age group at Seward, especially in class 2 and 3, with 140 and 188 basins respectively, the higher the number of adjoining basins and therefore overlapping buffer areas is. The buffer zones do not just overlap with each other, but also with areas of basins. A similar

problem to this is the inaccuracy of the digitalization at the Barrow site, where sometimes younger and older parts of a basin are included in one DTLB. The outlines are therefore sometimes not very precise when speaking about the differentiation of age classes or stadium within the thermokarst lake drainage cycle. This occurred, for example, at DTLB 14 at Barrow (fig. 16), where an older basin is included in a younger one.

Other structures, like residual ponds, channels and other ways of water discharge or deepening of the surface are pointwise influencing the minimum values of the basins and buffers. This leads to just certain, very low elevation values due to small structures. The minimum values do not resemble a bigger area, but mostly very little sections of either basins or buffers. Due to this fact, the minimum values and the differences between them, are not exactly useful for a comparison. The results of the differences of minimum values of buffer minus basin show a mix of positive and negative values. For all other values, the basin is usually, as expected, lower than the surrounded buffer area.

Regarding the files of the DTLB shapes as main data source, another big difference is the classification of the Seward data into five different age groups, whereas the Barrow data is not classified. Not just the age itself, but more factors, like vegetation and development of polygonal tundra, influence the state of the basins within the lake drainage cycle (Hinkel et al. 2003). It is not possible to say, which stage of the cycle is reached by a certain age of the basin since the drainage event. But it is easier to make a rough estimation of the stage within the cycle for DTLBs of a younger or older age class.

For the Seward peninsula, the age groups show features of an ongoing thaw lake cycle. In age group 1, there are still a lot of recent lakes overlapping with the basin (fig. 32 b), or big residual ponds within the basin (fig. 31 b), which might drain in the future, forming bigger multi-aged basins in the future. Additionally, there is mostly very little or no vegetation noticeable from World Imagery or Landsat images (fig. 30 b). In age group 2, there are not only some lake remains within the basins (fig. 34 b), but also a polygonal tundra pattern at an early stage and little vegetation (fig. 33b) can be determined. In the basins of age group 3, there are little to no lake remains to identify, more vegetation and some polygonal tundra forming (fig. 36 b). Within the basins of age group 4, a more distinct pattern of polygonal tundra can be found (fig. 39 b). At age group 5, mostly very distinct polygonal tundra structure is already developed, showing also small ponds (fig. 41 b, 42 b). Also, the elevation of these basins is already heightened due to an increase in the formation ground ice within the basin. Here, the start of a new lake and therefore a new cycle of the lake drainage cycle can be identified. Because of the low, to not existing height difference, not all those differences of age group 5 are useful for the height difference analysis. As a result, the landscape patterns match pretty good with the description of the Thermokarst Lake Drainage Cycle (Hinkel et al. 2003; Grosse et al. 2013).

The digitalized basins at Barrow were randomly picked, without a certain pattern or references of other projects. Basins of Barrow were categorized by Hinkel et al. (2003) into age groups by combining C14 ages, the vegetation cover extent and the analysis of the plant community composition for a study to determine the soil organic carbon (SOC) content. 558 basins were classified by Landsat- 7+ imagery, of which 77 basins were additionally verified in the field (Hinkel et al. 2003; Regmi et al. 2012). Hinkel et al. (2003) created four age groups for the 77 basins after the results of the C14 test results: one for “young” basins under 50 years since the

drainage; then a “medium” age class for basins drained in the last 50 to 300 years; followed by an “old” class for basins which drained 300 to 2000 years ago and the class “ancient” with basins, for which the drainage dates back to 2000 to 5500 years. These age groups do not differ much from the ones of the Seward data set by Jones et al. (2011), as the comparison of the two age classification in table 11 shows. The classification of Seward has one classified age class more and an additional one for basins of an unknown age. The advantage of the classification of the Barrow is the smaller age range of the medium group. But this is followed by an even larger range of age for the old age group from 300 to 5000 years in contrast to the medium class of Seward ranging from 500 to 2000 years, giving a clear disadvantage for this group. While the oldest age group of the Seward categorization is an open- end age range, the Barrow “ancient” class ends by the age of 5500 years and is not followed by an open range class. At both systems the age range increases by the older the age group gets.

Unfortunately, it was not possible to compare the digitalized DTLBs at Barrow of this study with the ones from Hinkel et al. (2003) to find out the age classes. Therefore, a direct comparison of basins with comparable age classes was not possible.

Table 11: Classification of age classes for Barrow and Seward after Jones et al. 2011 and Hinkel et al. 2003

Age class	Seward Jones et al. 2011	Barrow Hinkel et al. 2003
1	Modern 0 - 50	Young >50 years
2	Young 50 - 500	Medium 50 - 300 years
3	Medium 500 - 2000	Old 300 - 2000 years
4	Old 2000 - 5000	Ancient 2000 - 5500 years
5	Ancient >5000	---
0	unknown	---

For the Barrow research site, no placements of the basins within the Thermokarst Lake Drainage Cycle can be made from the gained results. But Bockheim/Hinkel (2012) found out, that for their established age classes of the DTLBs (see table 11) an increase of ice wedges from young to ancient from 0 % to 32 % can be determined. These results were gained by analyzing soil cores of a total of 138 basins and calculating the relation of soil cores with and without ice wedges per age group (Bockheim/Hinkel 2012). These results also indicate an increase in ice volume by an increasing age of the basins. This leads to the assumption, that by an increase in ice wedges, an increase of polygonal tundra structure is very likely. Both factors indicate an ongoing progress of the basins by age within the Thermokarst Lake Drainage Cycle.

Based on field sampling and the following analysis of those samples, Hinkel et al. (2003) gives an estimation of the “surface organic thickness” and the “ice content of uppermost permafrost (%)” per age class. The values of the ice content are fluctuating a lot between the age classes, but it can help, to get a rough estimation of how much ice can be expected in the ground.

Table 12: Extract of table to classify DTLBs from Hinkel et al. 2003

Age category	Young	Medium	Old	Ancient
Surface organic thickness (cm)	< 5	10 - 15	15 - 30	15 - 35
Ice content of uppermost permafrost (%)	30 - 70	15 - 50	20 - 60	30 - 65

More features than the already mentioned ones are to consider before interpreting the elevation difference between buffer and basin as the excess ice height/ volume. In general, there are different types of landscapes regarding how they developed and formed, which must be paid attention to. The basins do not have a straight cut off edge between the basin ground and the surrounding, but very diverse forms of slopes on the lake shores. Those need to be considered when digitalizing basins and when interpreting the results. It is an inconstant feature when it comes to the definition of the basin outline. Also, erosional remnants within the basins or remnants of lakes vary considerably between no remnants, to a mix of remaining lakes and uplifted ground due to various morphological reasons. Furthermore, is the observation of the sediments, the soil stratigraphy and possible taliks of interest.

At last, but as very important factor, it needs to be discussed on how important the distribution patterns of the elevation data are for the interpretation of the height differences. The four categories used are the one of normal, bimodal, multimodal distribution and one class without a pattern noticeable. The first assumption was to only use the class of normal distributed elevation data, because for those, the mean and median values resemble the best the whole distribution of the data. But the results show, that just very few basin and buffer elevation values are unimodal distributed. There are more basins than buffer with a unimodal pattern, but in general, the most data is of a bi - or multimodal distribution. Both research sites are showing these results. Analyzing just the unimodal class of elevation distribution would diminish the DTLB count tremendously. Therefore, all variations of distributions of elevation values should still be included. Only basins and buffer showing a negative difference of the surrounding minus the basin, are falsifying a result and should therefore be excluded. More important than the distribution is the displacement of the buffer values in comparison to the basin values, resulting in a positive height difference between the basin and the higher buffer around it.

All the mentioned points are important to include in the interpretation of the elevation differences. Table 13 summarizes the mean difference between buffer minus basin for Barrow and for Seward (SW) per age class.

Table 13: Mean differences of buffer - basin height

	Barrow	SW age 1	SW age 2	SW age 3	SW age 4	SW age 5
Diff. Buffer-DTLBs height mean [m]	0.64	1.50	1.22	0.27	0.08	2.40

These values should not be totally equalized with the absolute volume of excess ice in the surrounding of the basins. The absolute height above sea level and especially the local active layer depth and the permafrost depth need to be added. The mean elevation difference in addition with all the other named features to be included, can be used as basis for the estimation of the nowadays excess ice content. Whereas the maximum elevation difference can be interpreted as basis of the former content of excess ice. The higher the elevation difference is, the richer the areas ice content is.

Summarizing, that the values of the difference of the mean buffer minus basin values (table 13) need some deductions for all the named features, which need to be taken account of. Just after this, a height or better, a volume of excess ice can be given for the research sites by an interpolation of the small scaled values around the basins.

5.2. Evaluation of the Results and Outlook

The method used for this work is completely new. It was invented and executed for the first time. For a first attempt, the results are satisfying. Nevertheless, the method needs further work for improvement to be useful for bigger areas, a better handling of the data and especially concrete measurable results. For this, some considerations for improvements will be discussed in this chapter.

First, to make a better comparison between the two research sites of this work, more details about the data of Barrow need to be known. Additionally, the data sets should have the same number of basins. A good comparison is only possible when analyzing more DTLBs at Barrow and dividing the data in the same age classes as in the Seward data. For this, the basins of Barrow must be dated correctly, which most likely will need field work.

So far, the age group of the original Seward data was used with 5 different age classes at a logarithmic scale. It is uncertain, if another scale for the age groups might be more useful in terms of the interpretation of the results. Smaller age groups of less than 1000 years might be better for the interpretation. The range of age group 4 with 2000 to 5000 years is huge and differences within a 3000-year range of the draining of a basin might not be possible to determine.

One factor of inaccuracy is the determination of the outline of the basin and therefore the beginning of the buffer. This occurred especially at the Barrow site, where the basins were digitalized Landsat images. For this, a hypsometric analysis of the lakes and its surroundings might be useful. With this, a certain angle of basin to slope and to the surrounding could be determined in order to get a more comparable result for basin and buffer outlines.

Further on, some errors occurred because of overlapping of buffers with other basins or buffers. This mainly occurred at Seward peninsula, which has a higher density of DTLBs. Here, a topographic analysis of the intersections between buffers and basins could help to find errors or uncertainties.

Other possibilities of improvement for a more detailed or better proved excess ice content might be: An interpolation of the estimated excess ice content around the DTLBs over the whole area of the research site for a comprehensive result of the area, not just as pointwise measurements. Therefore, the mean elevation difference of a buffer could be used for an interpolation to get a first impression.

A comparison between the estimated results of excess ice values and the Northern Circumpolar Soil Map might be beneficial (Tarnocai et al. 2002). An additional idea is a comparison of the height differences of the basins and their surrounding with bathymetric profiles of the lake before they drained. For this, old bathymetric profiles would be needed, but a comparison could show, how the elevation difference changed from a water filled lake to a drained basin.

The Hillshades of the Arctic DEM, e. g. in figures 14 and 15, are showing some light stripes. These might have occurred due to certain signal error of the DEM data itself. Another source of error is the resampling with the method Nearest Neighbor. Other methods, like Bilinear or Cubic Convolution resampling could lead to better results for the Hillshade. But this is a minor error, since it does not directly influence the result, but just a form of displaying the data.

6. Conclusion

The results of the analysis of the elevation differences between the Drained Thermokarst Lake Basins and their surrounding are showing, that there are some differences between them, even if they are not enormous. So far, there cannot be a strict formula or way of interpretation given due to a number of varying factors which need to be considered. Determining the excess ice by a statistical analysis of a DEM by calculating the height differences between DTLBs and according buffer does work, but it needs to be calculated more detailed with more variables and is so far a very rough estimation. The result of this study is not one precise interpretation approach for excess ice from elevation difference of DTLBs and their surroundings, such an approach might be possible to establish with more data and with the validation of additional field sampling.

It was not possible to find a pattern of increasing or decreasing in the basin height, or the difference between basin and buffer, against the age of the basins. The biggest problem noticed is the correctness of DTLB outlines due to different age stadiums when digitalizing the DTLBs from satellite imagery. The outlines would partially be more differentiated, according to different ages. Further on, the rough age or a classification of the age, like for the Seward basins, is necessary for comparisons. This information was not available for the Barrow site at the time this research was done. This implies, that some more data, e.g. age estimations or more information on soil properties, would be necessary for proper comparisons. Additionally, it would be very interesting to compare the results of more research areas, either within Alaska, or also outside, like Northern Canada or Siberia. A validation with field samples could include soil profiles and their analysis, especially on ice and water content and dating with C14. Furthermore, a vegetation analysis of the basins including details on the vegetation species,

count and patterns is necessary together with characteristics on polygonal tundra and ice wedges. Certainly, the used methods will need an improvement as well.

All in all, the approach of estimating excess ground ice in Arctic tundra landscapes by a statistical analysis of drained thermokarst lake basins can be a good method for a mostly remote analysis of the change of thermokarst basins in the arctic. In the future there will be also methods like differential DEMs possible to include in order to see changes of DTLBs over the recent past. Methods and data sets can be improved to get more solid and concrete results out of the method. It is and will be even more important, to get to know more details on ground ice and its behavior within thermokarst structures and of course on permafrost ground in general. The importance of knowledge on ground ice for the behavior on permafrost degradation and thermokarst formation is very well summarized by a quote of Bockheim and Hinkel (2012):

“...the advantage of using excess ice metric is that it provides some indication of the potential morphological change resulting from volumetric loss and consolidation when the permafrost thaws and the embedded ice melts; loss of volume is reflected as overall surface subsidence or local thermokarst formation.”

The change of permafrost grounds by the degradation of excess ice and the change in thermokarst structures, involves a change in the whole system of this landscape type, including the physical, biological and social systems of those areas, as the IPCC quote on the cryosphere, mentioned in the introduction, states:

“The cryosphere is, however, not simply a passive indicator of climate change; changes in each component of the cryosphere have a significant and lasting impact on physical, biological and social systems.”
IPCC - Climate Change 2013 The Physical Science Basis (Vaughan et al. 2013)

Acknowledgements

First, I want to thank all the staff members at the Department of Physical Geography at the Catholic University of Eichstätt -Ingolstadt for the help and guidance throughout my master studies. A special thanks goes to the supervisor of my master thesis and several other projects during my master studies, Prof. Dr. Michael Becht, for the administrative support and his availability for questions.

The thesis was written at the Alfred-Wegener-Institute, where Dr. Moritz Langer, was my second supervisor. Thanks for your ideas for the thesis, instructions, discussions and help during the development of the topic. Other thanks go to the other students of the PermaRisk group, Tarek and Alex, for their help with R and general technical support.

Thanks to Julian for proof reading my thesis, and not only for your motivation, but also for the interesting scientific and off- topic discussions. I appreciate it a lot.

My biggest thanks go to my parents and my grandparents for their ongoing support and encouragement through my Bachelor and Master studies, all my travels in between and everything related to my years at University. You were a great help in various ways in those years!

My boyfriend Héctor was a great help for emotional support, proofreading and general motivation for the last part of my thesis. Thank you very much!

All my friends from University and outside University, thank you for your various ways of support throughout the last couple of years. It was you who made these years enjoyable and so memorable.

Bibliography

- Arp, C.; Jones, B.; Lu, Z.; Whitman, M. (2012): Shifting balance of thermokarst lake ice regimes across the Arctic Coastal Plain of northern Alaska. In *Geophys. Res. Lett.* 39 (16). DOI: 10.1029/2012GL052518.
- AWI (2019): Permafrost research at AWI. Available online at <https://www.awi.de/en/science/geosciences/permafrost-research.html>, checked on 12.09.2019.
- AWI PermaRisk (2019): Research group PermaRisk at AWI. Available online at <https://www.awi.de/forschung/nachwuchsgruppen/permarisk.html>, checked on 12.09.2019.
- Bockheim, J.; Everett, L.; Hinkel, K.; Nelson, F.; Brown, J. (1999): Soil Organic Carbon Storage and Distribution in Arctic Tundra, Barrow, Alaska. In *Soil Science Society of America Journal* 63 (4), p. 934. DOI: 10.2136/sssaj1999.634934x.
- Bockheim, J.; Hinkel, K. (2005): Characteristics and Significance of the Transition Zone in Drained Thaw-Lake Basins of the Arctic Coastal Plain, Alaska. In *ARCTIC* 58 (4), pp. 406–417.
- Bockheim, J.; Hinkel, K. (2012): Accumulation of Excess Ground Ice in an Age Sequence of Drained Thermokarst Lake Basins, Arctic Alaska. In *Permafrost and Periglacial Processes* 23 (3), pp. 231–236. DOI: 10.1002/ppp.1745.
- Boike, J.; Georgi, C.; Kirilin, G.; Muster, S.; Abramova, K.; Fedorova, I.; Chetverova, A.; Grigoriev, M.; Bornemann, N.; Langer, M. (2015): Thermal processes of thermokarst lakes in the continuous permafrost zone of northern Siberia – observations and modeling (Lena River Delta, Siberia). In *Biogeosciences* 12 (20), pp. 5941–5965. DOI: 10.5194/bg-12-5941-2015.
- Brown, J.; Ferrians, O.; Heginbottom, J.; Melnikov, E. (2002): Circum-Arctic Map of Permafrost and Ground-Ice Conditions, Version 2. [Indicate subset used]. Edited by National Snow and Ice Data Center. Available online at <https://nsidc.org/data/ggd318#>, checked on 05.06.2019.
- Brown, J.; Sidlauskas, F.; Delinski, G. (1997): Circum-Arctic map of permafrost and ground ice conditions. Reston Va., Denver Colo.: The Survey; For sale by Information Services.
- Candela, S.; Howat, I.; Noh, M.-J.; Porter, C.; Morin, P. (2017): ArcticDEM Validation and Accuracy Assessment. Available online at <http://adsabs.harvard.edu/abs/2017AGUFM.C51A0951C>, checked on 05.06.2019.
- Carson, C.; Hussey, K. (1962): The Oriented Lakes of Arctic Alaska. In *Iowa State University*, pp. 417–439.
- Climate Data (2019a): Climate Graph City of Barrow. Available online at <https://en.climate-data.org/north-america/united-states-of-america/alaska/barrow-1417/>, checked on 29.08.2019.

- Climate Data (2019b): Climate Graph of Deering. Available online at <https://en.climate-data.org/north-america/united-states-of-america/alaska/deering-124356/>, checked on 29.08.2019.
- Comiso, J.; Hall, D. (2014): Climate trends in the Arctic as observed from space. In *Wiley interdisciplinary reviews. Climate change* 5 (3), pp. 389–409. DOI: 10.1002/wcc.277.
- Dobinski, W. (2011): Permafrost. In *Earth-Science Reviews* 108 (3-4), pp. 158–169. DOI: 10.1016/j.earscirev.2011.06.007.
- ESRI (2019a): Arctic DEM Index & Data Download. Available online at <https://www.arcgis.com/apps/webappviewer/index.html?id=aff5fa8f5d5548c6bff44cc8be385f61>, checked on 05.05.2019.
- ESRI (2019b): World Imagery. Available online at <https://www.arcgis.com/home/item.html?id=10df2279f9684e4a9f6a7f08febac2a9>, checked on 05.06.2019.
- Frohn, R.; Hinkel, K.; Eisner, W. (2005): Satellite remote sensing classification of thaw lakes and drained thaw lake basins on the North Slope of Alaska. In *Remote Sensing of Environment* 97 (1), pp. 116–126. DOI: 10.1016/j.rse.2005.04.022.
- Gilbert, G.; Kanevskiy, M.; Murton, J. (2016): Recent Advances (2008-2015) in the Study of Ground Ice and Cryostratigraphy. In *Permafrost and Periglac. Process.* 27 (4), pp. 377–389. DOI: 10.1002/ppp.1912.
- Grosse, G.; Jones, B.; Arp, C. (2013): Thermokarst Lakes, Drainage, and Drained Basins. In J. Shroder, R. Giardino, J. Harbor (Eds.): *Treatise on geomorphology. Glacial and periglacial Geomorphology, Volume 8: Academic Press* (8), pp. 325–353.
- Grosse, G.; Romanovsky, V.; Jorgenson, T.; Anthony, K.; Brown, J.; Overduin, P. (2011): Vulnerability and Feedbacks of Permafrost to Climate Change // Vulnerability and feedbacks of permafrost to climate change. In *Eos Trans. AGU* 92 (9), p. 73. DOI: 10.1029/2011EO090001.
- Grosse, G.; Romanovsky, V.; Nelson, F.; Brown, J.; Lewkowicz, A. (2010): Why Permafrost Is Thawing, Not Melting. In *Eos Trans. AGU* 91 (9), p. 87. DOI: 10.1029/2010EO090003.
- Heginbottom, J. (2002): Permafrost mapping: a review. In *Progress in Physical Geography* 26 (4), pp. 623–642. DOI: 10.1191/0309133302pp355ra.
- Hinkel, K.; Eisner, W.; Bockheim, J.; Nelson, F.; Peterson, K.; Dai, X. (2003): Spatial Extent, Age, and Carbon Stocks in Drained Thaw Lake Basins on the Barrow Peninsula, Alaska. In *Arctic, Antarctic, and Alpine Research* 35 (3), pp. 291–300. DOI: 10.1657/1523-0430(2003)035[0291:SEAACS]2.0.CO;2.
- Hinkel, K.; Jones, B.; Eisner, W.; Cuomo, C.; Beck, R.; Frohn, R. (2007): Methods to assess natural and anthropogenic thaw lake drainage on the western Arctic coastal plain of northern Alaska. In *J. Geophys. Res.* 112 (F2), p. 241. DOI: 10.1029/2006JF000584.

- Hinkel, K.; Sheng, Y.; Lenters, J.; Lyons, E.; Beck, R.; Eisner, W.; Wang, J. (2012): Thermokarst Lakes on the Arctic Coastal Plain of Alaska: Geomorphic Controls on Bathymetry. In *Permafrost and Periglac. Process.* 23 (3), pp. 218–230. DOI: 10.1002/ppp.1744.
- Hope, C.; Schaefer, K. (2016): Economic impacts of carbon dioxide and methane released from thawing permafrost. In *Nature Clim Change* 6 (1), pp. 56–59. DOI: 10.1038/nclimate2807.
- Hopkins, D. (1949): Thaw Lakes and Thaw Sinks in the Imuruk Lake Area, Seward Peninsula, Alaska. In *The Journal of Geology* 57 (2).
- Jones, B.; Grosse, G.; Arp, C.; Jones, M.; Walter Anthony, K.; Romanovsky, V. (2011): Modern thermokarst lake dynamics in the continuous permafrost zone, northern Seward Peninsula, Alaska. In *J. Geophys. Res.* 116 (D15), p. 2422. DOI: 10.1029/2011JG001666.
- Jones, M.; Grosse, G.; Jones, B.; Walter Anthony, K. (2012): Peat accumulation in drained thermokarst lake basins in continuous, ice-rich permafrost, northern Seward Peninsula, Alaska. In *J. Geophys. Res.* 117 (G2), n/a-n/a. DOI: 10.1029/2011JG001766.
- Jorgenson, M.; Macander, M.; Jorgenson, J.; Ping, C.-L.; Harden, J. (2003): Ground ice and carbon characteristics of eroding coastal permafrost at Beaufort agoon, northern Alaska. In Marcia Phillips, Sarah M. Springman, Lukas U. Arenson (Eds.): *Proceedings of the 8th International Conference on Permafrost, 21-25 July 2003, Zurich, Switzerland*. Lisse: Balkema, 495-500.
- Jorgenson, T.; Yoshikawa, K.; Kanevskiy, M.; Shur, Y.; Romanovsky, V.; Marchenko, S.; Grosse, G.; Brown, J.; Jones, B. (2008): Permafrost Characteristics of Alaska. In *Institute of Northern Engineering, University of Alaska Fairbanks*.
- Larsen, J.; Fondahl, G. (2016): Arctic Human Development Report. In Igor S. Zonn, Andrey G. Kostianoy, Aleksandr V. Semenov (Eds.): *The Eastern Arctic Seas Encyclopedia*. Cham: Springer International Publishing, p. 22.
- Lee, H.; Swenson, S.; Slater, A.; Lawrence, D. (2014): Effects of excess ground ice on projections of permafrost in a warming climate. In *Environ. Res. Lett.* 9 (12), p. 124006. DOI: 10.1088/1748-9326/9/12/124006.
- Liu, L.; Schaefer, K.; Gusmeroli, A.; Grosse, G.; Jones, B.; Zhang, T.; Parsekian, A.; Zebker, H. (2014): Seasonal thaw settlement at drained thermokarst lake basins, Arctic Alaska. In *The Cryosphere* 8 (3), pp. 815–826. DOI: 10.5194/tc-8-815-2014.
- Muster, S.; Roth, K.; Langer, M.; Lange, S.; Cresto Aleina, F.; Bartsch, A.; Morgenstern, A.; Grosse, G.; Jones, B.; Sannel, A.; Sjöberg, Y.; Günther, F.; Andresen, C.; Veremeeva, A.; Lindgren, P.; Bouchard, F.; Lara, M.; Fortier, D.; Charbonneau, S.; Virtanen, T.; Hugelius, G.; Palmtag, J.; Siewert, M.; Riley, W.; Koven, C.; Boike, J. (2017): PeRL: a circum-Arctic Permafrost Region Pond and Lake database. In *Earth Syst. Sci. Data* 9 (1), pp. 317–348. DOI: 10.5194/essd-9-317-2017.
- National Snow and Ice Data Center (2019): Frozen ground. Available online at https://nsidc.org/cryosphere/frozenground/whereis_fg.html, checked on 29.05.2019.

- Polar Geospatial Centre (2018): Arctic DEM. With assistance of Claire Porter, Paul Morin, Ian Howat, Myoung-Jon Noh, Brian Bates, Kenneth Peterman et al. Available online at <https://www.pgc.umn.edu/data/arcticdem/>, checked on 31.05.2019.
- Regmi, P.; Grosse, G.; Jones, M.; Jones, B.; Anthony, K. (2012): Characterizing Post-Drainage Succession in Thermokarst Lake Basins on the Seward Peninsula, Alaska with TerraSAR-X Backscatter and Landsat-based NDVI Data. In *Remote Sensing* 4 (12), pp. 3741–3765. DOI: 10.3390/rs4123741.
- Rowland, J.; Jones, C.; Altmann, G.; Bryan, R.; Crosby, B.; Hinzman, L.; Kane, D.; Lawrence, D.; Mancino, A.; Marsh, P.; McNamara, J.; Romanvosky, V.; Toniolo, H.; Travis, B.; Trochim, E.; Wilson, C.; Geernaert, G. (2010): Arctic Landscapes in Transition: Responses to Thawing Permafrost. In *Eos Trans. AGU* 91 (26), pp. 229–230. DOI: 10.1029/2010EO260001.
- Sinergize (2019): Sentinel Hub. Available online at https://www.sentinel-hub.com/develop/documentation/eo_products/Landsat8EOproducts, checked on 30.08.2019.
- Stewart, M. (2018): World Imagery Map Contributors. Available online at <http://www.arcgis.com/home/item.html?id=10df2279f9684e4a9f6a7f08febac2a9>, checked on 21.09.2019.
- Tarnocai, C.; Kimble, J.; Swanson, D.; Goryachkin, S.; Naumov, Y.; Stolbovoi, V.; Jakobsen, B.; Broll, G.; Montanarella, L.; Arnoldussen, A.; Arnalds, O.; Yli-Halla, M. (2002): Northern Circumpolar Soil Map, Volume 1. National Snow and Ice Data Center. Available online at <https://nsidc.org/data/ggd602#>, checked on 16.09.2019.
- van Everdingen, R. (2005): Glossary of Permafrost and Related Ground-Ice Terms.
- Vaughan, D.; J.C. Comiso; I. Allison, J.; Carrasco, G.; Kaser, R.; Kwok; P. Mote; T. Murray; F. Paul; J. Ren; E. Rignot (2013): Observations: Cryosphere. In *Climate Change 2013: The Physical Science Basis. Contribution of Working Group I to the Fifth Assessment Report of the Intergovernmental Panel on*.
- Vonk, J.; Gustafsson, Ö. (2013): Permafrost-carbon complexities. In *Nature Geoscience* 6 (9), pp. 675–676. DOI: 10.1038/ngeo1937.

Eidesstaatliche Erklärung

Hiermit erkläre ich, **Lisa Annika Schramm**, geb. 13.07.1994 in Esslingen am Neckar, dass ich die vorliegende Masterarbeit mit dem englischen Titel „*Estimating excess ground ice in Arctic tundra landscapes by a statistical analysis of drained thermokarst lake basins - A comparison between research sites in Alaska*“ bzw. dem deutschen Titel „*Abschätzung von überschüssigem Bodeneis in arktischen Tundralandschaften anhand einer statistischen Analyse von Alasen - Ein Vergleich zwischen Untersuchungsgebieten in Alaska*“ selbstständig und ohne Hilfe Dritter verfasst habe.

Bei der Masterarbeit wurden keine anderen als die angegebenen Quellen und Hilfsmittel benutzt. Alle den angegebenen Quellen entnommenen wörtlichen oder sinngemäßen Inhalte wurden von mir entsprechend kenntlich gemacht. Die Arbeit wurde zu keiner anderen Prüfung eingereicht.

Potsdam, 24. September 2019

Lisa Schramm

Appendix

Appendix 1: Table Barrow, various buffer radii

I D	DTLB Size [m²]	Buffer 50m Size [m²]	Buffer 100m Size [m²]	Buffer 150m Size [m²]	Buffer 50m Mean	Buffer 100m Mean	Buffer 150m Mean	Buffer 50m Med	Buffer 100m Med	Buffer 150m Med	Buffer 50m Max	Buffer 100m Max	Buffer 150m Max	Buffer 50m Min	Buffer 100m Min	Buffer 150m Min
1	2419723	320295	655423	1005353	7.32	7.52	7.66	7.22	7.36	7.48	9.00	9.49	9.99	5.69	5.59	5.46
2	737345	212134	440012	683583	1.56	1.74	1.89	1.55	1.68	1.79	2.98	3.20	3.46	0.67	0.37	0.33
3	1904419	359585	731851	1117455	6.87	7.11	7.28	6.72	6.86	6.96	8.40	9.49	10.35	5.85	5.69	5.29
4	633220	157920	331547	520887	1.55	1.10	2.00	1.34	0.95	1.77	4.29	4.05	6.04	-1.30	-2.20	-1.42
5	3417157	349790	715237	1096340	1.15	1.31	1.40	1.36	1.49	1.56	3.29	4.18	5.42	-1.50	-1.63	-1.65
6	3046643	382351	778813	1187600	0.85	1.09	1.23	0.86	0.92	0.95	4.22	5.60	5.64	-2.09	-2.09	-2.70
7	3868608	396261	808340	1236069	16.32	16.36	16.37	16.27	16.33	16.40	17.20	19.25	19.66	14.75	14.60	14.35
8	11952064	710181	1435557	2176211	3.99	4.39	4.58	3.89	4.26	4.42	6.05	7.18	7.26	2.71	2.49	2.39
9	2431961	338854	693324	1063423	5.73	6.23	6.46	5.68	6.07	6.31	8.23	9.86	10.13	3.30	3.29	3.29
10	5624563	498794	1013288	1543462	6.99	7.04	7.02	6.91	6.91	6.88	8.46	9.18	9.46	5.71	5.20	4.54
11	2430490	305224	626184	962835	3.89	4.03	4.16	3.80	3.89	3.97	5.50	6.81	7.41	2.88	2.88	2.81
12	1436097	242264	499587	771996	3.01	3.22	3.38	3.02	3.15	3.26	4.65	5.32	6.68	1.22	1.06	1.06
13	791941	185206	385778	601449	4.42	4.74	5.03	4.16	4.41	5.02	7.51	8.84	9.91	3.55	3.47	3.27
14	3013737	391201	792560	1201484	1.09	1.23	1.34	1.04	1.17	1.26	1.97	2.55	2.59	0.34	0.25	0.18
15	2594511	337239	681082	1037117	3.16	3.50	3.70	2.92	3.29	3.56	7.49	7.77	7.82	0.59	0.59	0.54
16	3105136	425709	866977	1323743	10.47	10.56	10.60	9.96	9.91	9.90	14.31	14.67	14.80	8.94	8.94	8.84
17	1985544	320266	655917	1007007	8.41	8.65	8.81	8.70	8.77	8.78	12.10	13.87	14.20	6.10	6.10	6.06
18	1800122	276015	566525	871526	9.22	9.37	9.53	9.11	9.32	9.43	12.42	12.56	13.00	7.88	7.80	7.75
19	2753803	349356	714249	1094695	16.14	16.22	16.24	15.95	15.96	15.95	17.81	18.82	19.59	15.08	14.87	14.87
20	765907	186404	387777	604075	3.05	3.15	3.19	3.02	3.15	3.21	4.30	4.48	4.48	2.25	2.22	1.99

Appendix 2: Table Barrow, addition to table 3

<i>Lake OID</i>	DTLB Size [m²]	Buffer Size [m²]	Buffer Mean	DTLB Mean	Diff Buffer- DTLB Mean	Buffer Med	DTLB Med	Diff Buffer- DTLB Med	Buffer Max	DTLB Max	Diff Buffer- DTLB Max	Buffer Min	DTLB Min	Diff Buffer- DTLB Min
1	2419723	655423	7.52	6.85	0.66	7.36	6.79	0.57	9.49	9.37	0.12	5.59	5.58	0.006
2	737345	440012	1.74	1.17	0.57	1.68	1.16	0.51	3.20	2.21	0.99	0.37	0.53	-0.154
3	1904419	731851	7.11	6.29	0.81	6.86	6.29	0.57	9.49	6.97	2.52	5.69	5.74	-0.047
4	633220	331547	1.10	0.69	0.41	0.95	0.56	0.38	4.05	2.95	1.10	-2.20	-1.04	-1.152
5	3417157	715237	1.31	1.04	0.27	1.49	1.17	0.32	4.18	2.02	2.15	-1.64	-0.61	-1.024
6	3046643	778813	1.09	0.61	0.48	0.92	0.62	0.30	5.60	2.39	3.21	-2.10	-2.27	0.179
7	3868608	808340	16.36	15.98	0.37	16.33	15.95	0.37	19.25	16.87	2.37	14.60	14.73	-0.123
8	11952064	1435557	4.39	3.50	0.88	4.26	3.50	0.76	7.18	4.12	3.05	2.49	2.70	-0.208
9	2431961	693324	6.23	4.79	1.44	6.07	4.82	1.24	9.86	6.02	3.84	3.29	3.40	-0.104
10	5624563	1013288	7.04	6.76	0.27	6.91	6.73	0.18	9.18	7.80	1.38	5.20	5.69	-0.486
11	2430490	626184	4.03	3.43	0.59	3.89	3.38	0.51	6.81	4.88	1.93	2.88	2.91	-0.027
12	1436097	499587	3.22	2.49	0.72	3.15	2.47	0.68	5.32	3.67	1.64	1.06	1.17	-0.115
13	791941	385778	4.74	4.07	0.67	4.41	4.07	0.34	8.84	5.25	3.58	3.47	3.61	-0.143
14	3013737	792560	1.23	0.75	0.48	1.17	0.75	0.42	2.56	1.69	0.86	0.25	-2.05	2.312
15	2594511	681082	3.50	2.43	1.06	3.29	2.44	0.84	7.77	5.87	1.89	0.59	0.72	-0.127
16	3105136	866977	10.56	9.71	0.84	9.91	9.67	0.24	14.67	12.63	2.04	8.94	8.92	0.020
17	1985544	655917	8.65	8.25	0.39	8.77	8.30	0.47	13.87	9.32	4.55	6.10	6.09	0.012
18	1800122	566525	9.38	8.48	0.89	9.32	8.50	0.82	12.56	12.42	0.14	7.80	7.73	0.068
19	2753803	714249	16.22	15.78	0.44	15.96	15.76	0.19	18.82	16.72	2.10	14.87	14.83	0.040
20	765907	387777	3.15	2.61	0.54	3.15	2.59	0.55	4.48	3.45	1.02	2.22	2.171	0.050
∅	2835650	689001	5.93	5.28	0.64	5.79	5.28	0.52	8.86	6.83	2.07	3.97	4.02	0.007

Appendix 3: Table Seward age group 1, addition to table 4

ID	Object ID	DTLB Size [m²]	Buffer Size	Buffer Mean	DTLB Mean	Diff Buffer-DTLB Mean	Buffer Med	DTLB Med	Diff Buffer-DTLB Med	Buffer Max	DTLB Max	Diff Buffer-DTLB Max	Buffer Min	DTLB Min	Diff Buffer-DTLB Min
1	1	3588060.9	1108831.6	16.07	14.67	1.39	15.95	14.65	1.30	30.42	18.00	12.42	14.34	13.42	0.91
2	2	95896.4	197336.4	10.04	9.11	0.93	10.15	9.11	1.04	14.47	10.92	3.55	8.23	8.28	-0.05
3	3	3594678.3	813143.0	16.85	14.99	1.86	16.38	14.96	1.42	21.59	20.67	0.92	14.00	13.23	0.77
4	4	1054541.9	489509.7	14.42	12.50	1.92	14.09	12.52	1.58	20.93	14.94	5.99	11.23	11.39	-0.16
5	133	1722994.9	641490.4	17.29	16.16	1.13	17.20	16.08	1.12	24.18	24.40	-0.22	15.00	15.09	-0.09
6	137	184393.5	438206.7	24.32	19.72	4.60	21.43	17.93	3.50	39.29	32.11	7.18	4.31	13.69	-9.37
7	139	106026.2	207071.4	20.63	18.14	2.48	18.11	17.30	0.81	36.18	28.98	7.21	10.84	11.40	-0.55
8	178	566100.8	335422.5	18.09	17.31	0.78	17.89	17.22	0.67	22.45	22.32	0.13	13.64	12.45	1.19
9	186	487649.9	346831.8	18.60	17.19	1.40	17.66	17.12	0.55	31.27	26.84	4.43	11.28	11.26	0.02
10	211	180619.9	210161.7	11.62	11.16	0.46	11.71	11.16	0.56	14.24	13.77	0.47	7.81	9.86	-2.05
11	250	300535.7	407779.7	16.70	14.12	2.58	15.73	13.80	1.94	40.29	40.36	-0.07	12.16	12.00	0.17
12	258	707493.0	421885.6	24.59	23.08	1.52	23.89	23.17	0.72	37.20	28.28	8.92	20.19	15.11	5.08
13	294	127307.7	186473.8	19.17	18.26	0.91	19.00	18.39	0.61	22.46	20.95	1.51	16.68	16.57	0.11
14	296	370909.9	366250.2	12.73	12.08	0.66	12.76	12.15	0.61	14.47	13.83	0.63	10.57	10.02	0.55
15	334	451883.8	643820.7	15.81	15.70	0.11	15.63	15.66	-0.04	19.81	19.81	0.00	14.74	14.66	0.08
16	349	135551.6	199492.0	14.98	14.12	0.85	15.26	14.10	1.16	16.05	15.69	0.37	12.35	12.71	-0.36
17	352	380823.1	322797.9	9.95	8.68	1.27	10.02	8.48	1.55	11.68	11.14	0.55	7.06	7.18	-0.12
18	367	235116.4	331970.6	9.70	7.38	2.32	9.98	7.41	2.56	14.66	14.02	0.64	3.09	4.94	-1.85
19	420	435936.9	306578.2	12.09	10.46	1.63	11.73	10.46	1.28	17.60	16.11	1.49	8.66	6.58	2.08
20	422	497674.8	317371.6	15.01	13.72	1.28	14.87	13.68	1.19	21.10	16.03	5.07	12.19	12.36	-0.17
	Ø	761209.8	414621.3	15.93	14.43	1.50	15.47	14.27	1.21	23.52	20.46	3.06	11.42	11.61	-0.19

Appendix 4: Table Seward age group 2

ID	Object ID	DTLB Size	Buffer Size	Buffer Mean	DTLB Mean	Diff Buffer-DTLB Mean	Buffer Med	DTLB Med	Diff Buffer-DTLB Med	Buffer Max	DTLB Max	Diff Buffer-DTLB Max	Buffer Min	DTLB Min	Diff Buffer-DTLB Min
1	7	226860.9	111782.0	15.11	23.05	-7.94	15.15	23.12	-7.97	15.86	31.39	-15.53	13.88	17.52	-3.64
2	13	89443.8	173447.4	8.76	21.27	-12.51	8.80	20.95	-12.16	10.24	25.58	-15.34	4.65	16.96	-12.30
3	14	757868.6	335145.7	11.42	10.69	0.74	10.87	11.16	-0.29	15.41	17.55	-2.14	8.94	3.72	5.23
4	15	874022.9	176528.9	10.09	12.80	-2.70	10.65	11.74	-1.09	40.74	31.25	9.50	-5.33	2.61	-7.94
5	17	341100.3	141246.1	12.03	10.78	1.25	12.47	10.72	1.76	13.76	12.08	1.68	7.90	9.50	-1.59
6	19	35952.8	193172.7	15.08	10.83	4.25	15.37	10.68	4.69	15.86	14.40	1.46	12.68	9.38	3.30
7	20	472012.8	863674.3	32.59	12.64	19.96	27.03	11.29	15.74	205.48	32.99	172.50	-11.72	3.89	-15.61
8	24	126287.9	148794.6	13.10	8.02	5.08	12.80	8.33	4.47	17.43	9.16	8.27	9.06	5.04	4.02
9	25	102322.6	560764.9	15.76	8.88	6.88	15.54	8.61	6.92	26.54	12.29	14.24	-17.78	5.35	-23.13
10	28	168687.5	242887.6	14.64	19.44	-4.80	14.21	19.08	-4.87	20.64	33.52	-12.88	9.09	-2.29	11.39
11	29	938465.2	176155.5	9.75	10.15	-0.40	9.55	10.19	-0.64	13.53	35.27	-21.74	5.92	1.22	4.69
12	30	171475.0	108391.1	11.40	20.67	-9.28	11.49	19.29	-7.79	13.59	35.34	-21.75	9.52	13.66	-4.15
13	31	838784.2	239709.6	7.88	8.80	-0.92	7.95	9.05	-1.10	9.96	19.21	-9.24	4.33	-2.87	7.19
14	32	335508.7	368690.5	9.78	10.20	-0.43	10.31	10.25	0.06	12.97	12.49	0.48	-0.89	7.74	-8.63
15	40	2717620.4	428400.8	13.73	22.08	-8.35	13.87	22.12	-8.25	16.89	32.88	-15.99	9.01	8.80	0.21
16	43	370705.9	358370.5	12.64	25.03	-12.39	12.75	23.64	-10.89	15.23	48.81	-33.57	9.48	-1.29	10.77
17	44	816053.5	358622.7	13.74	20.83	-7.09	13.83	20.83	-6.99	18.28	27.23	-8.95	11.19	15.44	-4.25
18	46	223131.1	271025.1	13.84	18.11	-4.27	13.67	18.17	-4.50	19.58	24.35	-4.77	8.18	11.10	-2.93
19	47	283048.9	315400.6	14.15	17.71	-3.56	14.35	17.79	-3.43	17.25	20.62	-3.36	10.75	13.91	-3.16
20	50	260891.2	304795.8	10.70	16.30	-5.61	11.41	16.20	-4.79	17.82	26.27	-8.45	-7.98	10.50	-18.48
21	51	355829.9	187722.0	18.80	16.92	1.89	18.78	17.09	1.69	19.93	20.22	-0.30	17.25	13.70	3.55
22	54	868323.9	549912.7	21.17	24.09	-2.92	20.97	22.83	-1.86	29.42	40.84	-11.42	19.96	14.96	5.01
23	55	182548.5	456478.7	13.59	17.31	-3.72	13.16	16.55	-3.39	16.10	27.68	-11.58	10.34	14.34	-4.01
24	60	450706.8	495755.6	17.70	10.28	7.42	17.32	10.15	7.18	32.37	14.21	18.17	4.14	8.74	-4.61
25	64	94008.1	285114.0	14.48	9.58	4.90	13.61	10.09	3.52	27.25	18.53	8.72	8.11	1.42	6.69
26	67	379690.5	480751.8	10.55	10.62	-0.07	8.83	10.64	-1.81	112.97	15.18	97.79	-7.52	7.45	-14.98
27	71	793805.9	312823.2	8.43	17.53	-9.10	8.77	17.55	-8.78	11.12	19.69	-8.57	4.93	16.44	-11.51
28	72	356807.2	568041.8	23.79	20.01	3.78	23.92	20.27	3.65	29.32	25.38	3.94	14.39	15.43	-1.04

ID	Object ID	DTLB Size	Buffer Size	Buffer Mean	DTLB Mean	Diff Buffer-DTLB Mean	Buffer Med	DTLB Med	Diff Buffer-DTLB Med	Buffer Max	DTLB Max	Diff Buffer-DTLB Max	Buffer Min	DTLB Min	Diff Buffer-DTLB Min
29	73	350344.7	193971.9	15.84	21.74	-5.90	15.65	21.73	-6.08	20.01	26.80	-6.79	14.26	11.92	2.34
30	75	51627.2	617762.4	19.91	19.37	0.53	19.61	19.45	0.16	27.62	20.46	7.16	17.95	15.68	2.27
31	78	154886.9	183829.9	13.25	18.49	-5.24	13.11	18.76	-5.65	16.64	25.45	-8.81	10.63	9.87	0.76
32	82	140106.9	233984.4	7.32	15.46	-8.14	7.36	14.83	-7.46	8.78	26.54	-17.75	4.24	3.45	0.79
33	83	288495.1	265574.4	10.08	12.89	-2.82	11.44	12.87	-1.43	17.69	23.33	-5.64	0.40	9.96	-9.56
34	91	337315.1	136840.2	19.84	10.84	9.00	20.03	11.00	9.03	22.30	16.26	6.04	17.37	5.03	12.34
35	92	299518.9	315516.5	16.44	8.89	7.55	16.39	8.89	7.50	20.49	10.45	10.05	14.66	6.72	7.94
36	100	358497.0	208621.2	12.13	10.09	2.04	11.97	10.20	1.77	14.45	12.84	1.61	10.83	-9.64	20.47
37	102	1018538.2	421939.0	11.67	12.20	-0.53	11.60	12.21	-0.60	18.00	15.28	2.72	1.27	11.34	-10.08
38	107	286646.6	191474.2	7.23	12.63	-5.40	8.19	12.63	-4.44	10.41	13.68	-3.27	4.22	10.81	-6.59
39	108	797270.9	194804.0	12.82	13.35	-0.53	12.96	13.29	-0.33	22.11	16.15	5.96	4.56	8.08	-3.53
40	114	706048.5	268492.2	22.35	13.40	8.94	21.29	13.43	7.86	33.36	16.17	17.20	12.83	10.17	2.66
41	115	129048.7	235427.6	13.61	14.34	-0.73	13.14	13.66	-0.52	20.39	28.77	-8.37	11.35	3.82	7.53
42	117	1244448.4	352413.2	16.64	16.31	0.34	16.12	16.41	-0.29	22.00	27.51	-5.51	13.42	9.94	3.47
43	118	125345.8	430707.1	15.95	13.44	2.51	14.89	13.06	1.83	30.06	17.47	12.59	6.00	11.05	-5.06
44	120	157624.8	257965.1	18.19	15.52	2.66	15.27	15.52	-0.25	32.79	16.92	15.86	-0.42	14.72	-15.14
45	126	82034.9	351143.6	10.41	11.96	-1.55	10.18	11.91	-1.74	18.29	14.57	3.72	3.93	11.19	-7.26
46	128	322616.4	318272.8	23.39	13.28	10.11	21.96	13.22	8.74	37.80	23.64	14.16	11.39	7.73	3.66
47	130	251646.3	628955.2	8.77	16.30	-7.53	8.82	16.26	-7.44	10.74	18.79	-8.04	4.11	14.50	-10.39
48	131	69124.4	307390.9	15.29	11.44	3.84	15.38	11.16	4.23	17.98	15.47	2.50	10.38	5.32	5.06
49	135	1076818.3	433941.2	21.36	17.10	4.26	21.13	16.74	4.39	25.84	32.14	-6.30	19.13	13.71	5.42
50	136	230468.0	160594.9	22.81	17.36	5.45	21.95	17.46	4.49	33.91	19.00	14.92	15.98	11.37	4.62
51	140	95890.4	441678.5	18.25	25.01	-6.76	18.16	24.17	-6.01	19.90	32.17	-12.28	14.27	20.37	-6.10
52	142	2444251.4	125220.3	11.56	17.97	-6.40	11.36	17.81	-6.45	17.97	33.34	-15.38	9.36	14.07	-4.71
53	143	177015.9	229500.3	25.94	20.27	5.67	25.74	20.29	5.46	33.42	22.67	10.76	15.09	19.28	-4.19
54	149	491329.4	275713.4	10.92	16.23	-5.31	10.74	16.03	-5.29	15.27	29.46	-14.19	9.40	10.37	-0.97
55	150	298691.4	320414.8	18.56	17.01	1.55	18.60	17.01	1.58	26.95	19.01	7.94	13.28	14.19	-0.90
56	151	210197.4	555883.7	18.32	16.61	1.71	17.04	16.56	0.48	33.37	22.14	11.22	6.86	13.00	-6.15
57	153	417631.2	216765.0	19.81	15.03	4.78	17.65	15.16	2.49	31.24	19.61	11.62	15.53	7.63	7.89
58	154	233258.0	262063.1	9.55	16.61	-7.07	8.77	16.30	-7.52	17.68	21.16	-3.48	1.09	12.23	-11.14
59	158	106040.3	377620.4	19.43	40.85	-21.41	16.64	40.94	-24.30	36.02	49.83	-13.81	10.63	33.79	-23.16

ID	Object ID	DTLB Size	Buffer Size	Buffer Mean	DTLB Mean	Diff Buffer-DTLB Mean	Buffer Med	DTLB Med	Diff Buffer-DTLB Med	Buffer Max	DTLB Max	Diff Buffer-DTLB Max	Buffer Min	DTLB Min	Diff Buffer-DTLB Min
60	162	601351.7	303400.0	18.14	22.05	-3.91	17.93	21.79	-3.86	24.47	34.84	-10.37	13.64	2.93	10.70
61	163	997864.4	678210.7	13.50	23.52	-10.03	13.41	23.51	-10.10	15.04	25.69	-10.65	10.92	16.80	-5.87
62	164	148487.6	209799.6	17.71	25.44	-7.73	17.68	25.50	-7.82	25.50	31.71	-6.22	15.99	24.17	-8.19
63	170	478573.9	281537.5	11.88	19.08	-7.19	11.10	19.11	-8.01	26.16	20.03	6.13	4.55	16.92	-12.37
64	173	88519.7	212499.0	18.83	17.20	1.62	16.91	17.14	-0.23	27.51	21.29	6.21	9.66	15.60	-5.95
65	177	171501.3	253664.9	17.48	16.24	1.24	17.33	16.02	1.31	21.61	28.56	-6.94	13.65	6.71	6.94
66	179	281208.5	251552.7	25.92	17.88	8.04	24.50	17.93	6.56	37.37	18.62	18.75	17.21	16.80	0.41
67	185	665596.4	331657.9	12.88	17.24	-4.36	11.71	17.28	-5.57	29.23	20.28	8.95	7.79	14.22	-6.44
68	187	273793.5	659195.0	22.09	15.67	6.42	19.14	15.95	3.19	39.95	18.09	21.86	1.84	10.68	-8.84
69	193	464571.3	152749.0	13.36	13.50	-0.14	13.35	13.17	0.18	25.73	23.57	2.16	2.00	6.91	-4.92
70	198	601903.6	235599.6	19.05	13.93	5.11	18.53	13.73	4.79	33.14	21.01	12.13	1.18	10.86	-9.68
71	200	212912.8	221378.9	17.69	12.81	4.88	16.13	12.75	3.38	29.84	18.34	11.51	3.64	10.35	-6.70
72	203	106913.5	221161.4	16.56	12.08	4.48	16.21	11.86	4.35	25.37	20.54	4.83	14.13	6.58	7.56
73	205	416543.6	410187.0	16.60	10.81	5.80	15.23	11.09	4.14	29.50	14.64	14.86	-0.79	0.08	-0.87
74	209	665369.9	174935.3	15.40	12.40	3.00	15.30	12.55	2.75	26.67	15.53	11.15	7.64	10.64	-3.00
75	215	109677.3	297176.2	19.21	13.71	5.50	18.45	13.96	4.49	33.14	19.63	13.50	5.51	10.47	-4.96
76	216	101382.3	316340.0	18.42	13.22	5.20	18.53	12.87	5.66	21.23	19.33	1.89	13.76	12.10	1.66
77	221	188025.0	429594.9	12.45	16.48	-4.03	12.35	16.38	-4.03	15.40	20.85	-5.45	11.26	15.03	-3.77
78	223	73740.9	375008.5	11.76	16.59	-4.83	11.78	15.99	-4.21	12.94	24.28	-11.34	6.24	14.38	-8.14
79	224	84802.5	189893.4	16.29	17.81	-1.51	15.91	17.15	-1.24	22.44	29.30	-6.87	12.90	16.58	-3.68
80	225	205560.5	169763.8	15.59	22.03	-6.44	15.26	20.91	-5.65	23.72	30.75	-7.03	9.09	15.60	-6.51
81	226	171442.3	166520.8	28.15	15.56	12.59	30.89	15.49	15.41	34.90	19.75	15.15	17.38	13.36	4.02
82	229	126286.0	333249.2	23.15	15.38	7.77	21.91	15.19	6.72	35.57	25.30	10.26	16.03	6.49	9.54
83	230	1049741.3	475497.4	19.64	13.59	6.05	19.54	13.49	6.05	21.02	30.30	-9.28	18.95	11.93	7.02
84	235	601819.7	257603.3	9.53	12.72	-3.19	9.31	12.65	-3.34	15.49	19.15	-3.66	4.48	5.30	-0.81
85	236	198152.6	343594.8	10.46	11.97	-1.51	10.57	12.16	-1.59	14.83	12.87	1.96	-0.19	4.27	-4.46
86	237	235949.1	306096.5	18.49	11.43	7.06	18.27	11.35	6.92	21.63	21.49	0.14	14.61	1.33	13.28
87	238	68192.9	253217.8	28.03	11.39	16.64	27.95	11.19	16.76	31.81	13.07	18.73	26.18	8.56	17.62
88	239	191709.0	164756.0	11.02	11.27	-0.25	10.82	10.93	-0.10	12.69	22.93	-10.24	9.23	8.00	1.23
89	243	139194.6	244130.4	17.12	18.48	-1.36	17.17	18.51	-1.33	25.89	19.16	6.73	3.74	17.90	-14.15
90	249	435108.5	364658.3	11.38	13.54	-2.16	11.04	13.15	-2.11	13.41	26.56	-13.15	9.95	-1.69	11.63

ID	Object ID	DTLB Size	Buffer Size	Buffer Mean	DTLB Mean	Diff Buffer- DTLB Mean	Buffer Med	DTLB Med	Diff Buffer- DTLB Med	Buffer Max	DTLB Max	Diff Buffer- DTLB Max	Buffer Min	DTLB Min	Diff Buffer- DTLB Min
91	253	822492.2	591574.7	21.25	17.64	3.61	21.09	17.60	3.50	31.87	23.24	8.63	11.79	9.34	2.45
92	254	204774.2	340580.2	26.15	25.89	0.26	26.25	25.89	0.37	30.43	29.30	1.13	16.40	21.05	-4.65
93	257	807092.2	713152.2	24.30	23.63	0.67	21.02	23.46	-2.43	43.13	34.84	8.29	10.84	19.79	-8.95
94	260	207563.7	303034.4	8.53	28.14	-19.61	8.52	28.10	-19.58	10.10	30.80	-20.70	5.29	25.89	-20.60
95	262	283204.5	442298.0	35.50	27.83	7.68	37.52	26.76	10.76	49.18	43.94	5.23	10.69	13.61	-2.91
96	266	289616.8	237842.5	12.09	20.04	-7.95	10.75	19.83	-9.08	26.11	21.77	4.34	7.71	19.12	-11.41
97	267	391983.3	215238.3	20.55	19.14	1.40	16.65	19.17	-2.52	33.97	19.98	14.00	7.28	17.53	-10.25
98	274	1689103.8	198044.7	28.00	19.43	8.57	30.31	19.51	10.80	40.17	21.29	18.88	5.67	17.85	-12.18
99	275	279541.6	267411.8	17.99	20.86	-2.86	18.00	20.87	-2.87	20.61	26.89	-6.28	15.50	19.21	-3.70
100	276	184519.5	180412.2	46.07	21.08	25.00	47.77	20.90	26.87	51.82	29.57	22.25	31.67	19.90	11.76
101	277	1179087.6	281278.1	32.67	21.08	11.59	28.02	20.99	7.03	48.66	28.10	20.56	12.59	20.16	-7.57
102	284	394920.7	289208.1	16.43	15.80	0.64	15.09	15.81	-0.72	41.73	17.61	24.12	1.65	14.86	-13.21
103	285	106116.3	418259.5	10.37	15.56	-5.20	10.41	14.92	-4.51	12.89	22.60	-9.71	8.20	12.82	-4.62
104	289	232504.7	194553.6	8.82	15.43	-6.60	9.42	15.61	-6.19	11.78	20.71	-8.92	4.27	12.39	-8.12
105	297	263890.0	121639.3	7.73	12.49	-4.76	7.25	12.51	-5.25	11.10	14.28	-3.18	6.12	10.88	-4.77
106	298	72894.7	325430.8	10.29	10.95	-0.66	10.43	10.79	-0.36	12.09	12.99	-0.90	7.57	9.76	-2.20
107	299	118106.8	458447.1	17.31	10.50	6.81	17.36	10.35	7.01	20.15	19.25	0.90	14.61	8.59	6.01
108	301	465918.1	366232.1	12.79	9.89	2.90	12.65	10.01	2.64	15.30	17.07	-1.78	4.20	6.52	-2.32
109	305	198432.1	280439.8	21.00	7.11	13.89	20.98	7.15	13.83	24.63	7.76	16.87	19.82	5.87	13.95
110	314	122694.2	178319.5	13.50	8.79	4.71	13.24	8.78	4.46	15.93	9.14	6.79	12.83	8.44	4.39
111	319	605987.6	199750.9	20.11	10.74	9.37	20.58	10.55	10.03	21.70	13.30	8.40	17.00	10.13	6.86
112	320	2371242.2	240145.9	9.83	12.95	-3.12	9.90	12.94	-3.04	12.41	14.20	-1.79	5.09	10.96	-5.87
113	321	118062.5	252804.3	15.79	13.40	2.40	15.69	13.33	2.36	23.40	14.45	8.95	12.33	12.86	-0.53
114	333	357826.6	331073.9	9.77	13.49	-3.72	10.23	13.54	-3.31	12.11	15.96	-3.85	4.39	10.85	-6.46
115	335	923215.4	193960.9	13.78	10.25	3.54	13.72	10.09	3.63	18.17	12.27	5.90	9.63	7.90	1.73
116	336	447281.3	407762.1	19.26	9.95	9.31	19.33	9.89	9.44	20.69	12.90	7.79	17.34	7.30	10.04
117	340	198268.4	256727.2	17.68	13.75	3.94	17.92	13.70	4.22	19.35	17.45	1.90	15.83	13.33	2.50
118	341	433408.7	242373.0	9.42	13.61	-4.20	10.19	13.62	-3.43	12.01	17.49	-5.48	4.10	10.63	-6.53
119	353	181660.3	397572.3	19.06	9.60	9.46	18.50	9.65	8.85	31.73	11.64	20.09	16.15	5.78	10.36
120	354	37805.1	225813.5	15.11	8.39	6.72	13.90	8.33	5.57	24.05	10.83	13.22	9.30	6.38	2.91
121	355	134622.4	451922.1	14.22	10.01	4.21	13.85	10.16	3.69	17.69	11.50	6.19	9.03	6.41	2.62

ID	Object ID	DTLB Size	Buffer Size	Buffer Mean	DTLB Mean	Diff Buffer-DTLB Mean	Buffer Med	DTLB Med	Diff Buffer-DTLB Med	Buffer Max	DTLB Max	Diff Buffer-DTLB Max	Buffer Min	DTLB Min	Diff Buffer-DTLB Min
122	356	120802.5	266083.4	28.51	8.39	20.12	26.10	8.16	17.94	45.38	11.77	33.61	23.87	6.04	17.83
123	357	200109.2	301197.5	15.07	8.27	6.80	16.35	8.19	8.16	21.64	9.81	11.83	-15.06	6.20	-21.26
124	359	1744601.8	635882.6	25.41	9.06	16.35	23.47	9.10	14.37	118.79	10.53	108.25	17.89	6.18	11.70
125	366	197329.2	263354.3	12.10	8.25	3.84	12.39	8.36	4.03	21.74	10.22	11.52	-0.88	5.93	-6.81
126	368	107873.5	281521.1	14.17	7.90	6.27	13.34	8.02	5.31	30.48	9.05	21.43	2.17	6.82	-4.65
127	371	39648.0	340102.1	16.94	14.28	2.66	16.88	14.05	2.83	24.47	15.76	8.71	7.99	13.87	-5.89
128	373	129076.9	240580.1	12.43	15.21	-2.77	12.46	15.21	-2.76	14.78	16.04	-1.26	10.01	14.46	-4.44
129	375	109712.6	757873.5	23.57	12.57	11.00	22.28	12.12	10.16	37.93	14.68	23.26	9.51	11.28	-1.77
130	383	519948.0	291854.8	14.04	13.11	0.93	13.77	13.06	0.71	16.18	14.74	1.44	10.88	12.17	-1.29
131	390	250713.7	263080.4	22.72	12.25	10.47	27.24	12.35	14.89	34.19	18.66	15.53	2.11	9.72	-7.61
132	409	84803.0	1054065.5	16.60	12.62	3.98	13.67	12.40	1.27	35.87	16.81	19.06	1.48	7.80	-6.32
133	412	198175.2	663448.4	20.00	14.58	5.43	17.48	14.67	2.80	38.29	26.62	11.68	13.66	10.30	3.36
134	415	270059.6	263457.3	12.39	14.02	-1.63	12.41	13.83	-1.42	14.01	19.59	-5.58	9.73	12.85	-3.12
135	418	162215.0	664641.1	10.91	13.66	-2.75	10.57	13.69	-3.12	26.65	16.59	10.05	4.81	11.58	-6.77
136	426	240526.8	228232.8	12.18	9.57	2.61	12.30	7.75	4.55	19.15	17.94	1.21	4.20	2.81	1.38
137	428	402744.7	322628.5	16.01	9.48	6.53	16.61	9.24	7.37	19.12	11.83	7.30	9.92	6.15	3.76
138	433	114291.2	304941.2	16.00	13.85	2.15	13.77	14.15	-0.38	28.35	16.67	11.68	7.74	11.91	-4.17
139	436	29490.9	682993.4	17.19	10.81	6.39	16.91	10.73	6.18	31.16	11.76	19.40	-10.52	10.01	-20.53
140	440	606303.2	561906.1	17.06	11.49	5.57	13.61	11.52	2.09	37.97	13.20	24.77	2.68	6.23	-3.56
	Ø	402806.4	328599.0	16.35	15.13	1.22	15.95	15.00	0.95	26.31	21.03	5.28	8.68	10.59	-1.90

Appendix 5: Table Seward age group 3

ID	Object ID	DTLB Size	Buffer Size	Buffer Mean	DTLB Mean	Diff Buffer-DTLB Mean	Buffer Med	DTLB Med	Diff Buffer-DTLB Med	Buffer Max	DTLB Max	Diff Buffer-DTLB Max	Buffer Min	DTLB Min	Diff Buffer-DTLB Min
1	5	1519889.6	199848.9	9.925	24.560	-14.635	10.476	24.527	-14.051	14.058	34.496	-20.438	3.744	21.831	-18.087
2	6	2268685.0	350181.9	12.894	24.569	-11.676	12.773	24.618	-11.845	18.269	37.965	-19.696	10.865	15.541	-4.675
3	10	2497014.8	450885.7	17.924	16.409	1.515	18.044	15.753	2.291	19.258	34.454	-15.195	7.744	2.234	5.510
4	11	488687.0	245537.6	9.255	NA	NA	9.889	NA	NA	NA	NA	NA	7.531	NA	NA
5	12	2749650.8	251508.5	16.581	20.630	-4.049	16.634	20.438	-3.805	17.443	34.952	-17.509	15.707	8.592	7.115
6	16	782707.7	240382.4	14.920	9.907	5.013	14.939	10.542	4.397	15.986	18.044	-2.058	12.836	2.132	10.704
7	18	378887.2	149515.4	7.624	10.495	-2.871	4.485	11.020	-6.535	26.772	20.451	6.321	-0.684	2.771	-3.455
8	21	689568.9	531611.9	13.599	11.315	2.284	12.091	11.359	0.732	25.580	12.909	12.671	3.009	5.156	-2.146
9	22	617622.4	729954.4	17.204	9.741	7.463	17.247	10.187	7.060	21.383	14.015	7.368	14.242	4.403	9.839
10	23	351224.4	206225.7	14.877	9.893	4.983	14.906	9.998	4.908	15.731	12.030	3.701	13.654	7.979	5.674
11	26	64528.9	495975.0	12.031	8.485	3.546	11.915	8.702	3.213	16.809	10.574	6.235	8.762	3.880	4.882
12	33	75579.4	755059.7	15.140	10.182	4.958	14.917	10.807	4.110	21.890	12.577	9.313	13.140	1.260	11.880
13	34	398175.4	476181.1	12.142	10.813	1.330	12.275	11.573	0.702	19.302	15.107	4.195	7.904	0.390	7.514
14	36	907048.5	372552.1	16.446	10.492	5.954	16.259	10.541	5.718	19.516	14.319	5.196	15.558	4.586	10.972
15	38	733697.0	180935.4	16.978	10.740	6.238	17.056	11.314	5.742	18.735	16.621	2.114	12.939	-5.860	18.799
16	39	2540547.9	240481.3	18.501	11.516	6.985	18.582	11.478	7.104	22.716	23.537	-0.820	13.351	4.961	8.390
17	42	3799861.3	805483.9	12.752	21.459	-8.707	13.509	21.058	-7.548	18.420	32.645	-14.225	3.837	13.388	-9.550
18	45	991155.2	405266.7	16.804	18.713	-1.909	16.762	18.475	-1.713	18.415	31.074	-12.658	16.105	15.394	0.711
19	49	123525.3	463202.6	12.877	16.458	-3.581	12.859	16.395	-3.537	20.269	18.859	1.409	8.276	15.597	-7.321
20	52	888656.3	445530.6	11.468	17.225	-5.757	11.527	17.447	-5.920	13.120	25.093	-11.972	8.018	9.819	-1.802
21	53	765075.9	222907.4	10.498	13.726	-3.228	12.445	12.871	-0.426	13.842	30.168	-16.326	4.023	-14.895	18.918
22	57	299559.8	385148.3	8.883	10.764	-1.881	9.209	10.857	-1.648	11.488	14.053	-2.565	4.257	6.073	-1.816
23	58	804615.8	896491.3	8.615	10.066	-1.451	9.576	10.293	-0.717	11.909	14.254	-2.344	3.569	-0.114	3.683
24	62	1136380.2	324593.3	10.339	9.953	0.386	10.535	10.087	0.448	12.322	14.779	-2.457	7.937	-2.599	10.536
25	66	1740010.7	628430.0	19.198	11.595	7.603	18.042	11.610	6.432	33.938	27.163	6.775	14.757	1.056	13.702
26	69	506930.5	308961.1	10.194	16.856	-6.662	10.160	17.069	-6.909	11.301	26.633	-15.332	8.644	8.981	-0.337
27	70	753029.8	142616.5	8.168	20.491	-12.323	8.342	19.985	-11.643	11.423	33.151	-21.729	4.479	15.420	-10.940
28	74	655474.6	1107889.1	26.171	18.485	7.687	24.803	18.376	6.427	42.258	30.808	11.450	13.574	16.787	-3.213

ID	Object ID	DTLB Size	Buffer Size	Buffer Mean	DTLB Mean	Diff Buffer-DTLB Mean	Buffer Med	DTLB Med	Diff Buffer-DTLB Med	Buffer Max	DTLB Max	Diff Buffer-DTLB Max	Buffer Min	DTLB Min	Diff Buffer-DTLB Min
29	76	188064.3	614752.9	16.152	17.349	-1.197	16.445	17.460	-1.015	19.809	18.661	1.148	3.580	15.550	-11.970
30	77	164091.6	245429.4	15.555	17.176	-1.622	15.758	17.577	-1.819	17.613	19.645	-2.032	11.570	14.783	-3.214
31	79	1102580.3	138070.0	14.967	17.174	-2.207	15.347	17.168	-1.821	16.499	24.482	-7.983	13.228	7.957	5.271
32	81	3027213.1	335509.3	14.943	15.218	-0.275	14.909	15.230	-0.321	17.916	22.759	-4.843	12.781	10.815	1.967
33	84	95858.0	413405.5	19.382	11.623	7.759	18.025	11.627	6.398	29.511	13.539	15.971	15.519	9.118	6.400
34	85	78343.2	453798.1	15.323	11.215	4.108	14.563	11.234	3.329	27.073	12.909	14.164	12.919	8.920	3.999
35	86	158528.0	256622.0	15.008	12.280	2.728	14.625	12.145	2.480	18.438	23.769	-5.332	13.792	7.276	6.516
36	87	238705.2	388339.0	10.936	10.866	0.069	10.993	10.856	0.137	13.852	17.719	-3.867	5.352	7.235	-1.883
37	89	156677.0	170749.8	17.702	9.884	7.817	17.618	10.192	7.425	19.184	13.326	5.858	16.143	7.337	8.806
38	90	421186.5	173751.5	16.437	11.610	4.827	16.553	11.950	4.604	17.678	15.488	2.190	14.725	4.503	10.221
39	93	596264.9	346444.7	15.128	9.081	6.046	15.579	9.128	6.451	16.637	16.037	0.600	12.870	2.499	10.371
40	95	66354.8	147190.8	20.284	9.359	10.925	20.111	9.379	10.732	21.325	10.340	10.986	19.621	8.306	11.314
41	99	1088352.8	177004.9	11.412	11.639	-0.227	12.150	11.642	0.508	17.800	24.412	-6.612	-2.411	4.455	-6.867
42	101	371400.5	177814.7	15.994	9.703	6.290	16.177	9.664	6.513	17.553	13.308	4.246	10.941	2.609	8.331
43	103	416580.9	182360.2	9.435	12.319	-2.884	9.532	12.299	-2.767	11.479	13.776	-2.297	6.422	11.274	-4.852
44	106	494929.3	680587.1	14.768	11.426	3.342	14.695	11.338	3.358	20.732	13.094	7.638	10.106	9.242	0.864
45	109	1083890.6	145787.5	11.217	12.972	-1.755	11.584	12.982	-1.398	23.655	13.814	9.840	6.552	11.583	-5.031
46	110	400905.4	234917.1	12.003	12.592	-0.589	11.800	12.600	-0.799	17.697	13.578	4.119	7.592	10.910	-3.318
47	111	102296.6	449051.9	17.022	11.993	5.029	17.244	12.145	5.099	26.361	13.668	12.692	7.609	10.155	-2.546
48	112	88475.3	540435.5	7.719	12.086	-4.367	9.807	12.011	-2.204	21.502	14.371	7.132	-19.777	10.517	-30.294
49	119	264541.2	379782.8	16.857	14.406	2.451	16.235	14.354	1.881	26.302	16.511	9.791	-1.401	13.702	-15.103
50	123	427582.3	932128.0	14.454	7.512	6.943	11.968	7.410	4.558	30.760	10.909	19.850	1.535	4.110	-2.575
51	124	737368.8	330180.4	8.083	13.970	-5.887	8.326	13.895	-5.568	14.309	21.656	-7.348	2.643	12.723	-10.080
52	125	167752.8	153376.7	13.305	12.936	0.369	13.494	12.661	0.833	15.526	19.713	-4.186	9.994	9.060	0.934
53	127	490374.1	350745.7	20.166	13.670	6.496	19.709	13.656	6.053	28.044	15.035	13.009	11.829	12.681	-0.852
54	132	336457.5	211326.8	23.978	16.472	7.506	23.571	16.562	7.009	31.754	19.724	12.030	21.344	14.347	6.996
55	134	1085920.0	1509231.3	22.718	17.513	5.204	21.597	17.405	4.192	40.678	24.180	16.499	8.949	13.886	-4.937
56	138	254469.4	383971.6	8.412	19.216	-10.804	7.671	19.362	-11.691	14.127	22.093	-7.967	3.703	14.160	-10.458
57	141	650955.8	820390.3	22.189	30.448	-8.259	20.760	31.409	-10.649	39.156	33.963	5.193	17.599	17.526	0.073
58	144	710786.8	375887.6	13.333	20.585	-7.251	13.140	20.554	-7.414	22.095	21.795	0.300	8.323	18.432	-10.109
59	145	1133998.9	261861.8	11.305	21.550	-10.245	11.834	21.413	-9.579	14.278	35.469	-21.191	8.169	18.080	-9.911

ID	Object ID	DTLB Size	Buffer Size	Buffer Mean	DTLB Mean	Diff Buffer-DTLB Mean	Buffer Med	DTLB Med	Diff Buffer-DTLB Med	Buffer Max	DTLB Max	Diff Buffer-DTLB Max	Buffer Min	DTLB Min	Diff Buffer-DTLB Min
60	146	1114615.5	201675.6	10.614	19.301	-8.687	9.545	19.348	-9.804	23.493	20.197	3.296	3.650	18.387	-14.737
61	147	1443647.7	331015.9	21.418	18.355	3.063	19.811	18.547	1.264	36.036	25.764	10.272	4.524	15.438	-10.914
62	148	780783.8	911996.9	17.863	18.399	-0.537	16.057	18.425	-2.368	40.314	25.286	15.028	1.662	16.620	-14.958
63	156	1682672.7	209187.5	20.621	20.964	-0.343	19.157	20.895	-1.737	32.334	31.842	0.491	16.983	16.776	0.208
64	165	173372.6	247258.7	20.916	23.058	-2.142	20.942	23.055	-2.113	21.313	24.829	-3.517	20.509	21.658	-1.149
65	166	122652.8	383768.1	15.749	23.030	-7.281	15.871	23.039	-7.168	17.879	23.747	-5.868	14.545	22.483	-7.938
66	168	2028933.6	982879.5	15.892	21.033	-5.141	15.389	20.994	-5.605	30.361	31.008	-0.647	14.130	9.212	4.918
67	171	343013.1	415365.4	13.048	18.454	-5.406	12.967	18.499	-5.532	17.947	19.401	-1.454	9.675	17.376	-7.701
68	172	175199.8	1101388.2	17.772	18.361	-0.589	17.344	18.347	-1.003	28.555	21.753	6.802	4.108	16.021	-11.913
69	174	3407772.6	242474.7	19.303	17.746	1.557	19.240	17.795	1.445	21.534	25.090	-3.555	17.684	14.520	3.165
70	175	820614.4	949541.2	17.794	18.044	-0.250	18.194	18.090	0.104	21.932	18.886	3.046	14.470	16.439	-1.969
71	181	262775.0	240160.5	15.523	17.723	-2.199	15.530	17.880	-2.351	16.474	22.760	-6.286	13.867	14.573	-0.706
72	183	2681847.2	464300.0	19.419	16.904	2.515	19.251	16.977	2.273	24.798	19.589	5.209	17.153	15.493	1.661
73	188	118913.7	260428.8	15.114	17.627	-2.513	15.573	17.621	-2.048	17.686	18.504	-0.818	13.154	16.834	-3.680
74	190	218471.0	320372.2	9.078	19.449	-10.371	8.955	19.604	-10.649	10.679	20.955	-10.276	6.638	14.983	-8.345
75	191	480270.6	533335.2	6.134	17.086	-10.952	7.207	17.452	-10.245	11.060	22.643	-11.583	3.298	3.720	-0.422
76	195	324461.7	261357.7	15.128	16.412	-1.283	15.161	16.368	-1.207	17.333	18.135	-0.802	13.394	14.792	-1.398
77	196	70973.7	386509.2	20.110	15.173	4.937	20.642	15.235	5.408	22.091	16.125	5.966	18.264	13.504	4.760
78	197	127200.8	403304.9	13.850	15.551	-1.701	13.747	15.593	-1.846	16.896	16.313	0.583	11.617	14.797	-3.180
79	199	696827.5	411764.1	14.579	12.985	1.594	13.844	13.442	0.403	28.853	19.133	9.719	8.399	3.925	4.474
80	201	631371.3	1390293.1	16.631	14.030	2.601	16.348	14.021	2.327	21.307	16.639	4.668	14.732	11.126	3.605
81	202	919833.3	581312.2	13.551	13.298	0.254	10.830	13.629	-2.799	186.903	19.190	167.713	-7.321	8.472	-15.793
82	204	351146.8	814506.0	16.233	13.829	2.404	15.563	14.002	1.561	31.864	18.857	13.007	7.840	8.462	-0.621
83	206	651525.5	1013520.5	17.242	11.864	5.378	16.845	11.798	5.047	30.801	20.145	10.656	-2.424	6.174	-8.599
84	210	164035.4	273458.1	17.200	13.150	4.050	16.809	13.177	3.632	19.516	13.776	5.740	15.529	11.053	4.476
85	212	943679.7	311073.4	13.218	12.837	0.380	12.450	12.860	-0.409	31.178	14.298	16.880	-0.001	10.180	-10.181
86	213	845107.5	181797.1	23.072	12.813	10.259	23.207	12.826	10.381	24.285	14.347	9.938	20.831	11.243	9.588
87	217	1047944.6	958075.1	16.280	12.898	3.382	16.384	13.473	2.911	19.914	18.914	1.000	3.526	4.827	-1.301
88	218	1233969.9	501634.7	13.689	12.411	1.277	12.832	12.526	0.306	24.633	15.175	9.458	4.103	9.889	-5.786
89	219	1607495.4	239094.5	15.806	15.471	0.334	15.534	16.239	-0.704	21.937	21.617	0.320	11.955	6.801	5.153
90	220	200924.6	864659.5	12.829	15.259	-2.430	11.116	15.572	-4.456	60.531	16.274	44.257	-12.091	12.093	-24.184

ID	Object ID	DTLB Size	Buffer Size	Buffer Mean	DTLB Mean	Diff Buffer-DTLB Mean	Buffer Med	DTLB Med	Diff Buffer-DTLB Med	Buffer Max	DTLB Max	Diff Buffer-DTLB Max	Buffer Min	DTLB Min	Diff Buffer-DTLB Min
91	222	294015.7	211179.3	11.267	15.623	-4.356	10.154	15.739	-5.585	26.801	16.335	10.466	-12.267	13.260	-25.527
92	228	718003.0	227787.4	18.986	14.107	4.880	18.884	14.357	4.527	23.055	16.266	6.789	14.641	11.635	3.006
93	231	620227.5	538959.7	12.174	12.704	-0.530	12.140	12.747	-0.607	14.598	14.693	-0.095	11.103	11.154	-0.051
94	232	1038591.5	572721.1	8.006	11.297	-3.291	8.160	11.394	-3.234	21.224	13.134	8.090	1.478	9.875	-8.398
95	234	199066.8	424913.3	27.568	10.969	16.599	28.059	10.959	17.100	38.027	12.899	25.128	16.400	8.973	7.428
96	240	435036.4	288786.6	10.708	11.754	-1.046	12.699	11.903	0.796	14.510	19.716	-5.206	3.909	4.188	-0.278
97	242	448916.6	569820.8	11.055	17.090	-6.035	10.444	17.135	-6.691	26.606	23.010	3.597	-5.982	5.643	-11.625
98	244	232293.6	474275.9	11.145	18.911	-7.766	11.346	18.872	-7.526	20.147	20.658	-0.511	0.816	17.988	-17.172
99	245	782603.0	417964.6	15.654	15.504	0.150	15.535	15.747	-0.212	17.753	22.901	-5.147	9.241	8.776	0.465
100	247	4532966.1	169199.7	13.937	16.342	-2.405	13.588	16.300	-2.712	20.782	24.550	-3.769	11.142	5.430	5.712
101	251	304230.4	317584.3	10.687	15.930	-5.243	10.567	16.051	-5.484	14.411	18.185	-3.773	5.345	12.163	-6.818
102	252	423174.2	411767.7	9.895	17.523	-7.628	10.024	17.743	-7.719	14.291	19.159	-4.868	-9.639	15.688	-25.328
103	255	669689.0	580783.1	17.897	27.683	-9.785	18.353	27.964	-9.610	24.405	30.975	-6.570	13.798	25.586	-11.789
104	259	195572.7	295181.3	10.788	30.128	-19.339	10.569	30.307	-19.738	21.523	36.873	-15.350	-0.001	28.300	-28.300
105	261	562724.6	212348.1	12.161	28.436	-16.275	12.478	28.417	-15.938	18.269	34.985	-16.716	8.723	26.376	-17.653
106	263	3078854.4	284619.9	8.876	19.886	-11.010	8.509	19.930	-11.421	17.688	28.303	-10.615	5.215	16.068	-10.853
107	265	4827748.6	579635.1	18.519	17.660	0.859	17.374	17.732	-0.358	33.494	20.283	13.211	3.677	14.857	-11.180
108	268	2257960.9	367798.0	21.148	19.719	1.428	20.156	19.706	0.450	32.309	24.817	7.492	16.469	16.708	-0.239
109	269	76559.7	259725.3	9.844	20.435	-10.592	10.108	20.453	-10.345	12.515	20.935	-8.420	7.661	19.748	-12.088
110	271	574679.4	251807.2	14.496	19.545	-5.049	15.291	19.389	-4.098	17.317	26.593	-9.276	11.152	18.854	-7.702
111	273	1203861.2	449290.8	9.134	19.739	-10.605	9.326	19.775	-10.449	13.101	29.086	-15.984	3.203	17.305	-14.102
112	279	200201.6	854969.6	18.482	20.911	-2.429	17.481	20.875	-3.394	33.880	21.429	12.450	4.987	20.511	-15.524
113	280	1215988.3	455420.0	10.674	20.819	-10.145	11.669	20.917	-9.249	20.993	21.503	-0.510	-2.495	18.457	-20.951
114	286	539807.3	1519021.6	27.193	12.887	14.306	24.568	12.829	11.739	42.949	15.944	27.005	12.822	10.702	2.120
115	287	134725.1	526995.7	10.050	8.301	1.750	9.080	8.503	0.577	23.577	18.612	4.966	1.840	4.068	-2.227
116	288	1117367.3	975993.8	20.437	15.583	4.854	18.627	15.856	2.771	38.260	21.698	16.562	11.450	11.612	-0.162
117	290	886644.7	282127.8	10.160	12.871	-2.710	10.325	12.992	-2.667	16.008	20.385	-4.377	3.745	7.773	-4.029
118	292	521229.3	338203.0	11.967	20.734	-8.766	11.455	20.787	-9.332	29.066	26.576	2.490	2.231	17.824	-15.593
119	295	733388.6	509918.7	23.133	18.578	4.555	21.691	18.707	2.984	38.157	23.932	14.224	9.019	13.518	-4.499
120	303	210409.1	1281186.8	10.608	10.231	0.376	10.160	10.431	-0.270	19.202	11.267	7.936	7.121	7.570	-0.450
121	304	275942.1	560002.5	20.761	11.900	8.862	19.780	11.990	7.789	36.213	13.087	23.126	17.029	8.795	8.234

ID	Object ID	DTLB Size	Buffer Size	Buffer Mean	DTLB Mean	Diff Buffer-DTLB Mean	Buffer Med	DTLB Med	Diff Buffer-DTLB Med	Buffer Max	DTLB Max	Diff Buffer-DTLB Max	Buffer Min	DTLB Min	Diff Buffer-DTLB Min
122	306	828776.0	618167.8	28.888	8.104	20.783	28.417	8.329	20.088	41.764	12.934	28.831	24.752	3.117	21.635
123	308	1191919.7	537166.5	19.253	14.664	4.589	18.849	14.713	4.136	34.295	17.649	16.646	13.661	12.439	1.222
124	309	600539.4	1275960.8	24.103	14.593	9.510	21.749	14.497	7.252	41.405	22.549	18.856	8.188	13.588	-5.400
125	312	173424.7	373028.0	19.799	18.797	1.002	18.955	18.813	0.142	30.997	24.164	6.832	15.322	17.069	-1.747
126	315	221399.0	420581.8	18.002	8.851	9.151	18.007	8.835	9.172	25.499	9.924	15.575	15.605	7.994	7.610
127	316	4302131.1	564414.2	20.820	9.638	11.182	20.938	9.669	11.269	28.048	11.642	16.406	18.238	3.748	14.490
128	318	3735364.0	1096800.9	7.353	9.003	-1.650	9.110	9.287	-0.177	10.900	10.565	0.335	3.325	3.557	-0.232
129	322	1342044.9	1012338.0	15.681	13.066	2.615	15.916	13.135	2.781	16.950	13.841	3.109	14.066	10.929	3.138
130	324	862431.5	541593.2	16.814	16.910	-0.096	16.803	16.908	-0.105	18.749	17.866	0.883	14.989	15.738	-0.749
131	325	258259.5	287595.1	15.637	16.784	-1.146	15.574	16.720	-1.146	18.464	17.555	0.908	13.338	16.070	-2.732
132	326	254584.9	352107.2	17.378	16.777	0.601	17.288	16.769	0.519	20.791	19.312	1.478	13.746	15.687	-1.941
133	327	4002763.8	615118.5	14.395	16.530	-2.135	14.357	16.526	-2.169	18.552	21.606	-3.054	12.430	15.064	-2.634
134	329	497136.3	281816.1	16.244	15.399	0.845	15.986	15.572	0.414	22.676	16.873	5.802	13.543	13.085	0.458
135	330	1430421.0	352352.7	14.107	13.944	0.164	13.884	13.997	-0.113	16.417	15.327	1.090	6.119	11.472	-5.353
136	337	413162.5	654990.3	10.599	10.005	0.595	11.177	10.033	1.144	19.103	10.750	8.353	2.159	8.960	-6.801
137	338	1338175.8	1115308.8	19.699	10.459	9.240	19.540	10.465	9.075	26.593	18.047	8.546	16.484	7.387	9.096
138	339	232399.5	1190285.5	15.576	9.468	6.109	15.800	9.577	6.223	20.446	10.296	10.151	12.593	7.461	5.132
139	342	706353.9	474028.3	17.692	16.139	1.552	17.247	15.903	1.344	31.586	32.743	-1.157	4.520	12.387	-7.866
140	343	2131011.7	265358.0	15.330	15.774	-0.444	15.382	15.790	-0.408	16.689	22.981	-6.292	13.564	13.020	0.544
141	346	482244.9	485945.3	18.930	16.578	2.352	18.158	16.674	1.483	40.569	19.115	21.454	13.107	14.260	-1.153
142	348	244341.1	492841.5	12.895	15.283	-2.388	13.022	15.262	-2.240	14.241	16.049	-1.808	10.615	14.099	-3.484
143	350	970059.9	277779.6	7.710	15.179	-7.469	7.971	15.383	-7.412	10.493	17.826	-7.334	0.821	11.264	-10.443
144	351	236060.7	442819.9	15.550	11.292	4.258	14.603	11.451	3.152	24.119	13.044	11.075	7.572	8.049	-0.477
145	358	138319.2	291500.7	9.430	9.270	0.160	8.885	9.255	-0.370	11.391	11.343	0.048	7.836	7.906	-0.070
146	360	402934.9	302000.4	10.594	7.683	2.911	9.541	8.270	1.270	17.935	9.593	8.343	4.702	3.678	1.024
147	361	236965.4	211024.5	17.535	9.741	7.794	17.651	9.939	7.712	20.814	10.554	10.260	15.264	8.090	7.174
148	363	758787.8	535130.0	13.430	8.965	4.465	13.030	9.034	3.996	23.613	13.101	10.512	5.243	6.639	-1.395
149	364	839921.4	770576.7	21.069	11.160	9.909	20.248	11.971	8.277	33.344	14.117	19.227	15.781	4.251	11.530
150	365	516338.0	330461.3	14.178	10.069	4.109	13.831	10.145	3.686	25.443	11.309	14.133	2.293	8.587	-6.294
151	369	204681.3	725211.2	13.787	9.032	4.756	13.731	9.069	4.662	16.217	10.058	6.159	9.237	7.676	1.561
152	370	63616.1	430433.3	10.963	8.021	2.941	11.327	8.034	3.293	17.203	8.884	8.319	-1.357	7.381	-8.738

ID	Object ID	DTLB Size	Buffer Size	Buffer Mean	DTLB Mean	Diff Buffer-DTLB Mean	Buffer Med	DTLB Med	Diff Buffer-DTLB Med	Buffer Max	DTLB Max	Diff Buffer-DTLB Max	Buffer Min	DTLB Min	Diff Buffer-DTLB Min
153	372	128158.2	692316.5	12.993	16.778	-3.784	12.963	16.847	-3.884	16.054	17.420	-1.365	10.171	15.830	-5.659
154	376	503330.9	896062.3	21.730	8.460	13.270	20.907	8.764	12.144	39.377	13.028	26.349	17.236	3.862	13.373
155	377	213851.7	141422.0	9.503	12.448	-2.945	9.747	12.593	-2.845	10.664	13.494	-2.829	7.891	7.064	0.827
156	378	306949.2	644445.8	15.687	12.730	2.957	15.781	13.618	2.163	25.595	14.435	11.159	10.022	4.128	5.894
157	380	3571871.8	336653.8	16.472	13.490	2.982	14.701	13.533	1.168	30.252	17.610	12.642	12.808	4.420	8.388
158	382	908025.9	495856.0	28.528	10.987	17.541	29.974	11.186	18.788	36.700	14.825	21.876	15.377	8.343	7.035
159	385	2194076.6	1560554.8	24.283	14.819	9.465	21.507	14.827	6.679	40.044	20.696	19.349	3.153	13.472	-10.319
160	386	548501.3	252177.0	9.909	13.515	-3.606	9.711	13.465	-3.754	13.936	14.943	-1.007	7.312	12.391	-5.080
161	387	242428.3	228732.4	30.821	14.283	16.538	30.685	14.271	16.414	42.994	15.872	27.122	27.634	12.981	14.653
162	388	175142.3	530459.7	8.139	14.850	-6.711	8.587	14.838	-6.251	13.335	15.651	-2.317	-0.943	14.265	-15.208
163	392	3713125.8	286823.0	17.529	15.999	1.530	17.515	15.852	1.663	20.478	27.697	-7.219	13.454	14.292	-0.838
164	393	129994.2	732178.4	17.578	14.950	2.628	17.159	15.052	2.108	24.400	16.999	7.401	4.500	12.786	-8.285
165	395	2011744.0	217117.1	14.479	16.030	-1.551	13.676	15.944	-2.268	27.158	17.496	9.662	4.304	14.093	-9.790
166	397	3760706.0	469480.8	19.211	16.250	2.961	17.439	16.344	1.096	34.313	19.907	14.406	-16.393	8.435	-24.828
167	399	809547.5	418086.4	12.473	16.587	-4.114	12.595	16.563	-3.968	15.120	17.818	-2.697	10.725	16.073	-5.348
168	401	886180.3	314636.8	16.962	17.728	-0.767	16.789	17.741	-0.953	20.408	20.117	0.291	14.594	7.234	7.360
169	405	212056.9	308906.3	18.153	18.303	-0.150	17.932	18.305	-0.374	19.388	22.678	-3.291	16.029	14.375	1.654
170	406	424965.4	340753.7	16.274	16.538	-0.264	16.080	16.453	-0.373	19.660	19.021	0.639	11.524	15.793	-4.269
171	407	868299.1	292983.0	16.144	19.302	-3.158	15.483	19.213	-3.730	23.719	26.026	-2.307	10.489	16.152	-5.663
172	408	316183.0	473888.0	19.825	17.109	2.716	18.613	17.095	1.518	33.394	18.775	14.620	15.471	16.266	-0.794
173	410	1392771.7	388428.2	11.701	19.889	-8.188	11.666	19.914	-8.248	15.656	25.701	-10.045	7.796	15.253	-7.457
174	411	1451657.3	211651.4	16.423	16.396	0.027	16.148	16.477	-0.328	18.705	18.017	0.688	14.549	10.980	3.569
175	413	483911.5	550641.3	13.933	16.472	-2.539	13.518	16.847	-3.330	19.741	23.369	-3.628	8.850	12.782	-3.932
176	416	111526.2	767476.2	15.111	13.625	1.486	16.100	13.624	2.476	29.800	15.132	14.668	4.827	12.835	-8.009
177	417	543805.6	469718.3	19.529	15.174	4.354	19.482	15.123	4.359	24.817	20.930	3.888	17.303	9.005	8.298
178	421	547464.3	315744.7	16.262	14.936	1.326	16.727	14.934	1.793	19.360	15.892	3.468	12.357	13.308	-0.952
179	423	118887.0	312253.8	15.975	14.884	1.090	16.252	14.855	1.397	40.288	16.652	23.636	11.997	13.537	-1.540
180	424	269117.0	664110.3	12.054	15.620	-3.566	12.211	15.562	-3.351	19.984	16.577	3.407	6.771	13.837	-7.066
181	425	245141.8	160372.5	8.056	14.586	-6.530	8.830	14.458	-5.629	13.233	18.936	-5.703	2.706	12.680	-9.975
182	427	399047.3	460524.6	10.054	10.079	-0.025	10.408	10.005	0.403	20.829	15.136	5.693	1.246	6.792	-5.546
183	429	337299.4	264142.0	12.814	8.188	4.626	12.875	8.141	4.735	14.153	9.482	4.672	10.574	6.699	3.875

ID	Object ID	DTLB Size	Buffer Size	Buffer Mean	DTLB Mean	Diff Buffer- DTLB Mean	Buffer Med	DTLB Med	Diff Buffer- DTLB Med	Buffer Max	DTLB Max	Diff Buffer- DTLB Max	Buffer Min	DTLB Min	Diff Buffer- DTLB Min
184	430	745650.3	521862.2	13.828	15.151	-1.323	13.637	15.241	-1.604	20.980	17.150	3.830	10.275	11.573	-1.298
185	434	320762.9	567325.0	8.873	15.805	-6.932	9.657	15.939	-6.282	40.141	17.400	22.741	-2.431	14.690	-17.121
186	435	383451.0	555105.7	11.760	15.391	-3.630	12.675	15.340	-2.665	19.580	18.715	0.865	3.660	14.485	-10.825
187	437	1320832.0	589475.1	10.491	12.216	-1.725	10.831	12.233	-1.402	22.344	21.023	1.321	2.689	7.877	-5.188
188	442	140968.7	340713.4	17.960	9.883	8.077	18.241	10.290	7.950	25.499	22.323	3.177	11.966	-2.517	14.482
	Ø	858868.2	477072.2	15.140	14.895	0.276	14.931	14.973	-0.015	23.676	19.353	4.393	8.756	10.869	-2.107

Appendix 6: Table Seward age group 4

ID	Object ID	DTLB Size	Buffer Size	Buffer Mean	DTLB Mean	Diff Buffer-DTLB Mean	Buffer Med	DTLB Med	Diff Buffer-DTLB Med	Buffer Max	DTLB Max	Diff Buffer-DTLB Max	Buffer Min	DTLB Min	Diff Buffer-DTLB Min
1	1	988557.7	301712.8	19.467	20.629	-1.162	19.052	21.526	-2.474	25.407	33.262	-7.854	16.344	11.969	4.375
2	2	317112.4	297521.4	7.532	11.306	-3.774	7.827	10.504	-2.677	14.369	20.829	-6.461	3.583	4.216	-0.633
3	3	93096.6	374633.4	11.279	11.143	0.136	10.898	11.186	-0.288	16.876	12.648	4.228	7.616	9.643	-2.027
4	4	1491434.7	474247.8	12.452	11.618	0.834	10.508	11.758	-1.251	29.879	20.829	9.051	8.931	1.417	7.514
5	5	1436742.8	329021.1	8.928	24.869	-15.940	9.569	23.854	-14.285	11.545	40.483	-28.939	3.751	13.960	-10.209
6	6	2361091.0	815490.5	15.254	19.524	-4.269	15.184	19.436	-4.252	19.477	37.167	-17.689	11.474	13.540	-2.066
7	7	424918.3	543653.2	21.816	15.438	6.378	21.587	15.466	6.121	29.107	21.707	7.399	15.740	10.153	5.588
8	8	568674.4	500280.5	13.907	10.631	3.276	14.278	10.610	3.668	19.391	17.845	1.546	9.000	9.232	-0.232
9	9	174188.8	303561.7	14.446	8.878	5.568	14.161	9.618	4.543	20.988	11.868	9.120	8.987	0.555	8.432
10	10	966784.0	346709.1	15.456	11.302	4.154	14.370	11.494	2.876	26.528	26.457	0.071	11.893	-0.527	12.420
11	11	611213.0	487720.2	17.421	17.355	0.065	16.210	17.463	-1.253	26.438	19.962	6.477	10.430	14.524	-4.094
12	12	767767.4	568243.3	19.259	13.057	6.202	18.727	13.110	5.617	32.997	23.912	9.085	14.850	2.913	11.937
13	13	411936.8	475475.9	14.891	9.013	5.878	16.007	9.071	6.936	25.137	16.441	8.696	6.395	-1.916	8.312
14	14	377862.3	336130.8	27.449	10.485	16.963	23.518	10.462	13.056	43.887	18.431	25.457	19.825	5.339	14.486
15	15	663598.1	256480.8	18.391	13.331	5.060	18.127	13.724	4.402	19.778	21.041	-1.263	16.629	5.488	11.142
16	16	155738.5	786579.7	12.203	11.574	0.629	12.160	11.596	0.564	14.082	12.252	1.830	10.272	10.438	-0.167
17	17	487540.9	496881.5	12.713	11.228	1.485	12.870	11.354	1.516	14.835	13.292	1.543	4.399	9.565	-5.166
18	18	1951009.8	581453.1	17.771	12.255	5.516	17.758	12.277	5.481	19.660	15.040	4.620	8.412	10.587	-2.176
19	19	504194.5	562715.4	17.550	13.687	3.863	17.335	13.908	3.427	20.507	19.135	1.372	15.180	4.770	10.410
20	20	232297.5	325140.0	17.740	16.184	1.557	17.073	16.340	0.733	27.999	22.853	5.146	14.471	11.202	3.269
21	21	487608.4	648862.4	20.567	14.169	6.398	19.277	14.324	4.953	35.664	16.867	18.797	11.751	11.246	0.505
22	22	257112.2	379227.6	17.182	12.304	4.878	17.098	12.502	4.596	19.298	13.213	6.086	15.918	10.328	5.591
23	23	728211.0	1288086.8	13.335	17.056	-3.722	13.329	16.766	-3.436	19.722	29.713	-9.991	8.925	13.302	-4.378
24	24	1623480.1	569966.0	15.500	17.494	-1.994	15.257	18.041	-2.784	17.767	24.474	-6.707	14.281	7.676	6.605
25	25	1069496.4	864234.9	10.681	18.742	-8.061	11.154	18.308	-7.154	67.463	23.478	43.985	-35.391	12.295	-47.686
26	26	194369.5	606553.2	12.812	24.167	-11.355	11.903	22.829	-10.926	32.298	37.686	-5.389	-2.411	19.884	-22.296
27	27	672284.6	399874.3	17.372	21.417	-4.045	16.886	21.231	-4.345	20.681	28.502	-7.820	15.010	16.286	-1.276
28	28	844549.4	718835.4	12.011	18.447	-6.436	12.054	18.493	-6.439	18.636	22.239	-3.603	3.621	15.199	-11.578

ID	Object ID	DTLB Size	Buffer Size	Buffer Mean	DTLB Mean	Diff Buffer-DTLB Mean	Buffer Med	DTLB Med	Diff Buffer-DTLB Med	Buffer Max	DTLB Max	Diff Buffer-DTLB Max	Buffer Min	DTLB Min	Diff Buffer-DTLB Min
29	29	178869.0	560943.8	15.722	18.042	-2.320	15.375	18.050	-2.675	19.637	18.779	0.858	11.725	16.882	-5.158
30	30	1293479.3	838017.5	12.957	18.050	-5.093	11.653	18.110	-6.458	30.547	19.053	11.494	4.070	15.471	-11.401
31	31	551272.6	352276.5	28.605	16.376	12.229	28.258	16.535	11.723	33.315	24.519	8.796	23.036	11.548	11.489
32	32	685841.5	387494.9	9.071	15.428	-6.357	8.570	16.014	-7.444	15.722	20.569	-4.847	-0.561	8.254	-8.815
33	33	424043.8	224375.8	12.862	15.663	-2.801	12.778	16.332	-3.554	18.859	22.543	-3.684	5.775	7.437	-1.662
34	34	1045304.7	372719.6	21.393	17.459	3.933	21.414	17.260	4.153	28.165	26.130	2.034	19.044	12.492	6.551
35	35	895749.4	309388.5	21.235	12.388	8.847	17.296	12.678	4.618	35.197	16.527	18.669	12.956	7.363	5.593
36	36	395343.1	482594.8	14.081	13.074	1.007	14.369	13.220	1.149	27.263	18.392	8.871	-2.411	6.090	-8.501
37	37	144696.0	575426.1	23.104	12.956	10.147	23.228	12.922	10.306	37.865	15.681	22.184	-0.935	9.729	-10.663
38	38	1142943.1	497988.0	10.237	18.450	-8.214	9.146	17.764	-8.618	24.513	34.728	-10.215	-3.486	11.947	-15.433
39	39	677337.8	669400.1	9.462	10.355	-0.893	9.353	10.374	-1.022	25.765	13.462	12.303	3.697	8.804	-5.108
40	40	997317.5	239030.4	14.315	14.945	-0.630	13.745	15.555	-1.810	26.700	26.059	0.642	8.562	3.866	4.696
41	41	456320.1	334244.5	10.983	16.462	-5.479	10.257	16.438	-6.181	20.451	22.385	-1.934	3.282	13.369	-10.087
42	42	272859.1	294872.9	16.110	17.697	-1.587	15.975	16.680	-0.705	18.778	29.970	-11.192	14.528	13.278	1.249
43	43	312714.7	575108.4	17.884	28.540	-10.657	17.938	28.459	-10.521	24.960	29.808	-4.848	14.448	27.033	-12.585
44	44	2527985.2	231216.3	8.350	19.393	-11.043	9.558	19.445	-9.887	26.709	22.647	4.061	-14.004	17.223	-31.228
45	45	286858.9	463084.6	16.235	20.180	-3.945	16.432	20.255	-3.823	17.313	23.816	-6.504	14.689	18.890	-4.201
46	46	567316.9	712506.2	16.506	21.289	-4.783	16.458	21.252	-4.795	18.676	23.912	-5.236	14.488	19.266	-4.778
47	47	178976.4	1222176.9	15.954	20.711	-4.757	15.403	20.747	-5.344	30.420	21.766	8.654	13.862	19.456	-5.593
48	48	691988.9	394777.1	10.227	21.920	-11.694	10.438	21.965	-11.527	11.205	23.777	-12.573	8.895	20.145	-11.249
49	49	383800.5	219755.4	17.847	18.518	-0.672	17.950	18.601	-0.651	18.730	20.242	-1.512	16.352	17.452	-1.100
50	50	248168.0	322839.9	12.059	17.971	-5.911	12.083	18.248	-6.166	13.679	19.094	-5.415	9.477	13.615	-4.138
51	51	919899.9	491746.0	12.848	9.606	3.241	12.971	9.493	3.478	17.960	20.549	-2.588	10.898	3.822	7.076
52	52	398665.3	815648.2	15.042	8.096	6.945	14.895	8.613	6.282	20.631	12.107	8.524	8.044	3.649	4.395
53	53	291630.9	1084497.6	18.842	9.389	9.454	19.248	9.712	9.536	23.906	12.655	11.252	16.170	4.064	12.106
54	54	329336.3	468921.0	21.465	14.364	7.101	20.965	14.426	6.539	29.474	21.372	8.102	19.200	12.391	6.810
55	55	1642933.8	220069.2	11.234	14.934	-3.700	11.592	15.032	-3.440	12.358	17.967	-5.609	3.849	10.422	-6.573
56	56	743495.0	326378.9	19.459	18.588	0.871	18.939	18.807	0.132	23.187	28.874	-5.686	16.283	15.292	0.991
57	57	228777.1	182006.2	11.057	10.181	0.876	11.016	10.510	0.505	13.114	11.289	1.825	9.636	3.958	5.678
58	58	385567.2	327903.4	19.486	12.492	6.994	19.388	12.747	6.642	23.857	15.578	8.278	16.389	7.888	8.501
59	59	381855.0	413893.2	10.190	16.423	-6.233	9.508	16.535	-7.027	28.985	17.061	11.923	2.456	15.113	-12.657

ID	Object ID	DTLB Size	Buffer Size	Buffer Mean	DTLB Mean	Diff Buffer- DTLB Mean	Buffer Med	DTLB Med	Diff Buffer- DTLB Med	Buffer Max	DTLB Max	Diff Buffer- DTLB Max	Buffer Min	DTLB Min	Diff Buffer- DTLB Min
60	60	640979.4	1210740.7	16.665	18.964	-2.299	16.123	19.086	-2.963	31.054	21.566	9.488	12.176	15.120	-2.944
61	61	648372.8	682340.6	17.376	10.528	6.848	16.981	10.611	6.370	29.194	10.960	18.233	11.768	9.306	2.462
62	62	189957.0	363309.9	9.218	16.303	-7.085	9.285	16.381	-7.096	13.975	17.272	-3.297	3.599	14.878	-11.279
63	63	108803.1	476259.3	15.354	15.979	-0.625	15.223	15.911	-0.687	29.814	20.446	9.367	3.183	14.771	-11.588
64	64	431531.9	486227.7	11.897	16.510	-4.613	12.397	16.525	-4.127	18.534	18.350	0.184	5.508	15.232	-9.724
65	65	365118.8	298289.3	13.104	10.227	2.877	12.931	10.523	2.409	16.585	12.422	4.163	7.755	4.217	3.538
66	66	2162941.4	437993.5	15.928	15.637	0.291	16.843	15.726	1.117	26.438	17.894	8.545	3.720	12.741	-9.022
67	67	620369.5	393169.9	14.613	13.089	1.524	12.622	12.936	-0.314	27.686	14.482	13.204	6.936	7.136	-0.201
68	68	459063.0	235764.9	20.680	13.160	7.520	20.755	13.282	7.472	22.155	14.588	7.567	19.372	11.048	8.323
69	69	2239245.9	724142.7	17.433	13.525	3.909	15.862	13.613	2.249	35.654	19.349	16.305	12.085	9.196	2.890
70	70	359478.5	369024.9	12.493	14.074	-1.581	12.924	14.295	-1.371	20.766	17.211	3.555	6.169	10.541	-4.372
71	71	378902.6	1370089.0	16.578	16.105	0.473	16.749	16.327	0.421	26.469	17.970	8.498	7.223	14.399	-7.176
72	72	1262058.8	1408882.9	27.862	16.192	11.671	24.302	16.230	8.072	45.093	22.865	22.227	14.045	14.124	-0.079
73	73	449955.9	208516.4	16.235	16.290	-0.055	16.107	16.373	-0.267	20.495	17.211	3.285	12.921	13.292	-0.372
74	74	1202361.1	359084.0	16.010	16.755	-0.746	16.064	16.771	-0.707	19.596	18.192	1.403	11.980	14.608	-2.628
75	75	1323331.6	622747.4	12.938	18.395	-5.456	12.584	18.420	-5.836	30.068	19.454	10.615	3.981	16.283	-12.302
76	76	130943.7	326213.5	16.352	18.078	-1.726	16.270	18.107	-1.837	18.559	18.679	-0.119	13.765	17.022	-3.256
77	77	436214.4	241589.4	17.548	19.395	-1.847	18.381	19.290	-0.909	25.323	22.823	2.500	13.223	17.590	-4.367
78	78	341147.7	502826.3	11.220	17.052	-5.832	10.973	17.078	-6.105	17.441	18.343	-0.903	7.559	15.945	-8.386
79	79	90327.5	811691.9	18.923	13.976	4.947	19.476	13.854	5.622	24.798	20.542	4.256	7.633	10.680	-3.047
80	80	351157.8	1179626.1	17.851	11.952	5.899	15.894	12.000	3.894	36.886	14.537	22.349	11.114	8.281	2.833
81	81	442418.6	292697.8	17.127	16.518	0.609	16.277	16.934	-0.657	27.958	18.341	9.617	5.126	13.620	-8.494
82	82	54381.2	147744.6	16.092	16.832	-0.740	15.395	16.077	-0.682	23.719	23.568	0.151	12.494	13.942	-1.448
	Ø	673576.6	517067.9	15.606	15.522	0.084	15.254	15.566	-0.312	24.349	20.610	3.739	9.069	11.262	-2.193

Appendix 7: Table Seward age group 5, addition to table 8

Age group ID	Object ID	DTLB Size	Buffer Size	Buffer Mean	DTLB Mean	Diff Buffer- DTLB Mean	Buffer Med	DTLB Med	Diff Buffer- DTLB Med	Buffer Max	DTLB Max	Diff Buffer- DTLB Max	Buffer Min	DTLB Min	Diff Buffer- DTLB Min
1	8	1124200.6	221625.2	29.23	25.39	3.84	29.43	24.84	4.59	43.49	43.04	0.45	14.39	12.85	1.54
2	61	151155.9	530641.2	33.41	15.91	17.51	36.27	15.42	20.85	46.46	102.08	-55.62	12.85	8.82	4.02
3	68	335480.5	199765.5	42.27	20.81	21.46	43.42	21.04	22.38	52.72	26.07	26.65	30.46	12.58	17.88
4	157	248032.7	256617.9	32.59	27.22	5.37	36.02	27.54	8.49	46.38	41.72	4.65	17.85	18.32	-0.47
5	159	102325.5	642634.9	20.72	42.63	-21.91	20.57	43.87	-23.29	26.89	50.64	-23.74	19.11	28.51	-9.40
6	161	175208.9	270732.6	21.17	24.58	-3.41	24.27	24.14	0.13	30.14	36.72	-6.58	11.56	20.39	-8.83
7	167	2620139.1	1805823.3	23.65	22.55	1.10	23.25	23.07	0.18	46.85	39.38	7.47	10.61	10.90	-0.29
8	283	759267.5	222152.8	20.58	21.21	-0.64	19.85	21.17	-1.32	120.95	27.06	93.89	9.24	19.37	-10.13
9	293	708517.7	496316.8	18.94	20.71	-1.77	19.08	21.02	-1.94	21.50	25.77	-4.27	15.10	15.21	-0.11
	Ø	691592.1	516256.7	26.95	24.56	2.40	28.02	24.68	3.34	48.38	43.61	4.77	15.69	16.33	-0.64